

ALMA MATER STUDIORUM · UNIVERSITY OF BOLOGNA

---

School of Science  
Department of Physics and Astronomy  
Master Degree in Physics

# INTEGRAL REDUCTION IN COSMOLOGY

Supervisor:  
Prof. Fiorenzo Bastianelli

Submitted by:  
Andrea Pari

Co-Supervisor:  
Dr. Paolo Benincasa

Academic Year 2022/2023

# Contents

<b>1</b>	<b>Introduction</b>	<b>1</b>
<b>2</b>	<b>Integral reduction in flat space</b>	<b>5</b>
2.1	Scattering amplitudes . . . . .	5
2.2	Unitarity and Discontinuity . . . . .	6
2.3	Cutting rules . . . . .	9
2.4	Integral reduction . . . . .	12
<b>3</b>	<b>The analytic structure of the Bunch-Davies wavefunction</b>	<b>17</b>
3.1	The Bunch-Davies wavefunction . . . . .	17
3.2	The perturbative Bunch-Davies wavefunction . . . . .	18
3.3	Recursive relation for the universal integrand . . . . .	27
3.4	Singularities of the Bunch-Davies wavefunction . . . . .	29
<b>4</b>	<b>Integral reduction for the Bunch-Davies wavefunction</b>	<b>35</b>
4.1	Singularities and subgraphs . . . . .	35
4.1.1	Toy model . . . . .	37
4.1.2	Compatible subgraphs . . . . .	38
4.2	Tree-level reduction . . . . .	38
4.2.1	Wavefunction integral basis . . . . .	39
4.2.2	Computation of the coefficients at tree-level . . . . .	40
4.3	Tree-level examples . . . . .	44
4.4	1-Loop reduction . . . . .	57
4.4.1	Wavefunction integral basis . . . . .	57
4.4.2	Computation of the coefficients at 1-loop . . . . .	58
4.5	1-Loop example . . . . .	61
<b>5</b>	<b>Conclusion</b>	<b>67</b>
<b>A</b>	<b>Cauchy theorem and partial fractions</b>	<b>69</b>

## Abstract

Cosmic inflation is an hypothesis that predicts a near-exponential expansion of the universe in the first instants of its life. We can regard inflation as a “cosmological” particle accelerator where we can test new physics at higher energies than those accessible with experiments on earth. Indeed, a central challenge in cosmology is to extract fundamental physics from inflationary correlations. To accomplish this ambitious goal, innovative techniques for computing these correlations are needed. In this thesis, I consider the wavefunction of the universe, whose squared modulus provides the probability distribution for computing inflationary correlations. I focus on a class of scalar toy models in FRW cosmology and, drawing inspiration from integral reduction techniques for 1-loop flat-space amplitudes, I develop a systematic way to perform integral reduction for the wavefunction of the universe at tree-level and 1-loop. Here, the integral basis is determined by the singularity structure of a given process and the coefficients are determined by the wavefunction factorization conditions near singularities.

# Chapter 1

## Introduction

Our universe is presently expanding[1]. There was a time in the past, when it was smaller, denser and hotter. The theory of the hot Big Bang explains how the universe, from an initial state of high density and temperature, evolved into the universe we observe today. This theory describes, with reasonable confidence, the universe's evolution from  $t = 10^{-12}$  seconds after its birth, the Big Bang, to the current age of the universe, 13.8 billion years[2, 3, 4]. However, it is not a complete theory and presents some problems. In particular, two long-standing problems are the horizon problem and the flatness problem[5, 6].

Let us start by describing the former. Around 370 000 years after the Big Bang, during the epoch of recombination, the photons decoupled from the rest of the matter and started roaming freely across the universe which became transparent. We observe these photons today as the cosmic microwave background (CMB), which is a crucial observable to gather information on the primordial universe. The CMB that we measure today is homogeneous and isotropic. This is surprising, since in the context of the standard theory of the Big Bang, most of the universe appears not to have been in causal contact, the problem is even more serious considering that the epoch recombination is merely 370 000 years after the Big Bang. The fine-tuning problem concerning the homogeneity and isotropy of the CMB is known as the horizon problem. Furthermore, observed correlations in the CMB extend across regions of space that have never been in causal contact. An elegant hypothesis to solve these problems is inflation. This hypothesis predicts that the universe underwent a time of exponential expansion in the first instants of its life, allowing widely separated regions of spacetime to have been in causal contact in the past. As for the correlations observed in the CMB, they can be traced back to primordial density fluctuations at the end of inflation. It is hypothesised that these primordial density fluctuations were generated, during inflation, by small field quantum fluctuations that were stretched by the expansion of the spacetime and became the seeds for the large-scale structure of the universe[7, 5].

Let us now consider the flatness problem. Our universe appears flat and shows

no signs of curvature[8]. Since the curvature of a region of spacetime is determined by the potential and kinetic energy of that region via the Friedmann equations, a flat universe requires a precise fine tuning of the initial conditions for the hot Big Bang. An inflationary phase naturally resolves the flatness problem, as detailed calculations can be found in [5]. To provide an intuitive geometrical interpretation: if we consider a smooth, curved manifold and expand it, then any small region will appear increasingly flat[6].

To recapitulate, inflation predicts a quasi-exponential expansion of the universe in the first instants of its life. This hypothesis was originally proposed to address fine-tuning problems, including the horizon problem and the flatness problem. Nonetheless, it also offers a mechanism for generating the primordial density fluctuations that seeded the structures in the universe that we observe nowadays.

Let us summarize how inflation works[5]. The quasi-exponential expansion of the universe is driven by a scalar field  $\phi$  called inflaton. In the first stage of inflation, the inflaton is characterized by having a high potential energy compared to its negligible kinetic energy. During this phase, it behaves like a perfect fluid with negative pressure, driving the expansion of the universe. As the kinetic energy grows and the potential energy diminishes, inflation eventually ceases because the inflaton no longer behaves as a negative-pressure perfect fluid. We can regard the field  $\phi$  as a clock that determines the remaining duration of inflation. When treating the inflaton field quantum mechanically, it becomes subject to quantum fluctuations  $\delta\phi$ . Therefore, the end of inflation will vary across space. These small quantum fluctuations of the inflaton can lead to significant variations in local densities of the universe after inflation [5]. These variations are encoded in the correlations of the scalar field at the end of inflation and provide the initial conditions for the evolution of the universe. These correlations are referred to as inflationary correlations. Any measurable correlation today, such as temperature fluctuations in the CMB or the distribution of large-scale structures (LSS), can be traced back to inflationary correlations[9]. Being able to compute these inflationary correlations means understanding the physics at very high energies, 10-11 order of magnitudes higher than the energies at play at LHC. We can think of inflation as a “cosmological” particle accelerator where we can test new physics at higher energies than those accessible with experiments on earth.

The problem that we address in this thesis is to develop a systematic technique to compute inflationary correlations. To achieve this goal, a promising approach is represented by the wavefunction of the universe, which provides the probability distribution to compute inflationary correlations.

The advantage of considering the wavefunction of the universe is that, for conformally coupled scalars in FRW cosmology, it can be cast into a relatively simple form. In fact, in this context, the information on the cosmology can be extracted from the wavefunction of the universe by integrating a universal integrand on the space external energies with an appropriate measure, depending on the cosmology. The universal integrand is a rational function that encodes the analytic structure of the wavefunction and it is independent

on the cosmology[10, 11, 9].

The wavefunction of the universe is defined by the expectation value of the field evolution operator sandwiched between the Bunch-Davies vacuum at early times and the field configuration at the end of inflation. More precisely, it is referred to as Bunch-Davies wavefunction. A great deal of work has been done towards the understanding of the wavefunction of the universe for scalar fields in any FRW spacetime in the perturbative regime[10, 11, 9]. Specifically the Feynman rules of the Bunch-Davies wavefunction has been derived and the Bunch-Davies wavefunction can be expressed as a summation over the wavefunction contributions corresponding to all the possible Feynman graphs. Moreover, the analytic structure of the Bunch-Davies wavefunction corresponding to a single Feynman graph has been analyzed: such wavefunction is singular where energy conservation is imposed and factorizes, following specific rules, into flat space amplitudes and simpler wavefunctions, offering insights on understanding the relationship between flat-space amplitudes and the Bunch-Davies wavefunction in curved-space cosmology.

It is convenient to represent the singularity structure of the Bunch-Davies wavefunction of a single Feynman graph using its subgraphs. We represent an energy conservation constraint on a subprocess via a set of subgraphs on the Feynman graph of the process. In fact, there is a 1-1 correspondence between a singularity of codimension  $k$  of the wavefunction for a given process and a set of  $k$  subgraphs, enforcing energy conservation. Moreover, the Bunch-Davies wavefunction is an analytic function that has discontinuities and each singularity of given codimension corresponds to a discontinuity of the same codimension. The computation of such discontinuities is much simpler than performing the actual integration over the space of external energies[12]. These analytic properties can be exploited to compute the Bunch-Davies wavefunction, avoiding the direct integration.

In this thesis, we consider an integral reduction approach to compute the Bunch-Davies wavefunction of a single Feynman graph. We develop a systematic way to expand the Bunch-Davies wavefunction at tree-level and 1-loop in an integral basis where each integral term is determined by the singularity structure of a given process. The coefficients are fixed by matching the discontinuities of the wavefunction and the basis, and are determined by the wavefunction factorization conditions.

This work is important because it provides a systematic computational technique for calculating the Bunch-Davies wavefunction for a Feynman graph. The squared modulus of such wavefunction provides the probability distribution to compute inflationary correlations. Novel techniques of computation, such as the one presented here, are needed for a deeper understanding of such correlations. A more profound comprehension of inflationary correlations is crucial as it would shed more light on the physics of inflation and as these correlations provide the initial conditions for the evolution of the universe.

We begin this work by reviewing the flat-space scattering amplitudes, focusing on their analytic structure, and integral reduction for flat-space 1-loop amplitudes [13, 14, 12, 15, 16, 17]. A 1-loop amplitude becomes singular when intermediate particles go on

shell. For real momenta, we can send on-shell at most two particles simultaneously and the amplitude factorizes into two tree-level amplitudes, due to unitarity. Allowing the momenta to take complex values, we can send on-shell at most  $d$  particles simultaneously, where  $d$  is the dimension of the spacetime. In this limit, the amplitude factorizes at most into  $d$  tree-level amplitudes, due to generalized unitarity. These analytic properties can be exploited to compute 1-loop amplitudes using integral reduction. Specifically, a 1-loop amplitude is expanded in a basis of integrals that capture its singularity structure. The coefficients of the basis are determined by matching the discontinuities of the amplitude and those of the basis, and they are fixed by tree-level amplitudes [18, 10].

We consider this procedure as a guiding principle for the integral reduction of the Bunch-Davies wavefunction. We define a basis of integrals that capture the singularity structure of the wavefunction, encoded in the universal integrand. Then, by matching the discontinuities of the wavefunction and the basis, we determine the coefficients in terms of flat-space amplitudes and simpler wavefunctions, given by the factorization conditions. We develop an algorithm to perform the integral reduction for the Bunch-Davies wavefunction of a single Feynman graph at tree-level and we extend the treatment to the 1-loop case.

Let us summarize the procedure. First, we construct the integral basis for the wavefunction of a given graph by exploiting the 1-1 correspondence between sets of subgraphs of the given Feynman graph and the wavefunction singularities. We consider all the compatible sets of subgraphs, i.e. the subgraphs associated to a non-vanishing factorization of the wavefunction[9]. The basis is composed of an integral term for each compatible set of subgraphs. A basis term associated to a set of  $k$  subgraphs contains  $k$  poles in the external energy variables, where  $1 \leq k \leq n$  and  $n$  is the number of integration variables of the Bunch-Davies wavefunction. An integral basis term containing  $k$  poles is referred to as  $k$ -gon integral term and the associated coefficient as  $k$ -gon coefficient. We start by matching the discontinuities of highest codimension, thereby fixing the associated coefficient. These coefficients are fully determined by the factorized wavefunction into flat-space amplitudes. Then, we consider discontinuities of progressively lower codimension. For a general discontinuity of codimension- $k$ , the associated  $k$ -gon coefficient will be given by the pole at infinity of the  $k'$ -gon integral terms, where  $k \leq k' \leq n$ , and of the factorized wavefunction. We proceed until we have computed all the coefficients. The basis expansion is defined up to a rational function  $R$ , which cannot be computed in this manner since it does not have discontinuities.

This thesis is composed of five chapters. In chapter 2, we review scattering amplitudes in flat-space, their analytic structure and integral reduction for 1-loop flat-space amplitudes. In chapter 3, we review the Bunch-Davies wavefunction, along with its Feynman rules, analytic structure, and factorization conditions. In Chapter 4, we develop a systematic way to perform the integral reduction for the Bunch-Davies wavefunction for a single Feynman graph at tree-level and 1-loop and present some examples. Chapter 5 is the concluding chapter where we summarize the key points and discuss future directions.

# Chapter 2

## Integral reduction in flat space

In this chapter, we review scattering amplitudes in flat-space and discuss the optical theorem, which illustrates how unitarity constrains the analytic structure of the scattering amplitudes [15, 13]. Then, we present a systematic way to compute the discontinuities of a flat-space 1-loop amplitude using the cutting rules [19, 15, 10]. Firstly, we consider the application of the cutting rules in the context of unitarity, where the momenta of the amplitude are real. Secondly, we consider the context of generalized unitarity, where the momenta of the amplitude are analytically continued to complex values. Finally, we review a systematic approach to perform integral reduction for flat-space 1-loop amplitudes, employing the cutting rules for complexified momenta [12, 16]. We use the mostly plus convention,  $(- + ++)$ , for the signs of the Minkowski metric.

### 2.1 Scattering amplitudes

Let us consider scattering processes in Minkowski space-time [16, 15]. We assume that there are no interactions at asymptotic times, then the states we scatter can be defined as on-shell one-particle states of given momenta, known as asymptotic states. From a mathematical point of view, the asymptotic states are defined as the irreducible representations of the space-time isometry group, which in this case is the Poincaré group  $\Pi(d) = \mathbb{R}^{(d-1,1)} \ltimes SO(d-1,1)$ .  $\mathbb{R}^{(d-1,1)}$  is the  $d$ -dimensional translations group and  $SO(d-1,1)$  is the  $d$ -dimensional Lorentz group. Since the generators  $\hat{P}_\mu$  of  $\mathbb{R}^{(d-1,1)}$  commute, we can take the asymptotic states to be the direct product of  $\hat{P}_\mu$  with eigenvalue  $p_\mu$ .

Consider a scattering process of  $n$  total particles,  $n_{in}$  initial states and  $n_{out} = n - n_{in}$  final states. In the Schrodinger picture, the asymptotic states at infinite future and infinite past are respectively  ${}_{out} \langle p^{(1)} \dots p^{(n-n_{in})} |$  and  $| p'^{(1)} \dots p'^{(n_{in})} \rangle_{in}$  and they are time-dependent.

In the Heisenberg picture, the eigenstates of the momentum operator do not depend

on time and span respectively the whole future and past Hilbert spaces  $H_{out}$  and  $H_{in}$ . They are given by:  $\langle f | := \langle p^{(1)} \dots p^{(n-n_{in})} |$  and  $|i\rangle := |p^{(1)} \dots p^{(n_{in})}\rangle$ .

The S-matrix operator  $\hat{S}$  is a unitary operator such that [15, 16]:

$${}_{out}\langle p^{(1)} \dots p^{(n-n_{in})} | p^{(1)} \dots p^{(n_{in})} \rangle_{in} = \langle f | \hat{S} | i \rangle. \quad (2.1)$$

Thus, the S-matrix operator is a time evolution operators and evolves the initial asymptotic state  $|i\rangle$  in the Heisenberg picture to the future asymptotic time.

The  $\hat{S}$  operator satisfies the Heisenberg equation:

$$i\partial_t \hat{S}(t, t_0) = \hat{H}(t) \hat{S}(t, t_0) \quad (2.2)$$

therefore it is given by

$$\hat{S} = \hat{\mathcal{T}} \{ e^{-i \int_{t_0}^t \hat{H}(t') dt'} \}. \quad (2.3)$$

where  $\hat{\mathcal{T}}$  is the time ordering operator.

It is convenient to split the trivial part of the S-matrix and the scattering part:  $\hat{S} = \hat{I} + i\hat{T}$ , where  $\hat{T}$  is the transfer matrix. We define the scattering amplitude  $M_n$  as:

$$\langle f | i\hat{T} | i \rangle = M_n(\{p^{(1)} \dots p^{(n_{in})}\} \rightarrow \{p^{(1)} \dots p^{(n-n_{in})}\}). \quad (2.4)$$

Let us take as a convention that all the states are incoming, thus the scattering amplitude becomes  $M_n = M_n(p^{(1)}, \dots, p^{(n)})$  and all the different processes can be computed from it by analytic continuation.

The scattering amplitude  $M_n$  must be invariant under the Poincaré group. It is possible to define operators which act on the whole scattering amplitude as they do on the one-particle states. The action of the space-time translations on  $M_n$  is given by

$$M_n(p^{(1)}, \dots, p^{(n)}) = e^{ix \cdot \sum_{i=1}^n p^{(i)}} M_n(p^{(1)}, \dots, p^{(n)}) \quad (2.5)$$

In order to satisfy the above equation we must have  $\sum_{i=1}^n p^{(i)} = 0$ , i.e. total momentum conservation. In other words, invariance under space-time translation implies momentum conservation in the scattering process, leading to the appearance of a  $\delta$ -function enforcing momentum conservation. Additionally, Lorentz invariance implies that the scattering amplitude must be a function of a Lorentz invariant combination of the momenta[16].

## 2.2 Unitarity and Discontinuity

The time evolution operator  $\hat{S}$  is unitary:

$$\hat{S}^\dagger \hat{S} = \hat{I}. \quad (2.6)$$

In terms of the transfer matrix  $\hat{T}$  the above equation becomes

$$-i \left( \hat{T} - \hat{T}^\dagger \right) = \hat{T}^\dagger \hat{T}. \quad (2.7)$$

Sandwiching the relation (2.7) with the states  $\langle f|, |i\rangle$  and inserting on the left hand side the completeness relation for the Hilbert space:

$$\hat{I} = \sum_X \int d\Pi_X |X\rangle \langle X|, \quad d\Pi_X := \prod_{j \in X} \frac{d^3 p_j}{(2\pi)^3} \frac{1}{2E_j} \quad (2.8)$$

where the sum is performed over all the single and multi-particle states  $|X\rangle$ , we obtain the generalized optical theorem[13, 15]:

$$M(i \rightarrow f) - M^*(f \rightarrow i) = i \sum_X \int d\Pi_X (2\pi)^4 \delta^4(p_i - p_X) M(i \rightarrow X) M^*(f \rightarrow X). \quad (2.9)$$

The generalized optical theorem implies that the imaginary part of an amplitude is determined by amplitudes of lower loop and/or lower order in perturbation theory[15].

Additionally, let us consider the special case of the generalized optical theorem where the initial state and the final state coincide,  $|i\rangle = |f\rangle = |A\rangle$ . Eq. (2.9) becomes,

$$2 \operatorname{Im} M(A \rightarrow A) = \sum_X \int d\Pi_X (2\pi)^4 \delta^4(p_i - p_X) |M(A \rightarrow X)|^2. \quad (2.10)$$

If  $|A\rangle$  is a two-particle state, then the total cross section in the center-of-mass frame is given by[13]:

$$\sigma_{tot} = \sum_X \sigma_X = \sum_X \frac{1}{4E_{cm} |\vec{p}_{cm}|} \int d\Pi_X (2\pi)^4 \delta^4(p_A - p_X) |M(A \rightarrow X)|^2 \quad (2.11)$$

and the optical theorem is given by:

$$\operatorname{Im} M(A \rightarrow A) = 2E_{cm} |\vec{p}_{cm}| \sigma_{tot}, \quad (2.12)$$

where  $E_{cm}$  is the total center-of-mass energy and  $p_{cm}$  is the momentum of either particle in the center-of-mass frame. The imaginary part of the forward scattering amplitude is proportional to the total cross section [13, 15].

Let us take a closer look at where the imaginary part of a scattering amplitude comes from. We focus for simplicity on scalar theories, where the momentum space propagator is given by:

$$G = \frac{1}{p^2 + m^2 - i\epsilon}, \quad (2.13)$$

where the  $i\epsilon$  prescription ensures the correct boundary conditions for the Feynman propagator and it is always intended in the limit  $\epsilon$  going to zero.

Due to locality, poles can only arise from propagators[16]. In the tree-level case, a general amplitude contains only poles and it is given by:

$$M_{\text{tree}}(i \rightarrow f) = \sum_X \frac{n_X}{p_X^2 + m^2 - i\epsilon} + \text{contact} \quad (2.14)$$

where the summation runs over the momentum channels  $X$ ,  $n_X$  is a numerator that depends on the theory and 'contact' refers to the contact graphs. Let us substitute the general amplitude into the generalized optical theorem (2.9),

$$\begin{aligned} 2 \operatorname{Im} \left( \sum_X \frac{n_X}{p_X^2 + m^2 - i\epsilon} + \text{contact} \right) &= \\ &= \sum_X \int d\Pi_X (2\pi)^4 \delta^4(p_i - p_X) M_{\text{tree}}(i \rightarrow X) M_{\text{tree}}^*(f \rightarrow X) \end{aligned} \quad (2.15)$$

and consider the identity,

$$\operatorname{Im} \frac{1}{p^2 + m^2 - i\epsilon} = -\pi \delta(p^2 + m^2), \quad (2.16)$$

where the limit for  $\epsilon$  going to zero is implicit. The imaginary part on the left hand side (l.h.s) of eq. (2.15) is non-zero only when the propagator is on-shell. In this limit, the tree-level amplitude  $M_{\text{tree}}(i \rightarrow f)$  factorizes into two tree-level amplitudes with a lower number of external state, as shown in eq. (2.15).

Let us now consider a loop amplitude. In this case, the integration over the momenta of the propagators implies that the amplitude has branch cuts. Let us consider the amplitude as an analytic function of the complex variable  $s = E_{cm}^2$ , which is the analytic continuation of the center-of-mass energy. Let  $s_0$  be the threshold energy for production of the lightest multiparticle state. For  $s < s_0$  the intermediate state cannot go on-shell,  $s$  is real, and the Schwarz reflection principle implies:

$$M^*(s) = M(s^*). \quad (2.17)$$

Since for  $s < s_0$ , we do not cross any singularity, the above result can be analytically continued to the entire complex  $s$  plane. For  $s > s_0$ , there is a branch cut on the real axis starting at  $s > s_0$  and the discontinuity is given by:

$$\operatorname{Disc} M(s) = M(s + i\epsilon) - M(s - i\epsilon) = 2i \operatorname{Im} M(s + i\epsilon), \quad (2.18)$$

where we used (2.17) in the second equality[13].

Eq. (2.18) illustrates the connection between the discontinuity of a loop amplitude and its imaginary part. This, in turn, can be computed using the optical theorem and is expressed in terms of lower loop amplitudes.

In conclusion, the optical theorem implies that when the singularities of an amplitude are approached, one or more particles go on-shell and the amplitude factorizes into amplitudes with lower number of external states and/or at lower order in perturbation theory[16].

## 2.3 Cutting rules

In general, it is easier to compute the discontinuity of an amplitude than its imaginary part. Cutkosky proved that, for a general loop amplitude, the discontinuity can be computed using the following cutting rules [19, 15]:

1. Cut through the diagram in any way that can put all of the cut propagators on-shell without violating momentum conservation.
2. For each cut, replace  $k^2 + m^2 - i\epsilon \rightarrow -2i\pi\delta(k^2 + m^2)\vartheta(k^0)$
3. Sum over all cuts.
4. The result is the discontinuity of the diagram

For 1-loop amplitudes with real momenta, only two particles can be sent on-shell simultaneously and, thus, we can perform at most two cuts. By cutting two propagators, we compute a codimension-2 discontinuity. Approaching this singularity, the amplitude factorizes into two tree-level amplitudes, due to unitarity.

We can perform an analytic continuation on the momenta of the amplitude, allowing them to take complex values. For complex momenta, we can send on-shell  $d$  particles simultaneously, where  $d$  is the dimension of the spacetime. Thus, we can perform multiple cuts and compute discontinuities of higher codimension. By performing an  $n$ -cut, where  $n \leq d$ , we compute a discontinuity of codimension- $n$  and the amplitude factorizes into  $n$  tree-level amplitudes. This approach is referred to as generalized unitarity[12, 16].

Let us discuss the cutting rules in more details [12]. A general 1-loop amplitude has the form of an integral over the free loop-momentum  $k$ . Let us consider 1-loop amplitudes in  $d$  dimensions and split the measure  $d^d k$  as  $d^{d-1} \vec{k} dk^0$ . The  $k^0$  integral is then taken to be a contour integral along the real axis in the complex  $k^0$  plane. The Feynman  $i\epsilon$  prescription for propagators splits all poles of the real axis sending half of them to the upper half plane and the other half to the lower half plane. In order to compute the  $k^0$  integral we close the contour of integration in the lower plane selecting the solutions with positive energy  $k^0$ :

$$\int d^d k = \int d^{d-1} \vec{k} dk^0 \quad \text{where} \quad \int dk^0 = \int_C dk^0,$$

where  $C$  is the contour of integration closed in the lower plane.

Deforming the contour integral in the lower half plane gives rise to a sum of contour integrals enclosing each of the poles.

The residue of each of these poles can be computed replacing the propagator with a delta function, for instance:

$$\frac{1}{k^2 - i\epsilon} \rightarrow \delta^+(k^2),$$

where the (+) indicates choosing the solution which has  $k^0 > 0$ . This operation is called cutting the propagator.

We choose one propagator to cut and use the delta functions to perform the  $k^0$  integral, we are left with integrals over  $d^{d-1} \vec{k}$ .

It is convenient to express the integral in spherical variables and the radial part is of the form:

$$I = \int_0^\infty dE_{\vec{k}} F(E_{\vec{k}}, \theta_i). \quad (2.19)$$

The function  $F$  has poles which corresponds to the remaining propagators in the complex  $E_{\vec{k}}$  space.

Let us consider a single pole and vary the kinematical invariants in such a way that the pole travels in a circle around the origin of the complex plane. In the process, the pole crosses the domain of integration and drags it along. Completing a full circle, the pole picks up an integration contour, see fig. (2.1). If the integration along this small contour is non-zero, the integrated function  $I$  is not single-valued, but it has a branch cut. The discontinuity across the branch cut is given by the integration along the contour around the pole and it is precisely the residue of the function  $F$  at the pole. Again, this residue be computed by substitution with a  $\delta$ -function, i.e. cutting the propagator.

Therefore, the amplitude's discontinuity is determined by cutting two propagators, resulting in a codimension-2 discontinuity, known as double cut discontinuity. Approaching a codimension-2 singularity, by making 2 cuts, the amplitude factorizes into 2 tree-level amplitudes, due to unitarity (2.9).

If we allow the momenta to be complex, we can send on-shell at most  $d$  particles simultaneously and, in general, the remaining angular integrals possess branch cuts. By cutting the remaining poles, we compute higher codimension discontinuities and the amplitude factorizes further. If we perform  $n$  cuts, the amplitude factorizes into  $n$  tree-level amplitudes, due to generalized unitarity [12, 16].

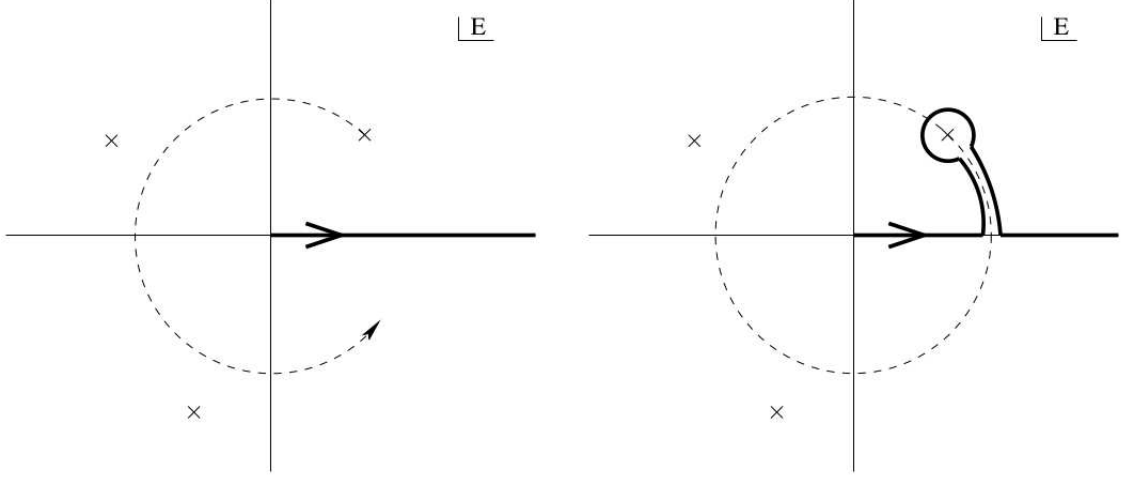


Figure 2.1: Complex  $E_{\vec{k}}$  space. We make the pole travel in a circle. It picks up an integration contour corresponding to the discontinuity of the branch cut [12].

**Example of a double cut** Let us consider a bubble integral in  $d$  dimensions:

$$M(p^2) = \int d^d k \frac{1}{(k^2 - i\epsilon)((k-p)^2 - i\epsilon)}. \quad (2.20)$$

We cut the first propagator by replacing  $\frac{1}{k^2 - i\epsilon}$  with  $\delta^+(k^2)$ , the single-cut amplitude is given by

$$M'(p^2) = \int d^d k \delta^+(k^2) \frac{1}{(k-p)^2 - i\epsilon} \quad (2.21)$$

where  $(+)$  indicates that we choose the positive energy solution. We split the integration in  $d^{d-1} \vec{k} dk^0$  and perform the  $k^0$  integration,

$$\begin{aligned} M'(p^2) &= \int d^{d-1} \vec{k} \int dk^0 \frac{\delta(k^0 - |\vec{k}|)}{2(|\vec{k}| - i\epsilon) - (k^0 - p^0)^2 + (\vec{k} - \vec{p})^2 - i\epsilon} \frac{1}{(k-p)^2 - i\epsilon} \\ &= \int d^{d-1} \vec{k} \frac{1}{2(|\vec{k}| - i\epsilon)} \frac{1}{(p^2 + 2|\vec{k}|p^0 - 2\vec{k} \cdot \vec{p} - i\epsilon)} \end{aligned} \quad (2.22)$$

We move to the center-of-momentum frame:  $p^\mu = (p^0, \vec{0})$  and express the integral in spherical coordinates,

$$\begin{aligned} M'(p^2) &= \text{Vol}(\mathbf{S}^{d-2}) \int_0^\infty k^{d-2} dk \frac{1}{2k} \frac{1}{(-(p^0)^2 + 2kp^0 - i\epsilon)} \\ &= \text{Vol}(\mathbf{S}^{d-2}) \int_0^\infty dk \frac{k^{d-3}}{2} \frac{1}{(-(p^0)^2 + 2kp^0 - i\epsilon)} \end{aligned} \quad (2.23)$$

The integral has a branch cut on the negative real  $k$  axis and a pole at  $k = \frac{p^0}{2}$ . Let us now vary the kinematical invariants in such a way that the pole travels in a circle around the origin of the complex plane. In the process the pole crosses the integration domain and picks up an integration contour. Therefore the discontinuity across the branch cut is given by the residue of the pole. As before, the residue of the pole can be computed by substituting it with a  $\delta$ -function. The discontinuity is given by:

$$\Delta M(p^2) = \int d^d k \delta^+(k^2) \delta^+((k-p)^2). \quad (2.24)$$

## 2.4 Integral reduction

One-loop amplitudes contain an integration over the virtual momenta of the propagators, giving rise to functions with branch cuts. These branch cuts lead to discontinuities that can be computed using the cutting rules, by substituting the appropriate propagators with delta functions, i.e. sending the propagators on-shell. When the propagators are sent on-shell, the amplitude factorizes into simpler tree-level amplitudes.

The aim of this section is to show how these analytic properties can be used to develop a computational method, the integral reduction, which let us reconstruct 1-loop amplitudes using on-shell tree-level amplitudes [12, 16].

**Integral basis** Integral reduction consists in expanding the 1-loop amplitude in an integral basis. For complex momenta, at most  $d$  particles can go on shell, where  $d$  is the dimension of the spacetime. Therefore, the amplitude contains at most singularities of codimension  $d$ . For this reason, the minimal integral basis on which a 1-loop amplitude in  $d$ -dimensions can be expanded shows at most  $d$ -gon integrals, and then the lower point ones [18, 12, 16]. For  $d$ -gon integral we refer to an integral which contains  $d$  propagators. The expansion of a 1-loop amplitude is given by

$$M^{1-loop} = \sum_{i \in X_d} C_d^i I_d^i + \sum_{i \in X_{d-1}} C_{d-1}^i I_{d-1}^i + \dots + \sum_{i \in X_2} C_2^i I_2^i + R \quad (2.25)$$

where the summation runs over all the possible momentum channels, each  $I_m$  is a scalar integral with  $m$  propagators and the coefficients  $C_m$  and  $R$  are rational functions of the kinematical invariants.

Since the two sides of equation (2.25) represent the same function, they must have the same analytic structure. Specifically, it is possible to get information on the coefficients from the fact that the discontinuities across given cuts on both sides of (2.25) must be equal. In order to compute the discontinuities, we use the cutting rules in the generalised unitarity case: we allow the momenta to be complex and we can cut at most  $d$  propagators.

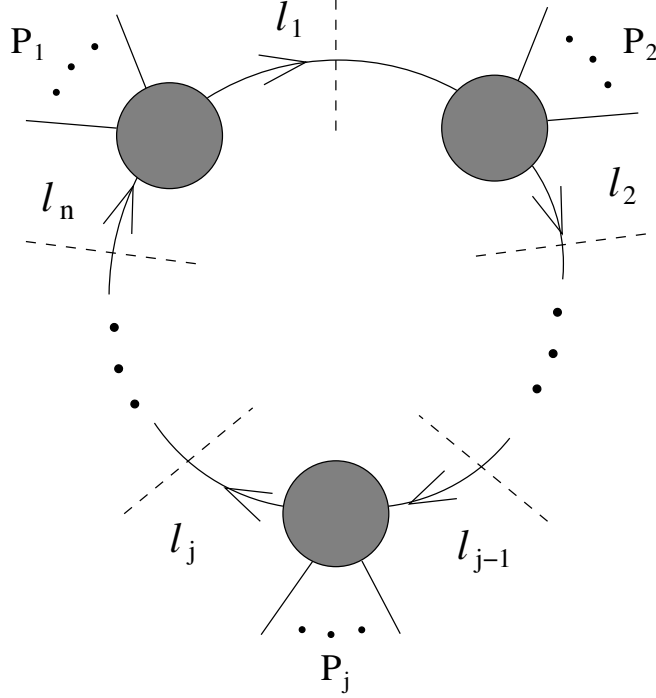


Figure 2.2: N-cut of a 1-loop amplitude in  $d$ -dimensions [12].

**General  $n$ -cut discontinuity** Starting from the left hand side (l.h.s) of (2.25), we perform a general  $n$ -cut on the 1-loop amplitude  $M$ , where  $n$  is such that  $n \leq d$  and it is the codimension of the discontinuity.

Let us divide the external states of the amplitude  $M$  into  $n$  groupings:  $\{1\}, \dots, \{n\}$ . The external momentum for each grouping is  $P_j$  and the loop momentum flowing between groupings  $\{j\}$  and  $\{j+1\}$  is  $l_j$ , as shown in fig. (2.2). By applying the cutting rules, we obtain the  $n$ -cut amplitude [12]:

$$\left[ \text{Cut}_{\{1\}, \dots, \{n\}}^{(n)} \right] M = \int \prod_{i=1}^n \frac{d^d l_i}{(2\pi)^d} \delta^+(l_i^2) \sum_{\text{species, spins}} \prod_{j=1}^n M_{\text{tree}}^{h_{j-1}, -h_j}(l_{j-1}, \{j\}, -l_j) \delta^d(l_{j-1} + P_j - l_j). \quad (2.26)$$

The amplitude factorizes into  $n$  tree-level amplitudes  $M_{\text{tree}}^{h_{j-1}, -h_j}$ . Each Dirac delta  $\delta^+(l_i^2)$  sends on-shell the propagator with momentum  $l_i$ , choosing the solution with positive energy. Each Dirac delta  $\delta^d(l_{j-1} + P_j - l_j)$  enforces momentum conservation for the tree level amplitude  $M_{\text{tree}}^{h_{j-1}, -h_j}$ .

Let us consider the right hand side (r.h.s.) of (2.25) and perform the  $n$ -cut of the

integral expansion:

$$\left[ \text{Cut}_{\{1\}, \dots, \{n\}}^{(n)} \right] M = \sum_{i \in X_d} C_d^i \left[ \text{Cut}_{\{1\}, \dots, \{n\}}^{(n)} \right] I_d^i + \dots + \sum_{i \in X_2} C_2^i \left[ \text{Cut}_{\{1\}, \dots, \{n\}}^{(n)} \right] I_2^i. \quad (2.27)$$

We perform the cuts on the basis terms by substituting the appropriate propagators with delta functions  $\delta^+$ . The terms that do not contain the appropriate propagators vanish.

**Cut equations** The discontinuity of the amplitude  $M$ , (2.26), must match the discontinuity of the integral basis, (2.27), for every possible set of cuts. In this way, we obtain a set of “cut equations” that relate the coefficients of the integral basis with tree-level on-shell amplitudes.

Let us now describe a systematic way to derive the “cut equations” and compute the coefficients.

The first step is to compute all the coefficients  $C_d^i$  by matching the discontinuities of highest codimension  $d$ . We perform a maximal cut of the amplitude on the l.h.s of (2.25). This amplitude factorizes into a product of  $d$  tree-level amplitudes. The same maximal cut is performed on the integral basis, isolating the appropriate coefficient on the r.h.s. of (2.25). We obtain a “cut equation” for each coefficient  $C_d^i$ , indexed by  $i$ . Specifically, the coefficients  $C_d^i$  associated to  $d$ -gon integral terms are determined by the appropriate  $d$  tree-level amplitudes.

Next, we compute the coefficients  $C_{d-1}^i$  by matching the discontinuities of codimension  $d-1$ . Performing a  $(d-1)$ -cut, on the l.h.s of (2.25), we obtain a factorized amplitude into  $d-1$  tree-level amplitudes; on the r.h.s, we are left with the appropriate  $d$ -gon integral terms and one  $(d-1)$ -gon integral term. The coefficients  $C_{d-1}^i$  are determined by the pole at infinite momentum of the  $d-1$  tree-level amplitudes, obtained by the factorization of the amplitude  $M$ .

We apply the same procedure for the coefficients  $C_{d-2}^i$ , which are determined by the pole at infinite momentum of the  $d-2$  tree-level amplitudes obtained by the factorization of the amplitude  $M$ . We proceed in this manner until we have computed the coefficients of lowest dimension  $C_2^i$ .

We are left with the rational term  $R$ , which does not have branch cuts and thus is invisible to the cutting procedure.

**Example of integral reduction** We present an example of integral reduction for a 1-loop amplitude in  $d=4$  dimensions [12, 16].

We start by matching the highest codimension discontinuities given by  $n=4$  cuts. We divide the external states in 4 groupings:  $\{1\}, \dots, \{4\}$ . We index all the possible groupings with the index  $k$ . We perform a 4-cut for each set of groupings  $k$ , obtaining a set of cut equations that fix the coefficients  $C_4^k$ :

$$\begin{aligned}
\left[\text{Cut}_k^{(4)}\right] M &= \int \frac{d^4 l}{(2\pi)^4} \delta^+(l^2) \delta^+((l - P_1)^2) \delta^+((l + P_2)^2) \delta^+((l - P_1 - P_4)^2) \prod_{m=1}^4 M_m^{\text{tree}}(l) \\
&= C_4^k \int \frac{d^4 l}{(2\pi)^4} \delta^+(l^2) \delta^+((l - P_1)^2) \delta^+((l + P_2)^2) \delta^+((l - P_1 - P_4)^2),
\end{aligned} \tag{2.28}$$

where  $l \equiv l_1$  is the magnitude of the loop momentum and  $P_1, \dots, P_4$  are the total momenta for each grouping of external states.

By performing the integration over the delta functions, we are solving quadratic equations and, thus, we have two solutions for  $l$ , which we refer to as  $l_*$ . The coefficient  $C_4^k$  is given by the product of four tree-level amplitudes summed over the two solutions  $l_*$  and the helicity states  $h$ :

$$C_4^k = \frac{1}{2} \sum_{l_*} \sum_h M_1^{\text{tree}}(l_* - P_1, P_1, -l_*) M_2^{\text{tree}}(l_*, P_2, -(l_* - P_2)) \times \tag{2.29}$$

$$\times M_3^{\text{tree}}(l_* + P_2, P_3, -(l_* - P_1 - P_2)) M_4^{\text{tree}}(l_* - P_1 - P_2, P_4, -(l_* - P_1)). \tag{2.30}$$

In this way we compute all the coefficients associated to basis terms with 4 propagators.

To compute the other coefficients, we have to match the discontinuities of lower codimension, starting from the triple cut. We divide the external states in 3 groupings:  $\{1\}, \{2\}, \{3\}$ . We index all the possible groupings with the index  $k$  and perform a 3-cut for each set of groupings  $k$ :

$$\left[\text{Cut}_k^{(3)}\right] M = C_3^k \int \frac{d^4 l}{(2\pi)^4} \delta^+(l^2) \delta^+((l - P_1)^2) \delta^+((l + P_2)^2) \prod_{m=1}^3 M_m^{\text{tree}}(l) \tag{2.31}$$

By performing the integration with the three delta functions, we do not localize the integral completely, the remaining integration can be parametrized by the variable  $z$ <sup>1</sup>. The three tree-level amplitudes, that we obtained by performing the triple cut, have poles in the variable  $z$ . These poles are connected to the box-integrals, i.e. 4-gon integrals. Therefore, the contributions to the triangle coefficients,  $C_3^k$ , are the ones that do not contain any pole at finite  $z$  and, thus, are given by the pole at infinity:

$$C_3^k = \frac{1}{2} \int_{\gamma_\infty} \frac{dz}{z} \sum_{l_*} \prod_{m=1}^3 M_m^{\text{tree}}(z), \tag{2.32}$$

---

<sup>1</sup>For a detailed calculation refer to [16].

where  $\gamma_\infty$  is a contour around the pole at infinity.

Finally, we consider the double cut. We divide the external states in 2 groupings:  $\{1\}, \{2\}$ . We index all the possible groupings with the index  $k$  and perform a double cut for each set of groupings  $k$ :

$$\left[ \text{Cut}_k^{(2)} \right] M = \int \frac{d^4 l}{(2\pi)^4} \delta^{(+)}(l^2) \delta^{(+)}((l - P_1)^2) \prod_{m=1}^2 M_m^{\text{tree}}. \quad (2.33)$$

We will not delve into the computation of the bubble coefficient since it is more involved<sup>2</sup>. The essential idea remains the same: the bubble coefficients are fixed by the poles at infinity of the double cut amplitude (2.33).

---

<sup>2</sup>For a detailed computation of the Bubble coefficients, refer to [12] and [16].

# Chapter 3

## The analytic structure of the Bunch-Davies wavefunction

A great deal of work has been done towards the understanding of the wavefunction of the universe, defined on the Bunch-Davies vacuum, in the perturbative regime. Specifically the Feynman rules of the Bunch-Davies wavefunction have been derived and the latter can be expressed as a summation over the wavefunction contributions corresponding to all the possible Feynman graphs. Moreover, the analytic structure of the Bunch-Davies wavefunction corresponding to a single Feynman graph has been analyzed[10, 11, 20, 9].

We focus on a class of toy models describing conformally coupled scalar in FRW cosmology. In this context, the information on the cosmology can be extracted from the wavefunction of the universe by integrating a universal integrand on the space of external energies with an appropriate measure, depending on the cosmology. The universal integrand is a rational function that encodes the analytic structure of the wavefunction and it is independent on the cosmology.

In this chapter, we review the aforementioned topics. In the next chapter, we will exploit the analytic properties of the Bunch-Davies wavefunction, which we review here, to compute it using the integral reduction technique.

### 3.1 The Bunch-Davies wavefunction

Consider a quantum mechanical system described by a hermitian hamiltonian,  $H(t)$ . The system's evolution operator is defined as[9]:

$$U := \hat{T} \left\{ \exp \left( -i \int_{-T}^0 dt H(t) \right) \right\}, \quad (3.1)$$

where the operator  $U$  is Hermitian, satisfying  $U^\dagger U = I = U U^\dagger$ . Let  $\Phi$  and  $\Phi'$  represent field configurations at times  $t = 0$  and  $t = -T$ , respectively. The transition amplitude

is given by:

$$\langle \Phi | U | \Phi' \rangle := \langle \Phi | \hat{T} \left\{ \exp \left( -i \int_{-T}^0 dt H(t) \right) \right\} | \Phi' \rangle = \mathcal{N} \int_{\phi(-T)=\Phi'}^{\phi(0)=\Phi} \mathcal{D}\phi e^{iS[\phi]}, \quad (3.2)$$

where  $S[\phi]$  represents the action describing the system in terms of field configurations and it is used to compute the transition amplitude between the initial and final field configurations in the path integral approach;  $\mathcal{N}$  denotes a normalization constant.

From the transition amplitude (3.2), by taking the limit  $T \rightarrow \infty(1 - i\epsilon)$ , we define the ground state wavefunction  $\Psi_{\circ}[\Phi]$  [9]:

$$\Psi_{\circ}^*[\Phi'] \Psi_{\circ}[\Phi] := \mathcal{N} \int_{\phi(-\infty(1-i\epsilon))=\Phi'}^{\phi(0)=\Phi} \mathcal{D}\phi e^{iS[\phi]}, \quad (3.3)$$

where the  $i\epsilon$  prescription is needed for the convergence of the Lorentzian path integral, accounting for oscillatory phases,  $\Psi_{\circ}^*[\Phi']$  denotes the complex conjugate of the ground state wavefunction for the configuration  $\Phi'$  and  $\Psi_{\circ}[\Phi]$  represents the ground state wavefunction for the configuration  $\Phi$ .

Setting the initial configuration to the vacuum,  $\Phi' = 0$ , we obtain the vacuum wavefunction:

$$\Psi_{\circ}[\Phi] = \langle \Phi | U | 0 \rangle = \mathcal{N} \int_{\phi(-\infty(1-i\epsilon))=0}^{\phi(0)=\Phi} \mathcal{D}\phi e^{iS[\phi]}, \quad (3.4)$$

where  $\phi(0) = \Phi$  denotes the configuration of the field at a later time  $t = 0$ , while  $\phi(-\infty(1 - i\epsilon)) = 0$  identifies a state at early times  $t = -\infty$ , specifically the Bunch-Davies vacuum state which is characterized by positive frequency modes only.

In a cosmological context,  $\phi$  represents a collection of all contributing modes, including gravitational ones. However, in this thesis, only scalar modes will be considered.

The Bunch-Davies wavefunction,  $\Psi_{\circ}[\Phi]$ , depends on the field configuration  $\Phi$  at a fixed time,  $t = 0$ , since the time evolution has been integrated out. Because  $\Psi_{\circ}[\Phi]$  exists on a fixed time slice, the time translation invariance is broken and energy is not conserved. Additionally, in cosmology we typically consider expanding spacetimes, which are not time-translation invariant. In such cases, the energy is not well-defined. Nonetheless, with an abuse of language, we refer to the energy as the absolute value of the momentum:  $E = |\vec{p}|$ .

## 3.2 The perturbative Bunch-Davies wavefunction

In this section, we review the Feynman rules for the Bunch-Davies wavefunction in the perturbative regime and we compute the Bunch-Davies wavefunction of a general Feynman graph [11, 9].

Let us consider a theory in  $d + 1$  dimensions described by an action that contains a conformally-coupled scalar field  $\phi$  in a FRW space-time with a space-like boundary at the conformal time  $\eta = 0$  where  $\eta \in ] - \infty, 0]$ .

We start by considering a lagrangian with non-conformal polynomial interactions. We will, then, extend the treatment to a lagrangian with a general interaction term, which contains derivatives of the field. The action is given by[21, 22, 10]:

$$S = - \int_{-\infty}^0 d\eta \int d^d x \sqrt{-g} \left[ \frac{1}{2} g^{\mu\nu} (\partial_\mu \phi) (\partial_\nu \phi) - \xi R \phi^2 - \sum_{k \geq 3} \frac{\lambda_k}{k!} \phi^k \right], \quad (3.5)$$

where the metric in comoving coordinates is

$$ds^2 = a^2(\eta) [-d\eta^2 + dx^i dx_i] \quad (3.6)$$

and  $\xi = \frac{d-1}{4d}$  corresponds the conformal coupling. It is convenient to perform a field redefinition [10, 11, 9]:

$$\phi \rightarrow a^{-\frac{d-1}{2}}(\eta) \phi. \quad (3.7)$$

The curved space action (3.5) is mapped into an flat space action with time dependent couplings,

$$S = - \int_{-\infty}^0 d\eta \int d^d x \left[ \frac{1}{2} (\partial\phi)^2 - \sum_{k \geq 3} \frac{\lambda_k(\eta)}{k!} \phi^k \right] \quad (3.8)$$

$$\lambda_k(\eta) = \lambda_k [a(\eta)]^{2 + \frac{(2-k)(d-1)}{2}} \quad (3.9)$$

where  $\cdot$  refers to the derivative with respect to the conformal time  $\eta$ .

The action (3.8) can be separated in a quadratic part and an interaction part:

$$S = S_2[\phi] + S_{\text{int}}[\phi]. \quad (3.10)$$

Additionally, we can split the field  $\phi$  into the classical free solution  $\phi_\circ$  and its quantum fluctuations  $\varphi$ :

$$\phi(\eta, \vec{x}) = \phi_\circ(\eta, \vec{x}) + \varphi(\eta, \vec{x}). \quad (3.11)$$

Then, it is necessary to translate the boundary condition on  $\phi$  to the pair  $(\phi_\circ, \varphi)$ . Since the fluctuations are required to vanish at the boundary, it is straightforward to derive the following boundary conditions:

$$\begin{aligned} \phi_\circ(-\infty(1 - i\epsilon), \vec{x}) &= 0, & \phi_\circ(0, \vec{x}) &= \Phi(\vec{x}) \\ \varphi(-\infty(1 - i\epsilon), \vec{x}) &= 0, & \varphi(0, \vec{x}) &= 0 \end{aligned} \quad (3.12)$$

where  $\Phi(\vec{x})$  is the field configuration at late time  $\eta = 0$ . Considering the splitting of the field given in (3.11), the action takes the form:

$$S = S_2[\phi_\circ] + S_2[\varphi] + S_{\text{int}}[\phi_\circ, \varphi], \quad (3.13)$$

where  $\phi_\circ(\eta, \vec{x})$  is the solution to the equation of motion obtained from the quadratic action,  $S_2[\phi_\circ]$ , endowed with the boundary conditions (3.12).

Due to the assumption of spatial translation invariance, we are able to reformulate the problem of computing  $\phi_\circ(\eta, \vec{x})$  in momentum space as:

$$\phi_\circ(\eta, \vec{x}) = \int \frac{d^d p}{(2\pi)^d} e^{i\vec{p}\cdot\vec{x}} \tilde{\phi}_\circ(\eta, \vec{p}). \quad (3.14)$$

The boundary conditions (3.12) and the Bunch Davies condition, which allows only positive frequency modes at early times, select the solutions of the equation of motion such that:

$$\tilde{\phi}_\circ(0, \vec{p}) = \tilde{\Phi}(\vec{p}), \quad \lim_{\eta \rightarrow -\infty(1-i\epsilon)} \tilde{\phi}_\circ(\eta, \vec{p}) \sim e^{iE\eta}, \quad (3.15)$$

where  $\tilde{\Phi}(\vec{p})$  is the Fourier transform of  $\Phi(\vec{x})$ .

Let us now compute the modes  $\phi_\circ$  for the model described by the action (3.8). The differential equation defining the modes is[11]:

$$\ddot{\phi}_\circ(\eta) + E^2 \phi_\circ(\eta) = 0 \quad (3.16)$$

where  $E = |\vec{p}|$ .

We impose the Bunch-Davies condition and the boundary conditions and we obtain the solution<sup>1</sup>:

$$\phi_\circ(\eta, \vec{x}) = \int \frac{d^d p}{(2\pi)^d} e^{i\vec{p}\cdot\vec{x}} \tilde{\Phi}(\vec{p}) e^{iE\eta} = \Phi(\vec{x}) e^{iE\eta}, \quad (3.17)$$

where the bulk-to-boundary propagator is given by:

$$\phi_+ = e^{iE\eta}. \quad (3.18)$$

Now that we have defined the toy model and derived the scalar modes, let's proceed to perturbatively expand the Bunch-Davies wavefunction[10, 11, 9].

Considering the splitting of the field (3.11), the Bunch-Davies wavefunction can be reformulated as,

$$\Psi_\circ[\Phi] = \mathcal{N} \exp(iS_2[\Phi]) \int_{\varphi(-\infty(1-i\epsilon))=0}^{\varphi(0)=0} \mathcal{D}\varphi e^{iS_2[\varphi] + iS_{\text{int}}[\Phi, \varphi]}. \quad (3.19)$$

---

<sup>1</sup>This solution can be generalized to the massive case, see [9].

Expanding perturbatively in the interactions, we obtain:

$$\begin{aligned}\Psi_{\circ}[\Phi] &= \mathcal{N} \exp(iS_2[\Phi]) \int_{\varphi(-\infty(1-i\epsilon))=0}^{\varphi(0)=0} \mathcal{D}\varphi e^{iS_2[\varphi]} \left( 1 + \sum_{j=0}^{\infty} \frac{i^j}{j!} S_{\text{int}}^j[\Phi, \varphi] \right) \\ &= \exp(iS_2[\Phi]) \sum_{j=0}^{\infty} \frac{i^j}{j!} \langle S_{\text{int}}^j \rangle[\Phi]\end{aligned}\quad (3.20)$$

where, in the first line,  $\langle S_{\text{int}}^j \rangle$  indicates the  $j$ -th term in the path-integrated sum, which includes the normalization,

$$\mathcal{N} = \frac{1}{\int \mathcal{D}\phi e^{iS_2[\phi]}}. \quad (3.21)$$

Considering the polynomial interaction term,

$$S_{\text{int}}[\phi_{\circ}, \varphi] = \int d^d x \int_{-\infty}^0 d\eta \frac{\lambda_k(\eta)}{k!} \phi^k \quad (3.22)$$

where  $\lambda_k(\eta)$  is a time-dependent function, we obtain:

$$\langle S_{\text{int}}^j \rangle = \mathcal{N} \int_{\varphi(-\infty(1-i\epsilon))=0}^{\varphi(0)=0} \mathcal{D}\varphi e^{iS_2[\varphi]} \prod_{r=1}^j \int d^d x_r \int_{-\infty}^0 d\eta_r \frac{\lambda_k(\eta_r)}{k!} \phi^k. \quad (3.23)$$

Given the polynomial dependence of the potential on fluctuations  $\varphi$  and the Gaussian form of  $S_2[\varphi]$ , only terms with an even number of  $\varphi$  contribute. The path integration over fluctuations yields the bulk-to-bulk propagators  $G(y_e; \eta_{v_e}, \eta_{v'_e})$ , which are required to vanish at the boundary, i.e. where  $\eta \rightarrow 0^-$ , and depend on the energy  $y_e$  running through them:

$$\begin{aligned}G(y_e; \eta_{v_e}, \eta_{v'_e}) &= \frac{1}{2y_e} \left[ e^{-iy_e(\eta_{v_e} - \eta_{v'_e})} \vartheta(\eta_{v_e} - \eta_{v'_e}) + e^{+iy_e(\eta_{v_e} - \eta_{v'_e})} \vartheta(\eta_{v'_e} - \eta_{v_e}) \right. \\ &\quad \left. - e^{+iy_e(\eta_{v_e} + \eta_{v'_e})} \right].\end{aligned}\quad (3.24)$$

The last term of the propagator is a boundary term and it ensures that the propagator vanishes approaching the late-time boundary.

The wavefunction of the universe (3.20) can be rewritten as

$$\Psi_{\circ}[\Phi] = e^{iS_2[\Phi]} \left\{ 1 + \sum_{k \geq 2} \int \prod_{j=1}^k \left[ \frac{d^d p^{(j)}}{(2\pi)^d} \Phi(\vec{p}^{(j)}) \right] \sum_{L=0}^{\infty} \psi_k^{(L)} \right\}, \quad (3.25)$$

where  $\psi_k^{(L)}$  is a function of spatial momenta and can be represented by connected graphs with the same number of bulk-to-boundary propagators and loops. If  $\mathcal{G}_k^{(L)}$  is the set of all contributing connected graphs, then:

$$\psi_k^{(L)} = \sum_{\mathcal{G} \subset \mathcal{G}_k^{(L)}} \psi_{\mathcal{G}}, \quad (3.26)$$

where  $\psi_{\mathcal{G}}$  represents the contribution of a specific graph  $\mathcal{G}$ . Each graph is defined by sets of sites  $\mathcal{V}$ , edges  $\mathcal{E}$  connecting the sites and external lines connecting the sites to the late-time space-like boundary. The functional form of  $\psi_{\mathcal{G}}$  is given by:

$$\psi_{\mathcal{G}} = \delta^{(d)} \left( \sum_{j=1}^k \vec{p}_j \right) \int_{-\infty}^0 \prod_{v \in \mathcal{V}} [d\eta_v e^{iX_v \eta_v} \lambda_k(\eta_v)] \prod_{e \in \mathcal{E}} G(y_e, \eta_{v_e}, \eta_{v'_e}). \quad (3.27)$$

Here, the bulk-to-boundary propagators  $\phi_+ = e^{iX_v \eta_v}$  are associated with external lines, where  $X_v$  is the energy at vertex  $v$ . Since  $\psi_{\mathcal{G}}$  depends on the total energies at each vertex, we can represent the Feynman graph  $\mathcal{G}$  as a reduced Feynman graph by removing the external legs. The bulk-to-bulk propagators  $G(y_e, \eta_{v_e}, \eta_{v'_e})$  are associated with the edges connecting the interaction sites. The function at the vertex, in the polynomial interaction case, is just the time-dependent coupling  $\lambda_k(\eta)$ :  $V_v = \lambda_k(\eta_v)$ . The spatial momentum conserving  $\delta$ -function is the result of the integration over spatial coordinates, stemming from the assumption of space-translation invariance. For a graph  $\mathcal{G}$  with  $n_s$  sites and  $n_e$  edges, the related wavefunction contribution involves  $3^{n_e}$  terms due to the three-term expression in (3.24).

The wavefunction contains an integration over the conformal times for each vertex, thus it is convenient to Fourier transform the time-dependent coupling  $\lambda_k(\eta)$ :

$$\lambda_k(\eta) = \int_{-\infty}^{+\infty} dz e^{iz\eta} \tilde{\lambda}_k(z). \quad (3.28)$$

Consider a FRW spacetime where the warp factor<sup>2</sup> is  $a(\eta) = (-\eta)^{-\alpha}$ ,  $\alpha \geq 0$ ;  $\lambda_k(\eta)$  is given by

$$\lambda_k(\eta) = \lambda_k \cdot (-\eta)^{-\alpha(2+(2-k)(d-1)/2)} \theta(-\eta) = \lambda_k \cdot (-\eta)^{\gamma_k} \theta(-\eta), \quad (3.29)$$

where  $\gamma_k = \alpha(2 + (2 - k)(d - 1)/2)$ ,  $\lambda_k$  is a constant[11, 9]. For  $\gamma_k > 0$ , we have the following<sup>3</sup>,

$$\lambda_k(\eta) = \lambda_k \int_{-\infty}^{+\infty} dz e^{iz\eta} z^{\gamma_k-1} \theta(z). \quad (3.30)$$

Let us substitute the Fourier transform of the coupling (3.28) into (3.27):

$$\tilde{\psi}_{\mathcal{G}} = \delta^{(d)} \left( \sum_{j=1}^k \vec{p}_j \right) \prod_{v \in \mathcal{V}} \int_{-\infty}^{+\infty} dz_v \tilde{\lambda}_k(z_v) \int_{-\infty}^0 d\eta_v e^{i(X_v + z_v)\eta_v} \prod_{e \in \mathcal{E}} G(y_e, \eta_{v_e}, \eta_{v'_e}) \quad (3.31)$$

<sup>2</sup>For a more general treatment, refer to [9].

<sup>3</sup>For  $\gamma_k < 0$ ,  $\tilde{\psi}_{\mathcal{G}}$  can be obtained by acting with derivative operator on  $\psi_{\mathcal{G}}$ , refer to [11, 9].

where  $X_v$  is the total energy at vertex  $v$ . We perform the change of variable  $x_v = X_v + z_v$ , obtaining:

$$\tilde{\psi}_{\mathcal{G}} = \delta^{(d)} \left( \sum_{j=1}^k \vec{p}_j \right) \prod_{v \in \mathcal{V}} \int_{-\infty}^{+\infty} dx_v \tilde{\lambda}_k(x_v - X_v) \int_{-\infty}^0 d\eta_v e^{ix_v \eta_v} \prod_{e \in \mathcal{E}} G(y_e, \eta_{v_e}, \eta_{v'_e}). \quad (3.32)$$

We can rewrite the wavefunction as

$$\tilde{\psi}_{\mathcal{G}} = \delta^{(d)} \left( \sum_{j=1}^k \vec{p}_j \right) \int_{-\infty}^{+\infty} \prod_{v \in \mathcal{V}} [dx_v \tilde{\lambda}_k(x_v - X_v)] \psi_{\mathcal{G}}(x_v, y_e). \quad (3.33)$$

All of the details of the cosmology are contained into the function  $\tilde{\lambda}_k(x_v - X_v)$ , while  $\psi_{\mathcal{G}}(x_v, y_e)$  does not depend on the cosmology and, for this reason, it is referred to as universal integrand:

$$\psi_{\mathcal{G}} = \int_{-\infty}^0 \prod_{v \in \mathcal{V}} [d\eta_v e^{ix_v \eta_v}] \prod_{e \in \mathcal{E}} G(y_e; \eta_{v_e}, \eta_{v'_e}). \quad (3.34)$$

By performing the time integration, it is clear that the universal integrand is a rational function, which depends on the energies of the vertices  $x_v$  and contains only poles.

For the rest of this treatment, we will focus on conformally coupled scalars in FRW cosmology with a warp factor of the type  $a(\eta) = (-\eta)^{-\alpha}$ ,  $\alpha \in \mathbf{R}_+$  and  $\gamma_k \in \mathbf{Z}_+$ . In this case, the wavefunction is given by[11, 9]:

$$\tilde{\psi}_{\mathcal{G}} = \delta^{(d)} \left( \sum_{j=1}^k \vec{p}_j \right) \int_{-\infty}^{+\infty} \prod_{v \in \mathcal{V}} [dx_v \lambda_k \cdot (x_v - X_v)^{\gamma_k - 1} \vartheta(x_v - X_v)] \psi_{\mathcal{G}}(x_v, y_e). \quad (3.35)$$

For the integral reduction procedure proposed in this thesis, we limit the case to where  $\gamma_k$  is an integer. Consequently, the integral measure,  $\lambda_k \cdot (x_v - X_v)^{\gamma_k - 1}$ , does not contain any branch points. Moreover, we specifically consider the scenario where  $\gamma_k$  is a positive integer, ensuring no poles arise from the integral measure. The integral reduction procedure that we propose in this thesis requires that the integral measure does not contain branch points.

Let us now consider a lagrangian interaction term which contains derivatives of the field:

$$S_{\text{int}}[\phi_{\circ}, \varphi] = \int d^d x \int_{-\infty}^0 d\eta \lambda_k(\eta) V_k(\phi_{\circ}, \varphi, \partial_{\eta}, \partial_i). \quad (3.36)$$

The universal integrand will contain a vertex function  $V_v$  which will have in general a dependence on the derivatives of the field:

$$\psi_{\mathcal{G}} = \int_{-\infty}^0 \prod_{v \in \mathcal{V}} [d\eta_v e^{ix_v \eta_v} V_v] \prod_{e \in \mathcal{E}} G(y_e; \eta_{v_e}, \eta_{v'_e}). \quad (3.37)$$

In the perturbative regime we consider the following splitting of the scalar field:  $\phi = \phi_o + \varphi$ , where  $\phi_o$  is the classical solution and  $\varphi$  represents the quantum fluctuations. The derivatives of the interaction term acting on  $\phi_o$  correspond to derivatives of the bulk-to-boundary propagator. Since we are considering conformally coupled scalars in FRW spacetime, the bulk-to-boundary propagator in momentum space, including the spatial part, is given by:

$$\phi_+ = e^{iE\eta + i\vec{p}\cdot\vec{x}} \quad (3.38)$$

and its derivatives are straightforward

$$\begin{aligned} \partial_\eta^k \phi_+ &= (iE)^k \phi_+ \\ \partial_{\vec{x}}^k \phi_+ &= (i\vec{p})^k \phi_+. \end{aligned} \quad (3.39)$$

The derivatives acting on the fluctuations  $\varphi$  correspond to derivatives of the bulk-to-bulk propagator. In the case of spatial derivatives the calculation is straightforward:

$$\partial_{\vec{x}_1}^k G(\eta_1 - \eta_2, \vec{x}_1 - \vec{x}_2, y) = (i\vec{p})^k G(\eta_1 - \eta_2, \vec{x}_1 - \vec{x}_2, y). \quad (3.40)$$

In the case of time derivatives the calculation is more involved and it might lead to the appearance of boundary terms. In any case, no additional poles to the universal integrand come from derivatives of the field.

**Example** Consider a  $\phi^3$  theory in flat spacetime with a space-like boundary such that  $\eta \in ] -\infty, 0]$  and a time-independent interaction coupling  $\lambda$ :

$$S = - \int_{-\infty}^0 d\eta \int d^d x \left[ \frac{1}{2} (\partial\phi)^2 - \frac{\lambda}{3!} \phi^3 \right]. \quad (3.41)$$

In the perturbative regime, the field  $\phi$  is split into a classical part and quantum fluctuations:  $\phi = \phi_o + \varphi$ . The path integration involves only the quantum fluctuations. The action can be rewritten as in (3.13) and the perturbative wavefunction is given by (3.20).

The equation of motion for the classical field  $\phi_o$  is obtained by setting to zero the variation of the quadratic part of the action,

$$\delta S_2 = \delta \left( \int_{-\infty}^0 d\eta \int d^d x \frac{1}{2} (\partial\phi)^2 \right) = 0 \implies \square\phi_o = 0. \quad (3.42)$$

The solution to the equation of motion is given by (3.17). Let us consider the interacting part of the action:

$$S_{\text{int}} = \int_{-\infty}^0 d\eta \int d^3 x \frac{\lambda}{3!} (\phi_o + \varphi)^3. \quad (3.43)$$

Let us expand explicitly the perturbative wavefunction to the first and second order in the action:

$$\begin{aligned}\Psi_o[\Phi] &= \exp(iS_2[\Phi]) \sum_{j=0}^{\infty} \frac{i^j}{j!} \langle S_{\text{int}}^j \rangle[\Phi] \\ &= \exp(iS_2[\Phi]) \left( 1 + i\langle S_{\text{int}} \rangle + \frac{i^2}{2!} \langle S_{\text{int}}^2 \rangle + \dots \right).\end{aligned}\quad (3.44)$$

Recall that the only contributions to the wavefunction come from terms with an even number of fields  $\varphi$  due to the symmetry of the Gaussian path integral. The first order term is the path integrated action,

$$\langle S_{\text{int}} \rangle = \mathcal{N} \int_{\varphi(-\infty(1-i\varepsilon))=0}^{\varphi(0)=0} \mathcal{D}\varphi e^{iS_2[\varphi]} \int_{-\infty}^0 d\eta \int d^3x \frac{\lambda}{3!} (\phi_o + \varphi)^3. \quad (3.45)$$

The only contribution at tree-level is the contact graph which corresponds to the term  $\phi_o^3$ , in fact the term  $3\phi_o\varphi^2$  is a tadpole.

$$\begin{aligned}\langle S_{\text{contact}} \rangle &= \int_{-\infty}^0 d\eta \int d^3x \frac{\lambda}{3!} \phi_o^3 \\ &= \lambda \int_{-\infty}^0 d\eta \int \prod_{j=1}^3 \left[ \frac{d^3p_j}{(2\pi)^3} \tilde{\Phi}(\vec{p}_j) \right] \delta(\vec{p}_1 + \vec{p}_2 + \vec{p}_3) e^{i(E_1+E_2+E_3)\eta},\end{aligned}\quad (3.46)$$

where  $\phi_o$  was substituted by (3.17) and the integration in the position space variable  $\vec{x}$  returns a  $\delta$ -function which enforces the spatial momentum conservation, which reflects the invariance of the action under spatial translations.

Let us focus on the time integration. To ensure the convergence of the time integral, we shift the extreme of integration:

$$\eta = -\infty \rightarrow \eta = -\infty(1 - i\varepsilon). \quad (3.47)$$

This shift regularises the integral but violates unitarity. The same result is obtained by applying the  $i\varepsilon$  prescription on the energy[9]:

$$E \rightarrow E - i\varepsilon \implies e^{iE\eta} e^{\varepsilon\eta}. \quad (3.48)$$

In this manner, the integral converges for  $\eta \rightarrow -\infty$  and unitarity is not violated.

Finally, the time integration can be performed:

$$\langle S_{\text{contact}} \rangle = \lambda \int \prod_{j=1}^3 \left[ \frac{d^3p_j}{(2\pi)^3} \tilde{\Phi}(\vec{p}_j) \right] \delta(\vec{p}_1 + \vec{p}_2 + \vec{p}_3) \frac{1}{i(E_1 + E_2 + E_3)} \quad (3.49)$$

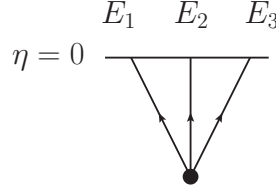
The wavefunction with the only contribution from the contact graph is given by:

$$\Psi_{\circ}[\Phi] = \exp(iS_2[\Phi]) \left( 1 + i\lambda \int \prod_{j=1}^3 \left[ \frac{d^3 p_j}{(2\pi)^3} \tilde{\Phi}(\vec{p}_j) \right] \delta(\vec{p}_1 + \vec{p}_2 + \vec{p}_3) \frac{1}{i(E_1 + E_2 + E_3)} \right). \quad (3.50)$$

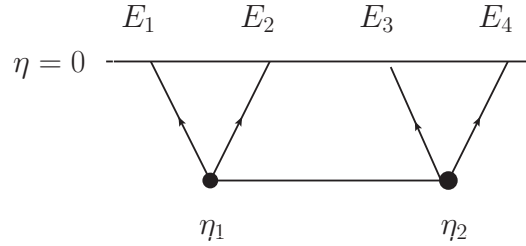
Conventionally the wavefunction is formulated as in (3.25), thus the contribution of the contact graph to the wavefunction reads:

$$\psi_{\text{contact}} = i\lambda \delta(\vec{p}_1 + \vec{p}_2 + \vec{p}_3) \frac{1}{i(E_1 + E_2 + E_3)}. \quad (3.51)$$

The associated Feynman diagram is:



Let us consider the contribution of second order in the action. Let us consider the following term without loops,  $[\phi_{\circ}^2(\eta_1, \vec{x}_1)\varphi(\eta_1, \vec{x}_1)][\phi_{\circ}^2(\eta_2, \vec{x}_2)\varphi(\eta_2, \vec{x}_2)]$ . The associated Feynman diagram  $\mathcal{G}$  is given by:



Let us start by computing the path integrated squared action:

$$\begin{aligned} \langle S_{\mathcal{G}}^2 \rangle &= \mathcal{N} \int_{\varphi(-\infty(1-i\varepsilon))=0}^{\varphi(0)=0} \mathcal{D}\varphi e^{iS_2[\varphi]} \int_{-\infty(1-i\varepsilon)}^0 d\eta_1 d\eta_2 \int d^3 x_1 d^3 x_2 \\ &\cdot \lambda^2 \varphi(\eta_1, \vec{x}_1)\varphi(\eta_2, \vec{x}_2) \int \left[ \prod_{j=1}^4 \frac{d^3 p_j}{(2\pi)^3} \tilde{\Phi}(\vec{p}_j) \right] e^{i(E_1+E_2)\eta_1 + i(E_3+E_4)\eta_2 + i(\vec{p}_1+\vec{p}_2)\vec{x}_1 + i(\vec{p}_3+\vec{p}_4)\vec{x}_2} \end{aligned}$$

Let us focus on the path integral which defines the bulk-to-bulk propagator  $G$ :

$$G(\eta_1, \eta_2; \vec{x}_1, \vec{x}_2) = \mathcal{N} \int_{\varphi(-\infty(1-i\varepsilon))=0}^{\varphi(0)=0} \mathcal{D}\varphi e^{iS_2[\varphi]} \varphi(\eta_1, \vec{x}_1) \varphi(\eta_2, \vec{x}_2). \quad (3.52)$$

The Gaussian path integral is proportional to the inverse of the differential operator associated to the quadratic action, in this case the flat space D'Alembert operator,

$$G \sim \frac{1}{\square}. \quad (3.53)$$

Since the fluctuations must vanish at the boundary, we impose the boundary conditions:

$$G(0, \eta_2) = 0, \quad G(\eta_1, 0) = 0. \quad (3.54)$$

Therefore, the bulk-to-bulk propagator is given by:

$$G(\eta_1 - \eta_2; \vec{x}_1 - \vec{x}_2; y) = \int \frac{d^3 p}{(2\pi)^3} e^{i\vec{p}(\vec{x}_1 - \vec{x}_2)} \frac{1}{2y} \left[ e^{-iy(\eta_1 - \eta_2)} \vartheta(\eta_1 - \eta_2) + e^{iy(\eta_1 - \eta_2)} \vartheta(\eta_2 - \eta_1) - e^{iy(\eta_1 + \eta_2)} \right]. \quad (3.55)$$

Let us focus again on the computation of  $\langle S_{\mathcal{G}}^2 \rangle$  and substitute the expression for the bulk-to-bulk propagator,

$$\langle S_{\mathcal{G}}^2 \rangle = \lambda^2 \int_{-\infty(1-i\varepsilon)}^0 d\eta_1 d\eta_2 \cdot \int \left[ \prod_{j=1}^4 \frac{d^3 p_j}{(2\pi)^3} \tilde{\Phi}(\vec{p}_j) \right] \cdot \delta(\vec{p}_1 + \vec{p}_2 + \vec{p}_3 + \vec{p}_4) G(\eta_1 - \eta_2; y) e^{i(E_1 + E_2)\eta_1 + i(E_3 + E_4)\eta_2}. \quad (3.56)$$

The contribution to the wavefunction coming from the graph  $\mathcal{G}$  is given by:

$$\psi_{\mathcal{G}} = \lambda^2 \frac{\delta(\vec{p}_1 + \vec{p}_2 + \vec{p}_3 + \vec{p}_4)}{(x_1 + y)(x_2 + y)(x_1 + x_2)}, \quad (3.57)$$

where  $x_1 = E_1 + E_2$ ,  $x_2 = E_3 + E_4$ .

### 3.3 Recursive relation for the universal integrand

Let us assume a theory where the lagrangian interaction term does not contain time derivatives of the fields and, thus, the function at each vertex  $V_v$  of the universal integrand

does not depend on time derivatives of the field. The universal integrand  $\psi_{\mathcal{G}}$  associated to a generic graph  $\mathcal{G}$  is, thus, given by

$$\psi_{\mathcal{G}} = \int_{-\infty}^0 \prod_{v \in \mathcal{V}} [d\eta_v e^{ix_v \eta_v} V_v] \prod_{e \in \mathcal{E}} G(y_e; \eta_{v_e}, \eta_{v'_e}) \quad (3.58)$$

where  $\mathcal{V}$  and  $\mathcal{E}$  are respectively the set of sites and of internal edges and the vertex function  $V_v$  does not depend on time derivatives of the field.

We will now show the derivation a useful recursive relation that let us identify easily the physical poles of the universal integrand[9]. Let us define the total time-translation operator as

$$\hat{\Delta} = -i \sum_{v \in \mathcal{V}} \partial_{\eta_v}. \quad (3.59)$$

If we act with it on the universal integral  $\psi_{\mathcal{G}}$  it returns zero: infinitely away from the boundary the modes are exponentially suppressed, while on the boundary the bulk-to-bulk propagator is zero,

$$0 = \hat{\Delta} \psi_{\mathcal{G}} = \int_{-\infty}^0 \hat{\Delta} \left\{ \prod_{v \in \mathcal{V}} [d\eta_v e^{ix_v \eta_v} V_v] \right\} \prod_{e \in \mathcal{E}} G(y_e; \eta_{v_e}, \eta_{v'_e}) + \int_{-\infty}^0 \prod_{v \in \mathcal{V}} [d\eta_v e^{ix_v \eta_v} V_v] \hat{\Delta} \left\{ \prod_{e \in \mathcal{E}} G(y_e; \eta_{v_e}, \eta_{v'_e}) \right\}. \quad (3.60)$$

When the operator acts on the external states it returns the sum of the energies. When it acts on each propagator, only the boundary term survives and the latter shifts the external energies of the corresponding external states by the energy  $+y_{\ell}$  flowing in the propagator. Overall, it returns a sum over the internal edges, where each term corresponds to erasing one edge and shifting the energies of the external states at its endpoints. We obtain the following relation:

$$\left( \sum_{v \in \mathcal{V}} x_v \right) \psi_{\mathcal{G}} = \sum_{\ell \in \mathcal{E}} \int_{-\infty}^0 \prod_{v \in \tilde{\mathcal{V}}} [d\eta_v e^{ix_v \eta_v} V_v] e^{i(x_{v_{\ell}} + y_{\ell}) \eta_{v_{\ell}}} e^{i(x_{v'_{\ell}} + y_{\ell}) \eta_{v'_{\ell}}} \prod_{e \in \mathcal{E} \setminus \{\ell\}} G(y_e; \eta_{v_e}, \eta_{v'_e}). \quad (3.61)$$

Graphically,

$$\left( \sum_{v \in \mathcal{V}} x_v \right) \psi_{\mathcal{G}} = \sum_{\ell \in \mathcal{E}} \psi_{\mathcal{L}} \overset{\bullet}{\text{---}} \overset{\bullet}{\text{---}} \psi_{\mathcal{R}} + \sum_{\ell \in \mathcal{E}} \psi_{\mathcal{G}'} \quad (3.62)$$

where the dashed red edges indicate the edges that get erased and the blobs represent the wavefunction associated to the subgraphs which the original graph reduces to upon the edge deletion.

This relation can be used recursively and it generates a representation of the wavefunctions with  $n_e!$  terms consisting of only physical poles.

It is important to emphasize that this relation is valid when considering universal integrands with vertex functions  $V_v$  which do not contain time derivatives, otherwise, in general, the total time translation operator acting on the universal integrand would not be zero.

**Example of the recursive relation** Let us apply the recursive relation for a bubble graph. We can split the loop into two 2-vertex graphs:

$$(x_1 + x_2) \begin{array}{c} \text{---} y_{12} \text{---} \\ \bullet \quad \bullet \\ \text{---} y_{21} \text{---} \\ x_1 \quad x_2 \end{array} = \begin{array}{c} \text{---} y_{12} \text{---} \\ \bullet \quad \bullet \\ x_1 + y_{21} \quad x_2 + y_{21} \end{array} + \begin{array}{c} x_1 + y_{12} \quad x_2 + y_{12} \\ \bullet \quad \bullet \\ \text{---} y_{21} \text{---} \end{array} \quad (3.63)$$

Using this relation, we are able to find a representation of loop graphs in terms of tree-level graphs, which are much simpler to deal with. Notice that we do not draw the external legs of the graphs, as they are reduced Feynman graphs.

### 3.4 Singularities of the Bunch-Davies wavefunction

In this section, we discuss the singularities of the Bunch-Davies wavefunction for a single Feynman graph, in the context of the scalar toy model in FRW cosmology, that we have defined in the previous section. For a more general treatment, refer to [9].

Considering the Bunch-Davies wavefunction for a graph  $\mathcal{G}$ , (3.35), we have denoted it as  $\tilde{\psi}_{\mathcal{G}}$  to distinguish it from  $\psi_{\mathcal{G}}$ , which we reserve for the universal integrand (3.37).

The singularities of the Bunch-Davies wavefunction  $\tilde{\psi}_{\mathcal{G}}$  are located at the poles of the universal integrand  $\psi_{\mathcal{G}}$ .

Since we restrict to the case where the parameter  $\gamma_k$  of the integral measure (3.29) is a positive integer, no poles or branch points come from the integral measure. Therefore, all the singularities of the Bunch-Davies wavefunction arise from the poles of the universal integrand.

We have chosen the Bunch-Davies vacuum state as the initial state for the vacuum wavefunction. The Bunch-Davies condition on the vacuum selects the modes with positive energy and such that they vanish at early times, i.e.  $\phi_+ \xrightarrow{\eta \rightarrow -\infty} e^{iE\eta}$ .

The Bunch-Davies condition implies that the physical region of the kinematical space is defined by all the energies being positive:

$$\{E_j \geq 0 \mid j = 1, \dots, n\} \text{ and } \left\{ y_{\mathcal{I}} := \left| \sum_{k \in \mathcal{I}} \vec{p}_k \right| \geq 0, \mid \forall \mathcal{I} \subset \{1, \dots, n\} \right\}. \quad (3.64)$$

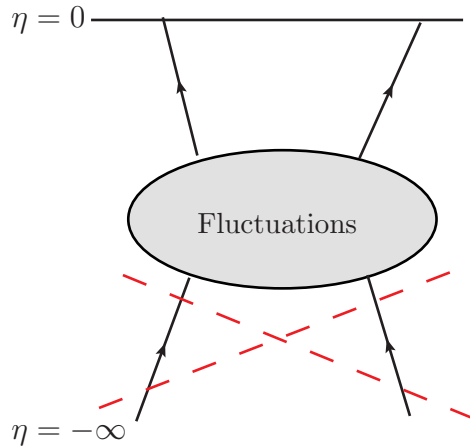


Figure 3.1: The Feynman diagrams satisfying the Bunch-Davies condition do not have external legs at early times and have only external legs corresponding to outgoing particles. Particle decay is prohibited at early times, allowing only quantum fluctuations. The theory of inflation predicts that these fluctuations are at the origin of all the cosmic structures [23].

Therefore the poles of the universal integrand are of the form:

$$\sum_j E_j + \sum_k y_k = 0. \quad (3.65)$$

This sheet in kinematic space can be reached, in the physical region, only if all the energies  $E_j$ 's and  $y_k$ 's all vanish. We refer to these combinations of energies as partial energies.

The absence of particle decay in the physical region is realized by the requiring that, in such region, we can only reach the singularities of the wavefunction in a trivial way, i.e. vanishing of all the energies.

It is possible to perform an analytic continuation such that some energies become negative and other stay positive and hence we can reach these sheets for non-zero external and internal energies. In these sheets, which are outside the physical region, the wavefunction can develop singularities. Approaching such singularities, the wavefunction factorizes into flat space amplitudes and simpler wavefunctions[9].

**Total energy singularity and flat space limit** Let us consider the time-integral representation of the wavefunction  $\tilde{\psi}_{\mathcal{G}}$  given by (3.27). Recall that for  $\eta \rightarrow -\infty(1 - i\epsilon)$  the mode functions are exponentially suppressed, (3.15). Let us define a “center-of-mass” time  $\bar{\eta}$ . Taking the early time limit of the “center-of-mass” time,  $\bar{\eta} \rightarrow -\infty(1 - i\epsilon)$ , is

equivalent to simultaneously taking the early time limit of every time  $\eta_v$  associated to each vertex  $v$ . In this limit  $\psi_{\mathcal{G}}$  takes the form[9]:

$$\psi_{\mathcal{G}} \sim \int_{-\infty(1-i\varepsilon)}^1 d\bar{\eta} f(\bar{\eta}) e^{iE_{\text{tot}}\bar{\eta}} \psi'_{\mathcal{G}}, \quad (3.66)$$

where  $f(\bar{\eta})$  is a function which depends on the cosmology and  $\psi'_{\mathcal{G}}$  is the part of the wavefunction obtained by the change of variable and can be expressed in terms of time integrals other than the “center-of-mass” time.

Due to the asymptotic behavior of the modes at early times, taking the early time limit of the “center-of-mass” time, ensures that the wavefunction gets a non-trivial contribution only for  $E_{\text{tot}} = 0$ . At that point the integral diverges.

From a physical point of view, shifting the “center-of-mass” time to early times means moving the entire process to an infinite distance from the space-like boundary at  $\eta = 0$ . By performing an analytic continuation of the energies, it is possible to reach the sheet where  $E_{\text{tot}} = 0$ . As the total energy approaches zero, certain states can be designated as in-states, while others as out-states and energy conservation is restored. In this scenario, the conditions reflect those of a flat-space scattering process.

**Example of total energy singularity** Let us consider the wavefunction contribution of the 2-vertex graph in flat space-time with a space-like boundary,

$$\begin{aligned} \psi_{\mathcal{G}} = \int_{-\infty(1-i\varepsilon)}^0 d\eta_1 d\eta_2 \frac{1}{2y} & \left[ e^{i(x_1-y)\eta_1} e^{i(x_2+y)\eta_2} \vartheta(\eta_1 - \eta_2) + \right. \\ & \left. + e^{i(x_1+y)\eta_1} e^{i(x_2-y)\eta_2} \vartheta(\eta_2 - \eta_1) - e^{i(x_1+y)\eta_1 + i(x_2+y)\eta_2} \right]. \end{aligned} \quad (3.67)$$

Let us perform the following change of variables,

$$\begin{aligned} \bar{\eta} &= \frac{1}{2}(\eta_1 + \eta_2) \\ \tilde{\eta} &= \frac{1}{2}(\eta_1 - \eta_2) \end{aligned} \quad (3.68)$$

where  $\bar{\eta}$  is the “center-of-mass” time.  $\psi_{\mathcal{G}}$  takes the form,

$$\psi_{\mathcal{G}} = \int_{-\infty}^0 d\bar{\eta} e^{i(x_1+x_2)\bar{\eta}} \int_{-\infty}^{+\infty} d\tilde{\eta} \frac{1}{2y} (e^{-i2y\tilde{\eta}} \vartheta(\tilde{\eta}) + e^{+i2y\tilde{\eta}} \vartheta(-\tilde{\eta}) - e^{i2y\bar{\eta}}) \cdot e^{i(x_1-x_2)\tilde{\eta}}. \quad (3.69)$$

Let us consider the limit  $\bar{\eta} \rightarrow -\infty(1-i\varepsilon)$ :

$$\begin{aligned} \lim_{\bar{\eta} \rightarrow -\infty(1-i\varepsilon)} \psi_{\mathcal{G}} &= \lim_{\bar{\eta} \rightarrow -\infty(1-i\varepsilon)} \left( \int_{-\infty}^0 d\bar{\eta} e^{i(x_1+x_2)\bar{\eta}} \right) \times \\ &\times \int_{-\infty}^{+\infty} d\tilde{\eta} \frac{1}{2y} (e^{-i2y\tilde{\eta}} \vartheta(\tilde{\eta}) + e^{+i2y\tilde{\eta}} \vartheta(-\tilde{\eta})) \cdot e^{i(x_1-x_2)\tilde{\eta}} \end{aligned} \quad (3.70)$$

In the limit  $\bar{\eta} \rightarrow -\infty(1 - i\varepsilon)$ , the integral in the variable  $\bar{\eta}$  gets a non-trivial contribution only at the point  $E_{\text{tot}} = x_1 + x_2 = 0$ . At this point, where  $x_1 = -x_2$ , one state is the in-state, and the other is the out-state. Moreover, the propagator's boundary term vanishes, transforming it into a Feynman propagator in flat space. From a physical point of view, we are moving the process infinitely far away from the boundary.

It is important to emphasize that as we approach the singularity, the wavefunction factorizes into a singularity and a flat space amplitude.

**Partial energy singularity and factorization** The discussion is similar to the previous one, but in this case energy conservation is imposed only on a subprocess[9].

Let  $\mathcal{L}$  and  $\mathcal{R}$  be two sets of external states such that  $\mathcal{L} \cup \mathcal{R} = \{1, \dots, n\}$ . We are interested in studying the behaviour of the Bunch-Davies wavefunction when  $E_{\text{tot}}^{\mathcal{L}} := E_{\mathcal{L}} + \sum_{e \in \mathcal{E}} y_e$  is taken to zero,  $E_{\mathcal{L}}$  and  $\mathcal{E} \subset \mathcal{E}$  being respectively the sum of all the energies of the external states in the subset  $\mathcal{L}$  and a subset of the internal states that connect the two subprocesses.

Let us reformulate the general wavefunction (3.27) into the two subprocesses  $\mathcal{L}$  and  $\mathcal{R}$ :

$$\begin{aligned} \psi_{\mathcal{G}} = & \int \prod_{e \in \mathcal{E}} \frac{d^d q_e}{(2\pi)^d} \left[ \int_{-\infty}^0 \prod_{v_{\mathcal{L}} \in \mathcal{V}_{\mathcal{L}}} [d\eta_{v_{\mathcal{L}}} e^{iX_{v_{\mathcal{L}}} \eta_{v_{\mathcal{L}}} V_{v_{\mathcal{L}}}}] \prod_{e_{\mathcal{L}} \in \mathcal{E}_{\mathcal{L}}} G(y_{e_{\mathcal{L}}}; \eta_{v_{\mathcal{L}}}, \eta_{v'_{\mathcal{L}}}) \right] \times \\ & \times \left[ \int_{-\infty}^0 \prod_{v_{\mathcal{R}} \in \mathcal{V}_{\mathcal{R}}} [d\eta_{v_{\mathcal{R}}} e^{iX_{v_{\mathcal{R}}} \eta_{v_{\mathcal{R}}} V_{v_{\mathcal{R}}}}] \prod_{e_{\mathcal{R}} \in \mathcal{E}_{\mathcal{R}}} G(y_{e_{\mathcal{R}}}; \eta_{v_{\mathcal{R}}}, \eta_{v'_{\mathcal{R}}}) \right] \times \\ & \times \prod_{\ell \in \mathcal{E}} G(y_{\ell}; \eta_{v_{\mathcal{L}\ell}}, \eta_{v'_{\mathcal{R}\ell}}) \end{aligned} \quad (3.71)$$

where  $\vec{q}_e$  is the momentum flowing the edge  $e \in \mathcal{E} = \mathcal{E}_{\mathcal{L}} \cup \mathcal{E}_{\mathcal{R}} \cup \mathcal{E}$ , with the relevant momentum conserving delta-functions left implicit. The propagators in the last line connect the two subsets  $\mathcal{L}$  and  $\mathcal{R}$ .

We impose energy conservation on the subprocess  $\mathcal{L}$  by taking the limit  $E_{\text{tot}}^{\mathcal{L}} \rightarrow 0$ . Let us see what happens to (3.71) piece by piece. Starting from the  $\mathcal{L}$  subprocess in first line of (3.71), we impose the total energy conservation on this subprocess by defining a "center-of-mass" time  $\bar{\eta}_{\mathcal{L}}$  and taking the limit  $\bar{\eta}_{\mathcal{L}} \rightarrow -\infty(1 - i\varepsilon)$ . Consider the bulk-to-bulk propagator of the  $\mathcal{L}$  subprocess. Taking the limit  $\bar{\eta}_{v_{\mathcal{L}}} \rightarrow -\infty(1 - i\varepsilon)$  means simultaneously taking the two limits:  $\eta_{v_{\mathcal{L}}} \rightarrow -\infty(1 - i\varepsilon)$  and  $\eta_{v'_{\mathcal{L}}} \rightarrow -\infty(1 - i\varepsilon)$ , therefore the boundary term is exponentially suppressed and we obtain a flat space Feynman propagator:

$$\lim_{\eta_{v_{\mathcal{L}}}, \eta_{v'_{\mathcal{L}}} \rightarrow -\infty(1-i\varepsilon)} G(y_e; \eta_{v_{\mathcal{L}}}, \eta_{v'_{\mathcal{L}}}) \sim \frac{1}{2y_e} \left[ e^{-iy_e(\eta_{v_{\mathcal{L}}} - \eta_{v'_{\mathcal{L}}})} \vartheta(\eta_{v_{\mathcal{L}}} - \eta_{v'_{\mathcal{L}}}) + e^{iy_e(\eta_{v_{\mathcal{L}}} - \eta_{v'_{\mathcal{L}}})} \vartheta(\eta_{v'_{\mathcal{L}}} - \eta_{v_{\mathcal{L}}}) \right]. \quad (3.72)$$

Let us now focus on the propagators which connect the two subprocesses. The propagator  $G(y_{\ell}; \eta_{v_{\mathcal{L}_{\ell}}}, \eta_{v'_{\mathcal{R}_{\ell}}})$  in the limit  $\eta_{v_{\mathcal{L}_{\ell}}} \rightarrow -\infty(1-i\varepsilon)$  returns a linear combinations of bulk-to-boundary propagators for the same state which differ by the sign of the energy:

$$\lim_{\eta_{\mathcal{L}_{\ell}} \rightarrow -\infty(1-i\varepsilon)} G(y_{\ell}; \eta_{v_{\mathcal{L}_{\ell}}}, \eta_{v'_{\mathcal{R}_{\ell}}}) \sim \frac{e^{iy_{\ell}\eta_{\mathcal{L}_{\ell}}}}{2y_{\ell}} \left[ e^{-iy_{\ell}\eta_{v'_{\mathcal{R}_{\ell}}}} - e^{iy_{\ell}\eta_{v'_{\mathcal{R}_{\ell}}}} \right]. \quad (3.73)$$

In conclusion, by imposing energy conservation on the subprocess  $\mathcal{L}$ , the wavefunction factorizes as follows:

$$\psi_G \sim \left( \int_{-\infty(1-i\varepsilon)} d\bar{\eta}_{\mathcal{L}} f_{\mathcal{L}}(\bar{\eta}_{\mathcal{L}}) e^{iE_{\text{tot}}^{(\mathcal{L})}\bar{\eta}_{\mathcal{L}}} \right) \times \mathcal{A}(\mathcal{L}, \mathcal{E}) \times \sum_{\{\sigma_{\ell}\}=\{\mp 1\}} \frac{\psi(\mathcal{E}(\sigma_{\ell}), \mathcal{R})}{2y_{\ell}}, \quad (3.74)$$

where the first term in parenthesis represents the singularity and it is non vanishing if and only if  $E_{\text{tot}}^{\mathcal{L}} \rightarrow 0$ ,  $\mathcal{A}(\mathcal{L}, \mathcal{E})$  is the flat space amplitude with external states given by  $\mathcal{L} \cup \mathcal{E}$ ,  $\psi(\mathcal{E}(\sigma_{\ell}), \mathcal{R})$  is the wavefunction with external states given by the set  $\mathcal{E} \cup \mathcal{R}$  and  $\sigma_{\ell}$  is the sign of the energy  $y_{\ell}$  of the state  $\ell \in \mathcal{E}$ .

**Example of partial energy singularity** Let us consider the wavefunction contribution of the 2-vertex graph in flat space-time with a space-like boundary,

$$\psi_G = \int_{-\infty(1-i\varepsilon)}^0 d\eta_1 d\eta_2 e^{ix_1\eta_1} e^{ix_2\eta_2} G(y; \eta_1 - \eta_2). \quad (3.75)$$

The subprocess containing the vertex  $x_1$  is the  $\mathcal{L}$  subprocess and the subprocess containing the vertex  $x_2$  is the  $\mathcal{R}$  subprocess.  $G(\eta_1 - \eta_2, y)$  is the bulk-to-bulk propagator connecting the two subprocesses.

Let us consider the limit  $\eta_1 \rightarrow -\infty(1-i\varepsilon)$ :

$$\lim_{\eta_1 \rightarrow -\infty(1-i\varepsilon)} \psi_G = \lim_{\eta_1 \rightarrow -\infty(1-i\varepsilon)} \left( \int_{-\infty(1-i\varepsilon)}^0 d\eta_1 e^{i(x_1+y)\eta_1} \int_{-\infty(1-i\varepsilon)}^0 d\eta_2 \frac{1}{2y} \left[ e^{i(x_2-y)\eta_2} - e^{i(x_2+y)\eta_2} \right] \right). \quad (3.76)$$

In the limit  $\eta_1 \rightarrow -\infty(1 - i\varepsilon)$ , the first term in the parenthesis is non-vanishing only when energy conservation is imposed on the subprocess  $\mathcal{L}$ , at which point it diverges.

The wavefunction factorizes into: a singularity for  $x_1 + y = 0$ , the flat space amplitude corresponding to the  $\mathcal{L}$  subprocess, which in this simple case is equal to 1, and a linear combination of the wavefunctions for the  $\mathcal{R}$  subprocess with the external state connecting to the  $\mathcal{L}$  subprocess shifted by minus and plus the energy  $y$  flowing in the propagator.

# Chapter 4

## Integral reduction for the Bunch-Davies wavefunction

In this chapter, we develop a systematic way to expand the Bunch-Davies wavefunction at tree-level and 1-loop in an integral basis where each integral term is determined by the singularity structure of a given process and the coefficients are determined by the wavefunction factorization conditions.

We begin by exploring the singularities of the Bunch-Davies wavefunction with higher codimension. We establish a correspondence between subgraphs of the Feynman graph representing the wavefunction and singularities of the wavefunction. Subsequently, we develop the algorithm for integral reduction, initially focusing on the tree-level case and later extending our approach to the 1-loop case.

### 4.1 Singularities and subgraphs

In the previous chapter, we have shown that the Bunch-Davies wavefunction is singular where energy conservation of a subprocess or the total process is imposed and factorizes approaching such singularities.

If we impose one energy constraint, the Bunch-Davies wavefunction factorizes into a codimension-1 singularity and a factorized wavefunction given by the factorization rules in section (3.4).

We can impose more energy constraints and factorize the wavefunction further, leading to higher codimension singularities. The codimension of the singularity is equal to the number of energy constraints.

Consider the Bunch-Davies wavefunction for a given process  $\mathcal{G}$ . An energy constraint can be represented by a subgraph of the Feynman graph  $\mathcal{G}$ . Such constraint is realized by setting the energy of the subgraph to zero.

The energy of a subgraph  $g$  is given by the sum of the energies of its vertices and the

internal energies flowing in the propagators that connect to its complementary subgraph:

$$E_g = \sum_{v \in \mathcal{V}_g} x_v + \sum_{e \in \mathcal{E}} y_e \quad (4.1)$$

where  $\mathcal{V}_g$  is the set of vertices inside the subgraph  $g$ ,  $\mathcal{E}$  is the set of the subgraph edges that connect the subprocess  $g$  with its complementary subgraph  $\bar{g}$ ,  $y_e$  is the energy flowing in the propagator of edge  $e$ .

There is 1-1 correspondence between sets of subgraphs taken on the graph  $\mathcal{G}$  and singularities. Therefore, we employ the subgraphs to study the analytic structure of the Bunch-Davies wavefunction for a given Feynman graph  $\mathcal{G}$ .

The vertices of a graph are labelled by the natural numbers and the edges are labelled by the two vertices at their extremes. In the case of a loop graph, the labels of the edges are assigned in clockwise direction. A given general graph is referred to as  $\mathcal{G}$ . A subgraph is referred to as  $g(\mathbf{v})$ , where  $\mathbf{v} = (1, 2, \dots)$  is the list of the internal vertices separated by a comma. For loop graphs, the order of the vertices is important: they have to be ordered following the loop direction, which is clockwise. The subgraph containing the entire graph is referred to as  $g(\mathcal{G})$ .

Let us consider the following subgraphs with the associated singularities:

$$g(1) = \begin{array}{c} \textcircled{\blacksquare} \xrightarrow{y_{12}} \blacksquare \\ x_1 \quad x_2 \end{array} \rightarrow \text{Sing}\{(x_1 + y) \rightarrow 0\} \quad (4.2)$$

$$g(1)g(\mathcal{G}) = \begin{array}{c} \textcircled{\textcircled{\blacksquare}} \xrightarrow{y_{12}} \blacksquare \\ x_1 \quad x_2 \end{array} \rightarrow \text{Sing}\{(x_1 + y) \rightarrow 0, (x_1 + x_2) \rightarrow 0\}. \quad (4.3)$$

$$g(1) = \begin{array}{c} \textcircled{\blacksquare} \quad \textcircled{\blacksquare} \\ \textcircled{\curvearrowright} \\ x_1 \quad x_2 \\ y_{21} \end{array} \xrightarrow{y_{12}} \rightarrow \text{Sing}\{(x_1 + y_{12} + y_{21}) \rightarrow 0\} \quad (4.4)$$

$$g(1)g(1, 2) = \begin{array}{c} \textcircled{\textcircled{\blacksquare}} \quad \textcircled{\textcircled{\blacksquare}} \\ \textcircled{\curvearrowright} \quad \textcircled{\curvearrowright} \\ x_1 \quad x_2 \\ y_{21} \end{array} \xrightarrow{y_{12}} \rightarrow \text{Sing}\{(x_1 + y_{12} + y_{21}) \rightarrow 0, (x_1 + x_2 + 2y_{21}) \rightarrow 0\} \quad (4.5)$$

These Feynman graphs are reduced, as we do not draw the external legs.

We refer to a set of subgraphs as  $\mathfrak{g}^d$ , where  $d$  is the cardinality of the set <sup>1</sup>. A set of subgraphs  $\mathfrak{g}^d$  is in correspondence to a singularity of codimension  $d$ . For instance,  $\mathfrak{g}^2 = \{g(1), g(1, 2)\}$  is a set containing 2 subgraphs and the associated singularity is codimension-2.

---

<sup>1</sup>In this chapter,  $d$  is the cardinality of the set of subgraphs  $\mathfrak{g}^d$ . It is not the dimension of the spacetime.

### 4.1.1 Toy model

In the previous chapter we have chosen a toy model described an action containing conformally coupled scalars in FRW cosmology with a warp factor of the type  $a(\eta) = (-\eta)^{-\alpha}$ ,  $\alpha \in \mathbf{R}_+$  and  $\gamma_k \in \mathbf{Z}_+$ . In this case the information on the cosmology can be extracted from the wavefunction by integrating on the external energies, leading to the following expression for the tree-level case:

$$\tilde{\psi}_{\mathcal{G}} = \int_{X_v}^{+\infty} \prod_{v \in \mathcal{V}} [dx_v \lambda_k \cdot (x_v - X_v)^{\gamma_k - 1}] \psi_{\mathcal{G}}(x_v, y_e), \quad (4.6)$$

where  $\mathcal{V}$  is the set of vertices. The internal energies  $y_e$  are fixed by the external momenta and are strictly positive  $y_e > 0$ .

We will refer to the full integrand including the measure as  $\bar{\psi}_{\mathcal{G}}$ :

$$\bar{\psi}_{\mathcal{G}} = \prod_{v \in \mathcal{V}} [\lambda_k \cdot (x_v - X_v)^{\gamma_k - 1}] \psi_{\mathcal{G}}(x_v, y_e). \quad (4.7)$$

$\psi_{\mathcal{G}}(x_v, y_e)$  is the universal integrand and it is a rational function which contains only simple poles and encodes the singularity structure of the Bunch-Davies wavefunction.

We restrict to the case where  $\gamma_k$  is a positive integer, thus no poles or branch points come from the integral measure. Moreover, no additional poles come from eventual derivative couplings. Therefore, all the poles are contained in the universal integrand.

In kinematical space, the singularities are located where we impose energy conservation constraints on a subprocess or the total process. When approaching a singularity of codimension  $d$  the Bunch-Davies wavefunction factorizes into a singularity of the same codimension and a factorized wavefunction. This factorized wavefunction is computed by taking  $d$  residues, enforcing energy conservation, on the wavefunction integrand  $\bar{\psi}_{\mathcal{G}}$ .

The factorized wavefunction and the associated singularity are identified by a set of subgraphs  $\mathbf{g}^d = \{g_1, \dots, g_i, \dots, g_d\}$  defining the energy constraints. This factorized wavefunction is given by:

$$\tilde{\psi}_{\mathbf{g}^d} = \int_{X_v}^{\infty} \prod_{v \in \mathcal{V}'} [dx_v] \text{Res}_{\mathbf{g}^d} \bar{\psi}_{\mathcal{G}}. \quad (4.8)$$

Here,  $\text{Res}_{\mathbf{g}^d} \equiv \text{Res}_{E_1 \rightarrow 0} \dots \text{Res}_{E_i \rightarrow 0} \dots \text{Res}_{E_d \rightarrow 0}$ , where  $E_i$  is the energy of the subgraph  $g_i \in \mathbf{g}^d$ . Therefore,  $\text{Res}_{\mathbf{g}^d}$  means taking  $d$  residues imposing energy conservation.

$\mathcal{V}'$  is the set of  $n_s - d$  integral variables left, where  $n_s$  is the number of vertices of the graph  $\mathcal{G}$  and  $d$  is the cardinality the set  $\mathbf{g}^d$ .

The residue of the wavefunction integrand can be computed by substituting the appropriate singularities in the wavefunction  $\tilde{\psi}_{\mathcal{G}}$  with  $\delta$ -functions enforcing energy conservation and performing the integration, thus every residue removes one integration variable.

Since the wavefunction  $\tilde{\psi}_{\mathcal{G}}$  is an integral function where the energy  $x_v$  associated to each vertex is an integration variable, we can impose at most  $n_s$  energy constraints (residues). Consider the 2-vertex graph example:

$$\tilde{\psi}_{\mathcal{G}} = \int_{X_1}^{+\infty} dx_1 \lambda \cdot (x_1 - X_1)^{\gamma-1} \int_{X_2}^{+\infty} dx_2 \lambda \cdot (x_2 - X_2)^{\gamma-1} \frac{1}{(x_1 + x_2)(x_1 + y)(x_2 + y)}. \quad (4.9)$$

The wavefunction obtained by performing the residue corresponding to the subgraph

$$g(1) = \begin{array}{c} \textcircled{\blacksquare} \xrightarrow{y} \blacksquare \\ x_1 \quad x_2 \end{array} \quad \text{is}$$

$$\begin{aligned} \tilde{\psi}_{g(1)} &= \int_{X_1}^{+\infty} dx_1 \lambda \cdot (x_1 - X_1)^{\gamma-1} \int_{X_2}^{+\infty} dx_2 \lambda \cdot (x_2 - X_2)^{\gamma-1} \frac{1}{(x_1 + x_2)(x_2 + y)} \delta(x_1 + y) \\ &= \int_{X_2}^{+\infty} dx_2 \lambda \cdot (-y - X_1)^{\gamma-1} \lambda \cdot (x_2 - X_2)^{\gamma-1} \frac{1}{(-y + x_2)(x_2 + y)}. \end{aligned} \quad (4.10)$$

### 4.1.2 Compatible subgraphs

Consider the wavefunction given by eq. (4.8), computed by taking  $d$  residues, enforcing energy conservation, on the wavefunction integrand  $\tilde{\psi}_{\mathcal{G}}$ . If such wavefunction,  $\tilde{\psi}_{\mathfrak{g}^d}$ , is zero for every order in which the residues are taken, then the set of subgraphs  $\mathfrak{g}^d$  is incompatible. When performing a sequential set of residues, we have to pay attention to the order. We must not take incompatible residues sequentially, otherwise we get a null amplitude.

If we let the internal energies  $y_e$  be non-negative, the compatibility rules for subgraphs are derived in [9]. In the tree-level case, the internal energies  $y_e$  must be strictly positive, so the compatibility of each set of subgraphs must be checked case by case.

We refer to set of all the compatible sets of  $d$  subgraphs as  $\mathfrak{G}^d$ . The elements of  $\mathfrak{G}^d$  are  $\mathfrak{g}_i^d$  where  $i \in [1, |\mathfrak{G}^d|]$ . The cardinality of  $\mathfrak{G}^d$  depends on the specific process  $\mathcal{G}$ .

## 4.2 Tree-level reduction

In order to perform the integral reduction for the Bunch-Davies wavefunction, we exploit its analytic structure. In analogy with the flat-space integral reduction, we require that the discontinuities of the wavefunction must match the discontinuities of the integral basis.

As we have seen in the flat-space integral reduction, taking residues of the wavefunction integrand corresponds to computing the discontinuities of the wavefunction integral. In fact, a discontinuity of codimension- $d$  is computed by taking  $d$  residues on the wavefunction integrand and corresponds to a specific set of subgraphs  $\mathfrak{g}_i^d \in \mathfrak{G}^d$ .

First, we are going to define an integral basis which captures the singularity structure of the Bunch-Davies wavefunction, which is encoded in the universal integrand. Second, we are going to match the discontinuities for every singularity to obtain the coefficients of the basis in terms of simpler wavefunctions and flat-space amplitudes.

### 4.2.1 Wavefunction integral basis

We exploit the 1-1 correspondence between singularities of the wavefunction and subgraphs to construct the integral basis. Each term of the integral basis corresponds to a set of subgraphs.

For a given process, consider all the compatible sets of  $d$  subgraphs where  $d \in [1, n_s]$ . We refer to this set as  $\mathfrak{G}^d$  and its elements are  $\mathfrak{g}_i^d$ .

Let us define a term of the basis associated to the set of subgraphs  $\mathfrak{g}_i^d$ :

$$I_{\mathfrak{g}_i^d} = \int_{X_v}^{+\infty} \prod_{v \in \mathcal{V}} [dx_v \lambda_k \cdot (x_v - X_v)^{\gamma_k - 1}] \prod_{j=1}^d \frac{1}{E_j}, \quad (4.11)$$

where  $E_j$  are the energies of the  $d$  subgraphs contained in  $\mathfrak{g}_i^d$ . The basis term  $I_{\mathfrak{g}_i^d}$  is a  $d$ -gon integral, meaning that it has  $d$  energy poles. We represent a term of the basis as the corresponding set of subgraphs on the graph  $\mathcal{G}$  with vertices drawn as black circles and subgraphs in dashed red. For instance, the 1-pole basis term for the subgraph  $g(1)$  of the 2-vertex graph is given by:

$$\begin{array}{c} \text{---} y \text{---} \\ \text{---} \bullet \text{---} \bullet \text{---} \\ \text{---} x_1 \quad x_2 \end{array} = \int_{X_1}^{+\infty} dx_1 \lambda_k \cdot (x_1 - X_1)^{\gamma_k - 1} \int_{X_2}^{+\infty} dx_2 \lambda_k \cdot (x_2 - X_2)^{\gamma_k - 1} \frac{1}{(x_1 + y)}. \quad (4.12)$$

We can expand the wavefunction as a linear combination of this basis up to a rational function  $R$ :

$$\begin{aligned} \tilde{\psi}_{\mathcal{G}} &= \sum_{d=1}^{n_s} \sum_{i=1}^{|\mathfrak{G}^d|} C_{\mathfrak{g}_i^d} I_{\mathfrak{g}_i^d} + R \\ &= \sum_{i=1}^{|\mathfrak{G}^1|} C_{\mathfrak{g}_i^1} I_{\mathfrak{g}_i^1} + \cdots + \sum_{k=1}^{|\mathfrak{G}^{n_s}|} C_{\mathfrak{g}_k^{n_s}} I_{\mathfrak{g}_k^{n_s}} + R. \end{aligned} \quad (4.13)$$

where, in the first line, the first summation runs over the  $d$ -gon basis terms, where  $d \in [1, n_s]$  and the second summation runs over every compatible set of  $d$  subgraphs  $\mathfrak{g}_i^d$  belonging to  $\mathfrak{G}^d$ .

The rational function  $R$  cannot be determined exploiting the discontinuities of the wavefunction and its determination is not within the scope of this thesis.

## 4.2.2 Computation of the coefficients at treel-level

The wavefunction and its integral representation are equal up to a rational function:

$$\int_{X_v}^{+\infty} \prod_{v \in \mathcal{V}} [dx_v \lambda_k \cdot (x_v - X_v)^{\gamma_k - 1}] \psi_{\mathcal{G}}(x_v, y_e) = \sum_{d=1}^{n_s} \sum_{i=1}^{|\mathfrak{G}^d|} C_{\mathfrak{g}_i^d} I_{\mathfrak{g}_i^d} + R. \quad (4.14)$$

In analogy with the discussion of flat-space integral reduction, we exploit the analytic structure of the amplitude to fix the coefficients. In particular, we match the discontinuities of the wavefunction with those of the basis. We start by matching the discontinuities of highest codimension and then proceed considering the discontinuities of lower codimension.

A discontinuity corresponds to a specific set of subgraphs  $\mathfrak{g}_i^d$ . By taking the appropriate residues on both sides of (4.14), for every compatible set of subgraphs  $\mathfrak{g}_i^d$ , we obtain a set of equations that relate the coefficients to simpler wavefunctions and flat space amplitudes, following the wavefunction factorization rules.

Let us describe the algorithm for computing the coefficients systematically. The algorithm follows an iterative structure. In the first step we consider the discontinuities of highest codimension,  $n_s$ , in the second step we consider discontinuities of lower codimension,  $n_s - 1$ , and we proceed until we get to the lowest codimension which is 1.

- (Codimension  $n_s$ ) We start by computing the coefficients  $C_{\mathfrak{g}_i^{n_s}}$  such that  $\mathfrak{g}_i^{n_s} \in \mathfrak{G}^{n_s}$ , namely the coefficients associated with integral terms having the highest number of poles. For each  $\mathfrak{g}_i^{n_s} \in \mathfrak{G}^{n_s}$ , we compute the corresponding set of residues, enforcing energy conservation, on the integrands of both sides of (4.14). Since we compute  $n_s$  residues, the wavefunction and the integral basis, which are defined by integration over  $n_s$  variables, are completely localized. On the l.h.s. we obtain a factorized wavefunction into flat-space amplitudes and on the r.h.s. we are left with only one basis term. We obtain immediately the expression of the coefficient  $C_{\mathfrak{g}_i^{n_s}}$ :

$$C_{\mathfrak{g}_i^{n_s}} = \text{Res}_{\mathfrak{g}_i^{n_s}} \psi_{\mathcal{G}} \quad (4.15)$$

where  $\text{Res}_{\mathfrak{g}_i^{n_s}}$  means taking  $n_s$  residues for the energies of the subgraphs belonging to  $\mathfrak{g}_i^{n_s}$  going to zero. The order of the residues matters, since two incompatible residues taken sequentially lead to a null amplitude. After calculating all the coefficients  $C_{\mathfrak{g}_i^{n_s}}$  for every  $\mathfrak{g}_i^{n_s} \in \mathfrak{G}^{n_s}$ , we proceed to the next step.

An important remark is in order: the coefficients associated with integral terms having the highest number of poles, i.e.  $n_s$  poles, are fully determined by flat-space amplitudes and do not depend on the cosmology.

- (Codimension  $n_s - 1$ ) To compute the coefficient  $C_{\mathfrak{g}_i^{n_s-1}}$ , we match the discontinuities of codimension  $n_s - 1$ . We perform  $n_s - 1$  residues on the integrands of both

sides of (4.14). We are left with one integration variable, we call  $\tilde{x}$ . The integral measure depends only on  $\tilde{x}$ :

$$\mu'(\tilde{x}) = \prod_{v \in \mathcal{V}} [\lambda_k \cdot (x_v - X_v)^{\gamma_k - 1}] \Big|_{\mathfrak{g}_i^{n_s - 1}}, \quad (4.16)$$

where the measure is evaluated for the energies of the subgraphs belonging to  $\mathfrak{g}_i^{n_s - 1}$  going to zero.

On the l.h.s, the universal integrand  $\psi_{\mathcal{G}}$  factorizes into simpler wavefunctions and flat space amplitudes, following the factorization rules, and it is given by

$$\psi_{\mathfrak{g}_i^{n_s - 1}}(\tilde{x}, y_e) = \text{Res}_{\mathfrak{g}_i^{n_s - 1}} \psi_{\mathcal{G}}(x_v, y_e). \quad (4.17)$$

On the r.h.s., we perform the same residues on the integrands of the basis terms, by substituting the appropriate poles with  $\delta$ -functions. Only the basis terms containing these poles will survive. We have contributions from  $n_s$ -gon basis terms and one  $(n_s - 1)$ -gon basis term:

$$\int_{\tilde{X}}^{+\infty} d\tilde{x} \mu'(\tilde{x}) \psi_{\mathfrak{g}_i^{n_s - 1}}(\tilde{x}, y_e) = \sum_j C_{\mathfrak{g}_i^{n_s - 1} \cup \mathfrak{g}_j^1} \int_{\tilde{X}}^{+\infty} d\tilde{x} \mu'(\tilde{x}) \frac{1}{E_j} + C_{\mathfrak{g}_i^{n_s - 1}} \int_{\tilde{X}}^{+\infty} d\tilde{x} \mu'(\tilde{x}) \quad (4.18)$$

where the sum is performed on the sets of one subgraph  $\mathfrak{g}_j^1 \in \mathfrak{G}^1$ , such that  $\mathfrak{g}_i^{n_s - 1} \cup \mathfrak{g}_j^1$  is a compatible set of cardinality  $n_s$ , i.e.  $\mathfrak{g}_i^{n_s - 1} \cup \mathfrak{g}_j^1 \in \mathfrak{G}^{n_s}$ .  $E_j$  is the energy of the one subgraph belonging to the set  $\mathfrak{g}_j^1$ .

We have to isolate the contributions to the coefficient  $C_{\mathfrak{g}_i^{n_s - 1}}$ . We expand the integrands on both sides of (4.18) using the relation (A.4), where the energy variable  $\tilde{x}$  has been shifted by  $\tilde{x} \rightarrow \tilde{x} + z$ . By matching the singularities, we obtain that the contributions to the coefficient  $C_{\mathfrak{g}_i^{n_s - 1}}$  come from the zeroth term of the Laurent series for  $z \rightarrow \infty$ :

$$\begin{aligned} \int_{\tilde{X}}^{+\infty} d\tilde{x} \mathcal{L}_{z \rightarrow \infty}^{(0)} \left\{ \mu'(\tilde{x}) \psi_{\mathfrak{g}_i^{n_s - 1}}(\tilde{x}, y_e) \right\} &= \sum_j C_{\mathfrak{g}_i^{n_s - 1} \cup \mathfrak{g}_j^1} \int_{\tilde{X}}^{+\infty} d\tilde{x} \mathcal{L}_{z \rightarrow \infty}^{(0)} \left\{ \mu'(\tilde{x}) \frac{1}{E_j} \right\} \\ &+ C_{\mathfrak{g}_i^{n_s - 1}} \int_{\tilde{X}}^{+\infty} d\tilde{x} \mathcal{L}_{z \rightarrow \infty}^{(0)} \left\{ \mu'(\tilde{x}) \right\} \end{aligned} \quad (4.19)$$

Here, we omit the shift of the variable  $\tilde{x}$ ; otherwise, the equation would become very cumbersome. Keep in mind that  $\tilde{x} \rightarrow \tilde{x} + z$ , and thus  $E_j(\tilde{x}) \rightarrow E_j(\tilde{x} + z)$  as well.

We can invert the above equation and obtain:

$$\begin{aligned}
C_{\mathfrak{g}_i^{n_s-1}} &= \frac{1}{\int_{\tilde{X}}^{+\infty} d\tilde{x} \mathcal{L}_{z \rightarrow \infty}^{(0)} \left\{ \mu(\tilde{x}) \right\}} \cdot \left\{ \int_{\tilde{X}}^{+\infty} d\tilde{x} \mathcal{L}_{z \rightarrow \infty}^{(0)} \left\{ \mu(\tilde{x}) \psi_{\mathfrak{g}_i^{n_s-1}}(\tilde{x}, y_e) \right\} \right. \\
&\quad \left. - \sum_j C_{\mathfrak{g}_i^{n_s-1} \cup \mathfrak{g}_j^1} \int_{\tilde{X}}^{+\infty} d\tilde{x} \mathcal{L}_{z \rightarrow \infty}^{(0)} \left\{ \mu(\tilde{x}) \frac{1}{E_j} \right\} \right\}. \tag{4.20}
\end{aligned}$$

After calculating all the coefficients  $C_{\mathfrak{g}_i^{n_s-1}}$  for every  $\mathfrak{g}_i^{n_s-1} \in \mathfrak{G}^{n_s-1}$ , we proceed to the compute the coefficients  $C_{\mathfrak{g}_i^{n_s-2}}$  for every  $\mathfrak{g}_i^{n_s-2} \in \mathfrak{G}^{n_s-2}$ . The next step involves computing generic  $d$ -gon coefficients.

- (Codimension  $d < n_s$ ) We now compute the coefficients  $C_{\mathfrak{g}_i^d}$  such that  $\mathfrak{g}_i^d \in \mathfrak{G}^d$ , by matching the discontinuities of codimension  $d$ . For each set of subgraphs  $\mathfrak{g}_i^d$  belonging to  $\mathfrak{G}^d$ , we compute the corresponding set of residues on the integrands of both sides of (4.14). The wavefunction contains  $n_s - d$  integration variables left. We call  $\mathcal{V}'$  the set of integration variables we are left with. On the l.h.s. we obtain a factorized wavefunction into flat-space amplitudes and simpler subgraphs wavefunctions. On the r.h.s., we have contributions from  $n_s$ -gon,  $(n_s - 1)$ -gon,  $\dots$ ,  $(d + 1)$ -gon basis terms and one  $d$ -gon term:

$$\begin{aligned}
&\int_{X_v}^{+\infty} \left[ \prod_{x_v \in \mathcal{V}'} dx_v \right] \mu'(x_v) \psi_{\mathfrak{g}_i^d}(x_v, y_e) \\
&= \sum_k C_{\mathfrak{g}_i^d \cup \mathfrak{g}_k^{n_s-d}} \int_{X_v}^{+\infty} \left[ \prod_{x_v \in \mathcal{V}'} dx_v \right] \mu'(x_v) \prod_{g_j \in \mathfrak{g}_k^{n_s-d}} \frac{1}{E_j} \\
&+ \sum_k C_{\mathfrak{g}_i^d \cup \mathfrak{g}_k^{n_s-d-1}} \int_{X_v}^{+\infty} \left[ \prod_{x_v \in \mathcal{V}'} dx_v \right] \mu'(x_v) \prod_{g_j \in \mathfrak{g}_k^{n_s-d-1}} \frac{1}{E_j} \\
&+ \dots \\
&+ \sum_k C_{\mathfrak{g}_i^d \cup \mathfrak{g}_k^1} \int_{X_v}^{+\infty} \left[ \prod_{x_v \in \mathcal{V}'} dx_v \right] \mu'(x_v) \frac{1}{E_k} \\
&+ C_{\mathfrak{g}_i^d} \int_{X_v}^{+\infty} \left[ \prod_{x_v \in \mathcal{V}'} dx_v \right] \mu'(x_v) \tag{4.21}
\end{aligned}$$

where the measure is evaluated at

$$\mu'(x_v, v \in \mathcal{V}') = \prod_{v \in \mathcal{V}} [\lambda_k \cdot (x_v - X_v)^{\gamma_k - 1}] \Big|_{\mathfrak{g}_i^d} \quad (4.22)$$

and

$$\psi_{\mathfrak{g}_i^d} = \text{Res}_{\mathfrak{g}_i^d} \psi_{\mathcal{G}}(x_v, y_e). \quad (4.23)$$

The first sum in (4.21) runs through all the sets  $\mathfrak{g}_k^{n_s-d}$  such that  $\mathfrak{g}_i^d \cup \mathfrak{g}_k^{n_s-d}$  is a compatible set of subgraphs, i.e.  $\mathfrak{g}_i^d \cup \mathfrak{g}_k^{n_s-d} \in \mathfrak{G}^{n_s}$ . The second sum runs through all the sets  $\mathfrak{g}_k^{n_s-d-1}$  such that  $\mathfrak{g}_i^d \cup \mathfrak{g}_k^{n_s-d-1} \in \mathfrak{G}^{n_s-1}$ . The same applies to the other sums. The product runs over the subgraphs  $g_j$ , indexed by  $j$ , belonging to the appropriate set of subgraphs. Each energy  $E_j$  represents the energy of the subgraph  $g_j$ . The product of the inverse of the energies  $E_j$  corresponds to the remaining poles of the basis terms.

We now have to isolate the contributions to the coefficient  $C_{\mathfrak{g}_i^d}$ . We expand the integrands on both sides of (4.21) using the relation (A.4), where the energy variables  $x_v$  have been shifted by  $x_v \rightarrow x_v + \alpha_v z$ . By matching the singularities, we obtain that the contributions to the coefficient  $C_{\mathfrak{g}_i^d}$  come from the zeroth term of the Laurent series for  $z \rightarrow \infty$ :

$$\begin{aligned} & \int_{X_v}^{+\infty} \left[ \prod_{x_v \in \mathcal{V}'} dx_v \right] \mathcal{L}_{z \rightarrow \infty}^{(0)} \left\{ \mu'(x_v) \psi_{\mathfrak{g}_i^d}(x_v, y_e) \right\} \\ &= \sum_k C_{\mathfrak{g}_i^d \cup \mathfrak{g}_k^{n_s-d}} \int_{X_v}^{+\infty} \left[ \prod_{x_v \in \mathcal{V}'} dx_v \right] \mathcal{L}_{z \rightarrow \infty}^{(0)} \left\{ \mu'(x_v) \prod_{g_j \in \mathfrak{g}_k^{n_s-d}} \frac{1}{E_j} \right\} \\ &+ \sum_k C_{\mathfrak{g}_i^d \cup \mathfrak{g}_k^{n_s-d-1}} \int_{X_v}^{+\infty} \left[ \prod_{x_v \in \mathcal{V}'} dx_v \right] \mathcal{L}_{z \rightarrow \infty}^{(0)} \left\{ \mu'(x_v) \prod_{g_j \in \mathfrak{g}_k^{n_s-d-1}} \frac{1}{E_j} \right\} \\ &+ \dots \\ &+ \sum_k C_{\mathfrak{g}_i^d \cup \mathfrak{g}_k^1} \int_{X_v}^{+\infty} \left[ \prod_{x_v \in \mathcal{V}'} dx_v \right] \mathcal{L}_{z \rightarrow \infty}^{(0)} \left\{ \mu'(x_v) \frac{1}{E_k} \right\} \\ &+ C_{\mathfrak{g}_i^d} \int_{X_v}^{+\infty} \left[ \prod_{x_v \in \mathcal{V}'} dx_v \right] \mathcal{L}_{z \rightarrow \infty}^{(0)} \left\{ \mu'(x_v) \right\} \end{aligned} \quad (4.24)$$

Here, we omit the shift of the variables  $x_v$ . Keep in mind that  $x_v \rightarrow x_v + \alpha_v z$ , and thus  $E_j(x_v) \rightarrow E_j(x_v + \alpha_v z)$  as well.

We have already computed all the coefficients of the previous iterations, thus by inverting the above equation we obtain an expression for  $C_{\mathfrak{g}_i^d}$ .

After calculating all the coefficients  $C_{\mathfrak{g}_i^d}$  for every  $\mathfrak{g}_i^d \in \mathfrak{G}^d$ , we proceed to compute the coefficients associated with integral terms having a lower number of poles.

An important remark is in order. In the previous steps of the algorithm we have shown that the  $n_s$ -gon coefficients, associated with integral terms having the highest number of poles, are fully determined by flat-space amplitudes and do not depend on the cosmology. The coefficients associated with integral terms having a lower number of poles depend on the cosmology, which is encoded in the integral measure. In a flat-space cosmology, the integral measure equals 1, resulting in  $d$ -gon coefficients, where  $d < n_s$ , to vanish.

### 4.3 Tree-level examples

We provide two examples of integral reduction for the wavefunction of a 2-vertex graph and a 3-vertex graph.

**2-vertex graph** Let us consider a 2-vertex graph with one time-independent interaction coupling  $\lambda$ ,

$$\tilde{\psi}_{\mathcal{G}} = \int_{X_1}^{+\infty} dx_1 \lambda \cdot (x_1 - X_1)^{\gamma-1} \int_{X_2}^{+\infty} dx_2 \lambda \cdot (x_2 - X_2)^{\gamma-1} \psi_{\mathcal{G}}. \quad (4.25)$$

where  $\psi_{\mathcal{G}}$  is the universal integrand of a 2-vertex graph. The integral basis has 6 terms. The expansion is as follows:

$$\begin{aligned} \tilde{\psi}_{\mathcal{G}} &= \int_{X_1}^{+\infty} dx_1 \lambda \cdot (x_1 - X_1)^{\gamma-1} \int_{X_2}^{+\infty} dx_2 \lambda \cdot (x_2 - X_2)^{\gamma-1} \psi_{\mathcal{G}} = \\ &= C_{g(1)g(1,2)} \int_{X_1}^{+\infty} dx_1 \lambda \cdot (x_1 - X_1)^{\gamma-1} \int_{X_2}^{+\infty} dx_2 \lambda \cdot (x_2 - X_2)^{\gamma-1} \frac{1}{(x_1 + x_2)(x_1 + y)} \\ &+ C_{g(2)g(1,2)} \int_{X_1}^{+\infty} dx_1 \lambda \cdot (x_1 - X_1)^{\gamma-1} \int_{X_2}^{+\infty} dx_2 \lambda \cdot (x_2 - X_2)^{\gamma-1} \frac{1}{(x_1 + x_2)(x_2 + y)} \\ &+ C_{g(1)g(2)} \int_{X_1}^{+\infty} dx_1 \lambda \cdot (x_1 - X_1)^{\gamma-1} \int_{X_2}^{+\infty} dx_2 \lambda \cdot (x_2 - X_2)^{\gamma-1} \frac{1}{(x_1 + y)(x_2 + y)} \\ &+ C_{g(1)} \int_{X_1}^{+\infty} dx_1 \lambda \cdot (x_1 - X_1)^{\gamma-1} \int_{X_2}^{+\infty} dx_2 \lambda \cdot (x_2 - X_2)^{\gamma-1} \frac{1}{(x_1 + y)} \\ &+ C_{g(2)} \int_{X_1}^{+\infty} dx_1 \lambda \cdot (x_1 - X_1)^{\gamma-1} \int_{X_2}^{+\infty} dx_2 \lambda \cdot (x_2 - X_2)^{\gamma-1} \frac{1}{(x_2 + y)} \end{aligned}$$

$$+ C_{g(1,2)} \int_{X_1}^{+\infty} dx_1 \lambda \cdot (x_1 - X_1)^{\gamma-1} \int_{X_2}^{+\infty} dx_2 \lambda \cdot (x_2 - X_2)^{\gamma-1} \frac{1}{(x_1 + x_2)} + R \quad (4.26)$$

Graphically (we omit the rational function  $R$ ),

$$\begin{aligned} \begin{array}{c} \blacksquare \xrightarrow{y} \blacksquare \\ x_1 \quad x_2 \end{array} &= C_{g(1)g(1,2)} \begin{array}{c} \bullet \text{---} \bullet \\ \text{(dashed red oval)} \end{array} + C_{g(2)g(1,2)} \begin{array}{c} \bullet \text{---} \bullet \\ \text{(dashed red oval)} \end{array} + C_{g(1)g(2)} \begin{array}{c} \bullet \text{---} \bullet \\ \text{(dashed red oval)} \end{array} \\ &+ C_{g(1)} \begin{array}{c} \bullet \text{---} \bullet \\ \text{(dashed red oval)} \end{array} + C_{g(2)} \begin{array}{c} \bullet \text{---} \bullet \\ \text{(dashed red oval)} \end{array} + C_{g(1,2)} \begin{array}{c} \bullet \text{---} \bullet \\ \text{(dashed red oval)} \end{array} \end{aligned} \quad (4.27)$$

where the wavefunction is represented with squared vertices labeled as:  $\blacksquare \text{---} \blacksquare$  and the

subgraphs drawn in dashed red correspond to the poles of the basis terms. Let us apply the algorithm for the computation of the coefficients.

- (Codimension  $d = 2$ ) We start by computing the coefficients associated to integral terms with two poles.

To compute the term  $C_{g(1)g(1,2)}$ , we limit the space of integration to a contour around the poles  $|x_1 + x_2| = \epsilon$  and  $|x_1 + y| = \epsilon$ , which corresponds to taking the residue of the wavefunction integrand at the poles. Such residue can be computed by substituting the singularities with  $\delta$ -functions:  $1/(x_1 + x_2) \rightarrow \delta(x_1 + x_2)$  and  $1/(x_1 + y) \rightarrow \delta(x_1 + y)$ .

The integrals are completely localized. On the l.h.s of (4.26), the wavefunction factorizes into two flat space amplitudes:

$$\begin{array}{c} \bullet \text{---} \bullet \\ \text{(solid red oval)} \\ x_1 \quad x_2 \end{array} = \frac{1}{2y} \begin{array}{c} \bullet \\ \text{(solid red circle)} \\ x_1 + y \end{array} \times \begin{array}{c} \bullet \\ \text{(solid red circle)} \\ x_2 - y \end{array} \quad (4.28)$$

where the subgraphs represented as solid red circles denote the computation of the appropriate residues on the wavefunction integrand.

On the r.h.s of (4.26) we have only the contribution from the basis term  $C_{g(1)g(1,2)}$ :

$$\begin{array}{c} \bullet \text{---} \bullet \\ \text{(solid red oval)} \\ x_1 \quad x_2 \end{array} = C_{g(1)g(1,2)} \begin{array}{c} \bullet \text{---} \bullet \\ \text{(solid red oval)} \end{array} \quad (4.29)$$

Therefore, we obtain:

$$C_{g(1)g(1,2)} = \frac{1}{2y} \mathcal{A}_1(x_1 + y) \times \mathcal{A}_2(x_2 - y). \quad (4.30)$$

Analogously, we compute  $C_{g(2)g(1,2)}$ ,

$$C_{g(1)g(2)} = \frac{1}{2y} \mathcal{A}_1(x_1 - y) \times \mathcal{A}_2(x_2 + y), \quad (4.31)$$



$$+ C_{g(1)g(2)} \int_{X_2}^{+\infty} dx_2 (x_2 - X_2)^{\gamma-1} \frac{1}{(x_2 + y)} + C_{g(1)} \int_{X_2}^{+\infty} dx_2 (x_2 - X_2)^{\gamma-1} \Big]. \quad (4.36)$$

We can represent the above equation graphically,

$$\begin{array}{c} \text{---} \bullet \text{---} \bullet \text{---} \\ x_1 \quad x_2 \end{array} \stackrel{y}{=} C_{g(1)g(1,2)} \begin{array}{c} \text{---} \bullet \text{---} \bullet \text{---} \\ \text{---} \bullet \text{---} \bullet \text{---} \end{array} + C_{g(1)g(2)} \begin{array}{c} \text{---} \bullet \text{---} \bullet \text{---} \\ \text{---} \bullet \text{---} \bullet \text{---} \end{array} + C_{g(1)} \begin{array}{c} \text{---} \bullet \text{---} \bullet \text{---} \\ \text{---} \bullet \text{---} \bullet \text{---} \end{array} \quad (4.37)$$

where the subgraph  $g(1)$  represented as a solid red circle denotes the computation of the appropriate residue on the wavefunction integrand and on the integrands of the basis terms. The subgraphs drawn in dashed red correspond to the remaining poles of the basis terms.

By demanding that the codimension-1 discontinuity of the wavefunction matches that of the integral basis, we derive the following equation:

$$\begin{aligned} & \int_{X_2}^{+\infty} dx_2 (x_2 - X_2)^{\gamma-1} \psi_{g(1)} \\ &= C_{g(1)g(1,2)} \int_{X_2}^{+\infty} dx_2 (x_2 - X_2)^{\gamma-1} \frac{1}{(x_2 - y)} \\ &+ C_{g(1)g(2)} \int_{X_2}^{+\infty} dx_2 (x_2 - X_2)^{\gamma-1} \frac{1}{(x_2 + y)} \\ &+ C_{g(1)} \int_{X_2}^{+\infty} dx_2 (x_2 - X_2)^{\gamma-1}. \end{aligned} \quad (4.38)$$

To compute the coefficient  $C_{g(1)}$ , we match the singularities of eq. (4.38), using partial fractions. We expand the integrands on both sides of the above equation using eq. (A.4), where we have shifted  $x_2 \rightarrow x_2 + z$ . The contributions to  $C_{g(1)}$  are given by the zeroth term of the Laurent series expansion of the integrands for  $z \rightarrow \infty$ . Namely,

$$\begin{aligned} & \int_{X_2}^{+\infty} dx_2 \mathcal{L}_{z \rightarrow \infty}^{(0)} \left\{ (x_2 + z - X_2)^{\gamma-1} \psi_{g(1)} \right\} \\ &= C_{g(1)g(1,2)} \int_{X_2}^{+\infty} dx_2 \mathcal{L}_{z \rightarrow \infty}^{(0)} \left\{ (x_2 + z - X_2)^{\gamma-1} \frac{1}{(x_2 + z - y)} \right\} \\ &+ C_{g(1)g(2)} \int_{X_2}^{+\infty} dx_2 \mathcal{L}_{z \rightarrow \infty}^{(0)} \left\{ (x_2 + z - X_2)^{\gamma-1} \frac{1}{(x_2 + z + y)} \right\} \\ &+ C_{g(1)} \int_{X_2}^{+\infty} dx_2 \mathcal{L}_{z \rightarrow \infty}^{(0)} \left\{ (x_2 + z - X_2)^{\gamma-1} \right\}, \end{aligned} \quad (4.39)$$

where  $\psi_{g(1)}$  is given by (4.35) where the variable  $x_2$  is shifted to  $x_2 + z$ .

Since the coefficients  $C_{g(1)g(1,2)}$  and  $C_{g(1)g(2)}$  have been computed in the previous iteration, by inverting the above equation, we have an expression for  $C_{g(1)}$ .

Due to symmetry arguments,  $C_{g(2)}$  is given by  $C_{g(1)}$  by exchanging:  $x_1 \leftrightarrow x_2$ ,  $X_1 \leftrightarrow X_2$ .

Let us compute  $C_{g(1,2)}$ . Starting from (4.26), we compute the residue at the pole  $(x_1 + x_2) = 0$  on the integrands of both sides:

$$\begin{aligned}
& \int_{X_2}^{-X_1} dx_2 (-x_2 - X_1)^{\gamma-1} (x_2 - X_2)^{\gamma-1} \mathcal{A}_{\mathcal{G}} = \\
& = C_{g(1)g(1,2)} \int_{X_2}^{-X_1} dx_2 (-x_2 - X_1)^{\gamma-1} (x_2 - X_2)^{\gamma-1} \frac{1}{(-x_2 + y)} \\
& + C_{g(2)g(1,2)} \int_{X_2}^{-X_1} dx_2 (-x_2 - X_1)^{\gamma-1} (x_2 - X_2)^{\beta} \frac{1}{(x_2 + y)} \\
& + C_{g(1,2)} \int_{X_2}^{-X_1} dx_2 (-x_2 - X_1)^{\gamma-1} (x_2 - X_2)^{\gamma-1} \tag{4.40}
\end{aligned}$$

where  $\mathcal{A}_{\mathcal{G}} \equiv \mathcal{A}_{\mathcal{G}}(x_1 + x_2)$  is the flat space amplitude associated to the subgraph of the total process  $\mathcal{G}$ . In order to have a non-null integral, the extremes of integration have to be such that  $X_2 \leq x_2 \leq -X_1$ , consequently,  $X_1$  must be negative. We interpret  $X_1$  being negative as an incoming state and  $X_2$  positive as an outgoing state. Since we imposed total energy conservation, we recover a flat space amplitude which is characterized by having both incoming and outgoing states.

We can represent the above equation graphically,

$$\begin{aligned}
\text{[Diagram: } \square_{x_1} \text{---}^y \text{---} \square_{x_2} \text{]} & = C_{g(1)g(1,2)} \text{[Diagram: } \bullet \text{---} \bullet \text{]} + C_{g(1)g(2)} \text{[Diagram: } \bullet \text{---} \bullet \text{]} + C_{g(1)} \text{[Diagram: } \bullet \text{---} \bullet \text{]} \tag{4.41}
\end{aligned}$$

To compute the coefficient  $C_{g(1,2)}$ , we match the singularities of eq. (4.40), using partial fractions. We expand the integrands on both sides of the above equation using eq. (A.4), where we have shifted  $x_2 \rightarrow x_2 + z$ . The contributions to  $C_{g(1,2)}$  are given by the zeroth term of the Laurent series expansion of the integrands for  $z \rightarrow \infty$ :

$$\begin{aligned}
& \int_{X_2}^{-X_1} dx_2 \mathcal{L}_{z \rightarrow \infty}^{(0)} \left\{ (-x_2 + z - X_1)^{\gamma-1} (x_2 + z - X_2)^{\gamma-1} \mathcal{A}_{\mathcal{G}} \right\} = \\
& = C_{g(1)g(1,2)} \int_{X_2}^{-X_1} dx_2 \mathcal{L}_{z \rightarrow \infty}^{(0)} \left\{ (-x_2 - z - X_1)^{\gamma-1} (x_2 + z - X_2)^{\gamma-1} \frac{1}{(-x_2 - z + y)} \right\}
\end{aligned}$$

$$\begin{aligned}
& + C_{g(2)g(1,2)} \int_{X_2}^{-X_1} dx_2 \mathcal{L}_{z \rightarrow \infty}^{(0)} \left\{ (-x_2 - z - X_1)^{\gamma-1} (x_2 + z - X_2)^{\gamma-1} \frac{1}{(x_2 + z + y)} \right\} \\
& + C_{g(1,2)} \int_{X_2}^{-X_1} dx_2 \mathcal{L}_{z \rightarrow \infty}^{(0)} \left\{ (-x_2 - z - X_1)^{\gamma-1} (x_2 + z - X_2)^{\gamma-1} \right\}
\end{aligned} \tag{4.42}$$

By inverting the above equation, we have an expression for  $C_{g(1,2)}$ .

Notice that 1-gon coefficients depend on the cosmology, encoded in the integral measure, as well as on flat-space amplitudes and simpler wavefunctions.

**3-vertex chain** The wavefunction of a 3-vertex chain graph is given by

$$\tilde{\psi}_{\mathcal{G}} = \int_{X_1}^{+\infty} dx_1 \lambda \cdot (x_1 - X_1)^{\gamma-1} \int_{X_2}^{+\infty} dx_2 \lambda \cdot (x_2 - X_2)^{\gamma-1} \int_{X_3}^{+\infty} dx_3 \lambda \cdot (x_3 - X_3)^{\gamma-1} \psi_{\mathcal{G}}, \tag{4.43}$$

where  $\psi_{\mathcal{G}} \equiv \psi_{\mathcal{G}}(x_1, x_2, x_3, y_{12}, y_{23})$  is the universal integrand.

Considering the compatibility rules for subgraphs in [9], we find two incompatible sets of subgraphs:

$$g(2)g(\mathcal{G}) = \text{---} \bullet \text{---} \bullet \text{---} \bullet \quad g(1,2)g(2,3) = \text{---} \bullet \text{---} \bullet \text{---} \bullet \tag{4.44}$$

There are additional incompatible sets of subgraphs if we restrict to the tree-level case, since we have the additional constraint that the internal energies  $y_{12}$  and  $y_{23}$  must be strictly positive.

There are sets of subgraphs which contain the incompatible subgraphs in (4.44) but are not incompatible sets. In this case, it is important to pay attention to the order of the residues that we compute to obtain the associated wavefunction. Let us consider, for instance, the wavefunction associated to the set of subgraphs  $\mathfrak{g}^3 = \{g(2), g(1,2), g(2,3)\}$ :

$$\begin{array}{c} \text{---} \bullet \text{---} \bullet \text{---} \bullet \\ \text{\scriptsize } x_1 \quad x_2 \quad x_3 \end{array} \quad \begin{array}{c} \text{---} \bullet \text{---} \bullet \text{---} \bullet \\ \text{\scriptsize } x_1 \quad x_2 + y_{23} \end{array} \quad \times \quad \frac{1}{2y_{23}} \begin{array}{c} \bullet \\ \text{\scriptsize } x_3 - y_{23} \end{array} = \frac{1}{4y_{12}y_{23}} \begin{array}{c} \bullet \\ \text{\scriptsize } x_1 - y_{12} \end{array} \times \begin{array}{c} \bullet \\ \text{\scriptsize } x_2 + y_{23} \end{array} \times \begin{array}{c} \bullet \\ \text{\scriptsize } x_3 - y_{23} \end{array} \tag{4.45}$$

where solid red circles denotes the computation of the appropriate residues on the wavefunction integrand. The associated universal integrand is given by:

$$\psi_{g(2)g(1,2)g(2,3)} = \frac{1}{4y_{12}y_{23}} \mathcal{A}_1(x_1 - y_{12}) \mathcal{A}_2(x_2 + y_{23}) \mathcal{A}_3(x_3 - y_{23}). \tag{4.46}$$

Although the incompatible set  $\mathfrak{g}^2 = \{g(1,2), g(2,3)\}$  is contained into the set  $\mathfrak{g}^3 = \{g(2), g(1,2), g(2,3)\}$ , the latter is compatible.

After having identified all the compatible sets of subgraphs, we can expand the 3-vertex chain in the integral basis:

$$\begin{aligned}
\begin{array}{c} y_{12} \quad y_{23} \\ \blacksquare \quad \blacksquare \quad \blacksquare \\ x_1 \quad x_2 \quad x_3 \end{array} &= C_{g(1)g(1,2)g(\mathcal{G})} \begin{array}{c} \bullet \text{---} \bullet \text{---} \bullet \\ \text{(red dashed ovals around } \{1,2\} \text{ and } \{1,2,3\}) \end{array} + C_{g(2)g(1,2)g(\mathcal{G})} \begin{array}{c} \bullet \text{---} \bullet \text{---} \bullet \\ \text{(red dashed ovals around } \{2,3\} \text{ and } \{1,2,3\}) \end{array} \\
&+ C_{g(2)g(2,3)g(\mathcal{G})} \begin{array}{c} \bullet \text{---} \bullet \text{---} \bullet \\ \text{(red dashed ovals around } \{2,3\} \text{ and } \{1,2,3\}) \end{array} + C_{g(3)g(2,3)g(\mathcal{G})} \begin{array}{c} \bullet \text{---} \bullet \text{---} \bullet \\ \text{(red dashed ovals around } \{1,2\} \text{ and } \{2,3\}) \end{array} \\
&+ C_{g(1)g(1,2)g(3)} \begin{array}{c} \bullet \text{---} \bullet \text{---} \bullet \\ \text{(red dashed ovals around } \{1,2\} \text{ and } \{3\}) \end{array} + C_{g(2)g(1,2)g(3)} \begin{array}{c} \bullet \text{---} \bullet \text{---} \bullet \\ \text{(red dashed ovals around } \{1,2\} \text{ and } \{3\}) \end{array} \\
&+ C_{g(1)g(3)g(2,3)} \begin{array}{c} \bullet \text{---} \bullet \text{---} \bullet \\ \text{(red dashed ovals around } \{1\} \text{ and } \{2,3\}) \end{array} + C_{g(1)g(2)g(2,3)} \begin{array}{c} \bullet \text{---} \bullet \text{---} \bullet \\ \text{(red dashed ovals around } \{1\} \text{ and } \{2,3\}) \end{array} \\
&+ C_{g(1)g(2)g(3)} \begin{array}{c} \bullet \text{---} \bullet \text{---} \bullet \\ \text{(red dashed ovals around } \{1\} \text{ and } \{2\}) \end{array} + C_{g(1)g(1,2)g(2,3)} \begin{array}{c} \bullet \text{---} \bullet \text{---} \bullet \\ \text{(red dashed ovals around } \{1,2\} \text{ and } \{2,3\}) \end{array} \\
&+ C_{g(2)g(1,2)g(2,3)} \begin{array}{c} \bullet \text{---} \bullet \text{---} \bullet \\ \text{(red dashed ovals around } \{1,2\} \text{ and } \{2,3\}) \end{array} + C_{g(3)g(1,2)g(2,3)} \begin{array}{c} \bullet \text{---} \bullet \text{---} \bullet \\ \text{(red dashed ovals around } \{1,2\} \text{ and } \{2,3\}) \end{array} \\
&+ C_{g(1,2)g(2,3)g(\mathcal{G})} \begin{array}{c} \bullet \text{---} \bullet \text{---} \bullet \\ \text{(red dashed ovals around } \{1,2\} \text{ and } \{2,3\}) \end{array} + C_{g(1)g(1,2)} \begin{array}{c} \bullet \text{---} \bullet \text{---} \bullet \\ \text{(red dashed ovals around } \{1,2\}) \end{array} \\
&+ C_{g(2)g(1,2)} \begin{array}{c} \bullet \text{---} \bullet \text{---} \bullet \\ \text{(red dashed ovals around } \{1,2\}) \end{array} + C_{g(3)g(1,2)} \begin{array}{c} \bullet \text{---} \bullet \text{---} \bullet \\ \text{(red dashed ovals around } \{1,2\}) \end{array} \\
&+ C_{g(1)g(2,3)} \begin{array}{c} \bullet \text{---} \bullet \text{---} \bullet \\ \text{(red dashed ovals around } \{2,3\}) \end{array} + C_{g(2)g(2,3)} \begin{array}{c} \bullet \text{---} \bullet \text{---} \bullet \\ \text{(red dashed ovals around } \{2,3\}) \end{array} \\
&+ C_{g(3)g(2,3)} \begin{array}{c} \bullet \text{---} \bullet \text{---} \bullet \\ \text{(red dashed ovals around } \{2,3\}) \end{array} + C_{g(1)g(3)} \begin{array}{c} \bullet \text{---} \bullet \text{---} \bullet \\ \text{(red dashed ovals around } \{1\} \text{ and } \{3\}) \end{array} \\
&+ C_{g(1)g(2)} \begin{array}{c} \bullet \text{---} \bullet \text{---} \bullet \\ \text{(red dashed ovals around } \{1\} \text{ and } \{2\}) \end{array} + C_{g(2)g(3)} \begin{array}{c} \bullet \text{---} \bullet \text{---} \bullet \\ \text{(red dashed ovals around } \{2\} \text{ and } \{3\}) \end{array} \\
&+ C_{g(1)g(\mathcal{G})} \begin{array}{c} \bullet \text{---} \bullet \text{---} \bullet \\ \text{(red dashed oval around } \{1\}) \end{array} + C_{g(3)g(\mathcal{G})} \begin{array}{c} \bullet \text{---} \bullet \text{---} \bullet \\ \text{(red dashed oval around } \{3\}) \end{array}
\end{aligned}$$

$$\begin{aligned}
& + C_{g(1,2)g(\mathcal{G})} \text{ (diagram with 3 nodes, 2 edges, 2 dashed red ovals)} + C_{g(2,3)g(\mathcal{G})} \text{ (diagram with 3 nodes, 2 edges, 2 dashed red ovals)} \\
& + C_{g(1)} \text{ (diagram with 3 nodes, 2 edges, 1 dashed red oval)} + C_{g(2)} \text{ (diagram with 3 nodes, 2 edges, 1 dashed red oval)} \\
& + C_{g(3)} \text{ (diagram with 3 nodes, 2 edges, 1 dashed red oval)} + C_{g(1,2)} \text{ (diagram with 3 nodes, 2 edges, 1 dashed red oval)} \\
& + C_{g(2,3)} \text{ (diagram with 3 nodes, 2 edges, 1 dashed red oval)} + C_{g(\mathcal{G})} \text{ (diagram with 3 nodes, 2 edges, 1 dashed red oval)}
\end{aligned} \tag{4.47}$$

where the subgraphs drawn in dashed red correspond to the poles of the basis terms. Let us now apply the algorithm for the computation of the coefficients. We will show the computation of one coefficient for each discontinuity codimension.

- (Codimension  $d = 3$ ) Let us start by considering coefficients associated to integral terms containing three poles. By taking 3 residues on the integrands of the wavefunction and the basis terms, the integrals are completely localized. Let us consider the coefficient associated to the set  $\mathfrak{g}^3 = \{g(2), g(1, 2), g(2, 3)\}$ . By performing the three residues on (4.47), we obtain:

$$\begin{array}{c}
\text{■} \xrightarrow{y_{12}} \text{■} \xrightarrow{y_{23}} \text{■} \\
x_1 \quad x_2 \quad x_3
\end{array} = C_{g(2)g(1,2)g(2,3)} \text{ (diagram with 3 nodes, 2 edges, 2 overlapping dashed red ovals)} \tag{4.48}$$

The coefficient  $C_{g(2)g(1,2)g(2,3)}$  is, thus, given by:

$$C_{g(2)g(1,2)g(2,3)} = \text{Res}_{\mathfrak{g}^3} \psi_{\mathcal{G}} \equiv \text{Res}_{\substack{x_2+y_{12}+y_{23}=0 \\ x_1+x_2+y_{23}=0 \\ x_2+x_3+y_{12}=0}} \psi_{\mathcal{G}} \tag{4.49}$$

where the factorization of the universal integrand is given by (4.46) and we obtain the coefficient in terms of flat space amplitudes:

$$C_{g(2)g(1,2)g(2,3)} = \frac{1}{4y_{12}y_{23}} \mathcal{A}_1(x_1 - y_{12}) \mathcal{A}_2(x_2 + y_{23}) \mathcal{A}_3(x_3 - y_{23}). \tag{4.50}$$

- (Codimension  $d = 2$ ) Let us consider coefficients associated to integral terms containing two poles.

Let us work on a specific example where we compute the coefficient  $C_{g(1,2)g(\mathcal{G})}$  associated to the following basis term:

$$\begin{aligned}
\text{Diagram} &= \int_{X_1}^{+\infty} dx_1 \lambda \cdot (x_1 - X_1)^{\gamma-1} \int_{X_2}^{+\infty} dx_2 \lambda \cdot (x_2 - X_2)^{\gamma-1} \\
&\cdot \int_{X_3}^{+\infty} dx_3 \lambda \cdot (x_3 - X_3)^{\gamma-1} \frac{1}{(x_1 + x_2 + y_{23})(x_1 + x_2 + x_3)}.
\end{aligned} \tag{4.51}$$

The factorized wavefunction  $\tilde{\psi}_{g(1,2)g(\mathcal{G})}$ , is computed by taking the residues at the poles  $x_1 + x_2 + y_{23} = 0$  and  $x_1 + x_2 + x_3 = 0$  of the wavefunction integrand  $\bar{\psi}_{\mathcal{G}}$  and it is given by:

$$\tilde{\psi}_{g(1,2)g(\mathcal{G})} = \lambda^3 \cdot (y_{23} - X_3)^{\gamma-1} \int_{X_1}^{+\infty} dx_1 (-x_1 - y_{23} - X_2)^{\gamma-1} (x_1 - X_1)^{\gamma-1} \psi_{g(1,2)g(\mathcal{G})}, \tag{4.52}$$

where we have integrated out the variables  $x_2$  and  $x_3$  and the wavefunction factorizes as:

$$\begin{aligned}
\text{Diagram} &= \text{Diagram} \times \frac{1}{2y_{23}} \text{Diagram}
\end{aligned} \tag{4.53}$$

Therefore, the universal integrand is given by:

$$\psi_{g(1,2)g(\mathcal{G})} = \frac{1}{2y_{23}} \mathcal{A}_{1,2}(x_1 + x_2 + y_{23}) \mathcal{A}_3(x_3 - y_{23}). \tag{4.54}$$

Computing the two residues on the integrands of the basis terms yields:

$$\begin{aligned}
\tilde{\psi}_{g(1,2)g(\mathcal{G})} &= C_{g(1)g(1,2)g(\mathcal{G})} \lambda^3 \cdot (y_{23} - X_3)^{\gamma-1} \\
&\cdot \int_{X_1}^{+\infty} dx_1 (-x_1 - y_{23} - X_2)^{\gamma-1} (x_1 - X_1)^{\gamma-1} \frac{1}{x_1 + y_{12}} \\
&+ C_{g(2)g(1,2)g(\mathcal{G})} \lambda^3 \cdot (y_{23} - X_3)^{\gamma-1} \\
&\cdot \int_{X_1}^{+\infty} dx_1 (-x_1 - y_{23} - X_2)^{\gamma-1} (x_1 - X_1)^{\gamma-1} \frac{1}{-x_1 + y_{12}} \\
&+ C_{g(1,2)g(\mathcal{G})} \lambda^3 \cdot (y_{23} - X_3)^{\gamma-1}
\end{aligned}$$

$$\cdot \int_{X_1}^{+\infty} dx_1 (-x_1 - y_{23} - X_2)^{\gamma-1} (x_1 - X_1)^{\gamma-1} \quad (4.55)$$

where we have integrated out the variables  $x_2$  and  $x_3$ . We represent the above equation graphically as:

$$= C_{g(1)g(1,2)g(\mathcal{G})} \text{ (diagram 1) } + C_{g(2)g(1,2)g(\mathcal{G})} \text{ (diagram 2) } + C_{g(1,2)g(\mathcal{G})} \text{ (diagram 3) } \quad (4.56)$$

The codimension-2 discontinuity of the wavefunction and the integral basis, given by (4.52) and (4.55) respectively, must be equal. Therefore we obtain the following equation:

$$\begin{aligned} & \int_{X_1}^{+\infty} dx_1 (-x_1 - y_{23} - X_2)^{\gamma-1} (x_1 - X_1)^{\gamma-1} \psi_{g(1,2)g(\mathcal{G})} = \\ & = C_{g(1)g(1,2)g(\mathcal{G})} \int_{X_1}^{+\infty} dx_1 (-x_1 - y_{23} - X_2)^{\gamma-1} (x_1 - X_1)^{\gamma-1} \frac{1}{x_1 + y_{12}} \\ & + C_{g(2)g(1,2)g(\mathcal{G})} \int_{X_1}^{+\infty} dx_1 (-x_1 - y_{23} - X_2)^{\gamma-1} (x_1 - X_1)^{\gamma-1} \frac{1}{-x_1 + y_{12}} \\ & + C_{g(1,2)g(\mathcal{G})} \int_{X_1}^{+\infty} dx_1 (-x_1 - y_{23} - X_2)^{\gamma-1} (x_1 - X_1)^{\gamma-1} \end{aligned} \quad (4.57)$$

The coefficient  $C_{g(1,2)g(\mathcal{G})}$  is obtained by matching the singularities of the integrands, using partial fractions (A.4). We shift the variable  $x_1 \rightarrow x_1 + z$  and pick the zeroth term of the Laurent series of the integrands for  $z \rightarrow \infty$ :

$$\begin{aligned} & \int_{X_1}^{+\infty} dx_1 \mathcal{L}_{z \rightarrow \infty}^{(0)} \left\{ (-x_1 - y_{23} - X_2)^{\gamma-1} (x_1 - X_1)^{\gamma-1} \psi_{g(1,2)g(\mathcal{G})} \right\} = \\ & = C_{g(1)g(1,2)g(\mathcal{G})} \int_{X_1}^{+\infty} dx_1 \mathcal{L}_{z \rightarrow \infty}^{(0)} \left\{ (-x_1 - y_{23} - X_2)^{\gamma-1} (x_1 - X_1)^{\gamma-1} \frac{1}{x_1 + y_{12}} \right\} \\ & + C_{g(2)g(1,2)g(\mathcal{G})} \int_{X_1}^{+\infty} dx_1 \mathcal{L}_{z \rightarrow \infty}^{(0)} \left\{ (-x_1 - y_{23} - X_2)^{\gamma-1} (x_1 - X_1)^{\gamma-1} \frac{1}{-x_1 + y_{12}} \right\} \\ & + C_{g(1,2)g(\mathcal{G})} \int_{X_1}^{+\infty} dx_1 \mathcal{L}_{z \rightarrow \infty}^{(0)} \left\{ (-x_1 - y_{23} - X_2)^{\gamma-1} (x_1 - X_1)^{\gamma-1} \right\}. \end{aligned} \quad (4.58)$$

Here, the shift in  $z$  is omitted for the sake of clarity and  $\psi_{g(1,2)g(\mathcal{G})}$  is given by (4.54). Inverting the above equation, we find an expression for  $C_{g(1,2)g(\mathcal{G})}$ .

- (Codimension  $d = 1$ ) Let us consider the computation of coefficients associated to an integral term with one pole.

Let us consider, for instance, the computation of the coefficient  $C_{g(1,2)}$  of the basis term:

$$\begin{aligned}
 \text{---} \bullet \text{---} \bullet \text{---} \bullet &= \int_{X_1}^{+\infty} dx_1 \lambda \cdot (x_1 - X_1)^{\gamma-1} \int_{X_2}^{+\infty} dx_2 \lambda \cdot (x_2 - X_2)^{\gamma-1} \\
 &\int_{X_3}^{+\infty} dx_3 \lambda \cdot (x_3 - X_3)^{\gamma-1} \frac{1}{(x_1 + x_2 + y_{23})}. \quad (4.59)
 \end{aligned}$$

The factorized wavefunction  $\tilde{\psi}_{g(1,2)}$ , computed by taking the residue at the pole  $x_1 + x_2 + y_{23} = 0$  of the wavefunction integrand  $\tilde{\psi}_{\mathcal{G}}$ , is given by

$$\tilde{\psi}_{g(1,2)} = \lambda^3 \int_{X_2}^{+\infty} \int_{X_3}^{+\infty} dx_2 dx_3 (-x_2 - y_{23} - X_1)^{\gamma-1} (x_2 - X_2)^{\gamma-1} (x_3 - X_3)^{\gamma-1} \psi_{g(1,2)} \quad (4.60)$$

where we have integrated out the variable  $x_1$  and the wavefunction factorizes as:

$$\begin{aligned}
 \text{---} \blacksquare \text{---} \blacksquare \text{---} \blacksquare &= \text{---} \blacksquare \text{---} \blacksquare \text{---} \times \frac{1}{2y_{23}} \left( \text{---} \blacksquare \text{---} \blacksquare \text{---} \right). \quad (4.61) \\
 &\quad \begin{matrix} y_{12} & y_{23} \\ \blacksquare & \blacksquare & \blacksquare \\ x_1 & x_2 & x_3 \end{matrix} \quad \begin{matrix} y_{12} \\ \blacksquare & \blacksquare \\ x_1 & x_2 + y_{23} \end{matrix} \quad \begin{matrix} \blacksquare & \blacksquare \\ x_3 - y_{23} & x_3 + y_{23} \end{matrix}
 \end{aligned}$$

The universal integrand is given by:

$$\psi_{g(1,2)} = \frac{1}{2y_{23}} \mathcal{A}_{1,2}(x_1 + x_2 + y_{23}) \times \left( \psi_3(x_3 - y_{23}) - \psi_3(x_3 + y_{23}) \right). \quad (4.62)$$

Computing the two residues on the integrands of the basis terms yields:

$$\begin{aligned}
 \tilde{\psi}_{g(1,2)} &= C_{g(1)g(1,2)g(\mathcal{G})} \lambda^3 \int_{X_2}^{+\infty} \int_{X_3}^{+\infty} dx_2 dx_3 \frac{(-x_2 - y_{23} - X_1)^{\gamma-1} (x_2 - X_2)^{\gamma-1} (x_3 - X_3)^{\gamma-1}}{(x_3 - y_{23})(-x_2 - y_{23} + y_{12})} \\
 &+ C_{g(2)g(1,2)g(\mathcal{G})} \lambda^3 \int_{X_2}^{+\infty} \int_{X_3}^{+\infty} dx_2 dx_3 \frac{(-x_2 - y_{23} - X_1)^{\gamma-1} (x_2 - X_2)^{\gamma-1} (x_3 - X_3)^{\gamma-1}}{(x_3 - y_{23})(x_1 + y_{12} + y_{23})} \\
 &+ C_{g(1)g(1,2)g(3)} \lambda^3 \int_{X_2}^{+\infty} \int_{X_3}^{+\infty} dx_2 dx_3 \frac{(-x_2 - y_{23} - X_1)^{\gamma-1} (x_2 - X_2)^{\gamma-1} (x_3 - X_3)^{\gamma-1}}{(x_3 + y_{23})(-x_2 - y_{23} + y_{12})} \\
 &+ C_{g(2)g(1,2)g(3)} \lambda^3 \int_{X_2}^{+\infty} \int_{X_3}^{+\infty} dx_2 dx_3 \frac{(-x_2 - y_{23} - X_1)^{\gamma-1} (x_2 - X_2)^{\gamma-1} (x_3 - X_3)^{\gamma-1}}{(x_3 + y_{23})(x_2 + y_{12} + y_{23})} \\
 &+ C_{g(1)g(1,2)g(3)} \lambda^3 \int_{X_2}^{+\infty} \int_{X_3}^{+\infty} dx_2 dx_3 \frac{(-x_2 - y_{23} - X_1)^{\gamma-1} (x_2 - X_2)^{\gamma-1} (x_3 - X_3)^{\gamma-1}}{(x_2 + x_3 + y_{12})(-x_2 - y_{23} + y_{12})} \\
 &+ C_{g(2)g(1,2)g(2,3)} \lambda^3 \int_{X_2}^{+\infty} \int_{X_3}^{+\infty} dx_2 dx_3 \frac{(-x_2 - y_{23} - X_1)^{\gamma-1} (x_2 - X_2)^{\gamma-1} (x_3 - X_3)^{\gamma-1}}{(x_2 + x_3 + y_{12})(-x_2 y_{23} + y_{12})}
 \end{aligned}$$

$$\begin{aligned}
& + C_{g(3)g(1,2)g(2,3)}\lambda^3 \int_{X_2}^{+\infty} \int_{X_3}^{+\infty} dx_2 dx_3 \frac{(-x_2 - y_{23} - X_1)^{\gamma-1} (x_2 - X_2)^{\gamma-1} (x_3 - X_3)^{\gamma-1}}{(x_2 + x_3 + y_{12})(x_3 + y_{23})} \\
& + C_{g(1,2)g(2,3)g(\mathcal{G})}\lambda^3 \int_{X_2}^{+\infty} \int_{X_3}^{+\infty} dx_2 dx_3 \frac{(-x_2 - y_{23} - X_1)^{\gamma-1} (x_2 - X_2)^{\gamma-1} (x_3 - X_3)^{\gamma-1}}{(x_2 + x_3 + y_{12})(x_3 - y_{23})} \\
& + C_{g(1)g(1,2)}\lambda^3 \int_{X_2}^{+\infty} \int_{X_3}^{+\infty} dx_2 dx_3 \frac{(-x_2 - y_{23} - X_1)^{\gamma-1} (x_2 - X_2)^{\gamma-1} (x_3 - X_3)^{\gamma-1}}{(-x_2 - y_{23} + y_{12})} \\
& + C_{g(2)g(1,2)}\lambda^3 \int_{X_2}^{+\infty} \int_{X_3}^{+\infty} dx_2 dx_3 \frac{(-x_2 - y_{23} - X_1)^{\gamma-1} (x_2 - X_2)^{\gamma-1} (x_3 - X_3)^{\gamma-1}}{(x_2 + y_{23} + y_{12})} \\
& + C_{g(3)g(1,2)}\lambda^3 \int_{X_2}^{+\infty} \int_{X_3}^{+\infty} dx_2 dx_3 \frac{(-x_2 - y_{23} - X_1)^{\gamma-1} (x_2 - X_2)^{\gamma-1} (x_3 - X_3)^{\gamma-1}}{(x_3 + y_{23})} \\
& + C_{g(1,2)g(\mathcal{G})}\lambda^3 \int_{X_2}^{+\infty} \int_{X_3}^{+\infty} dx_2 dx_3 \frac{(-x_2 - y_{23} - X_1)^{\gamma-1} (x_2 - X_2)^{\gamma-1} (x_3 - X_3)^{\gamma-1}}{(x_3 - y_{23})} \\
& + C_{g(1,2)}\lambda^3 \int_{X_2}^{+\infty} \int_{X_3}^{+\infty} dx_2 dx_3 (-x_2 - y_{23} - X_1)^{\gamma-1} (x_2 - X_2)^{\gamma-1} (x_3 - X_3)^{\gamma-1}
\end{aligned} \tag{4.63}$$

where we have integrated out the variable  $x_1$ . We represent such equation graphically as:

$$\begin{aligned}
& \begin{array}{c} \blacksquare \quad \blacksquare \quad \blacksquare \\ x_1 \quad x_2 \quad x_3 \end{array} \quad \begin{array}{c} y_{12} \quad y_{23} \end{array} = C_{g(1)g(1,2)g(\mathcal{G})} \text{ (diagram)} + C_{g(2)g(1,2)g(\mathcal{G})} \text{ (diagram)} \\
& + C_{g(1)g(1,2)g(3)} \text{ (diagram)} + C_{g(2)g(1,2)g(3)} \text{ (diagram)} \\
& + C_{g(1)g(1,2)g(3)} \text{ (diagram)} + C_{g(2)g(1,2)g(2,3)} \text{ (diagram)} \\
& + C_{g(3)g(1,2)g(2,3)} \text{ (diagram)} + C_{g(1,2)g(2,3)g(\mathcal{G})} \text{ (diagram)} \\
& + C_{g(1)g(1,2)} \text{ (diagram)} + C_{g(2)g(1,2)} \text{ (diagram)} \\
& + C_{g(3)g(1,2)} \text{ (diagram)} + C_{g(1,2)g(\mathcal{G})} \text{ (diagram)}
\end{aligned}$$



$$+ C_{g(1,2)} \int_{X_2}^{+\infty} \int_{X_3}^{+\infty} dx_2 dx_3 \mathcal{L}_{z \rightarrow \infty}^0 \left\{ (-x_2 - y_{23} - X_1)^{\gamma-1} (x_2 - X_2)^{\gamma-1} (x_3 - X_3)^{\gamma-1} \right\} \quad (4.65)$$

where  $\psi_{g(1,2)}$  is given by (4.62). By inverting the above equation we find an expression for  $C_{g(1,2)}$ , in terms of flat-space amplitudes and simpler wavefunctions.

## 4.4 1-Loop reduction

Let us consider the integral reduction for the Bunch-Davies wavefunction of a 1-loop Feynman graph. The only addition with respect to the tree-level case is the integration over the free loop momentum  $\vec{\ell}$ ,

$$\tilde{\psi}_{\mathcal{G}} = \int_{X_v}^{+\infty} \prod_{v \in \mathcal{V}} [dx_v \lambda_k \cdot (x_v - X_v)^{\gamma_k-1}] \int d\vec{\ell} \psi_{\mathcal{G}}(x_v, y_e). \quad (4.66)$$

The integral in the free loop momentum can be rewritten in terms of integrals over the energies flowing through the loop with an appropriate measure  $\mu_{\ell}$  and domain of integration  $\Gamma$ , this result is derived in [24]. The number of integral variables corresponding to one integration in the free loop momentum  $d^D \vec{\ell}$ , depends on the dimension  $D$  of the spatial momentum and on the number of loop edges  $n_e^{(\ell)}$ . In fact, the number of integral variables  $n_{\ell}$  is given by

$$n_{\ell} = \min(D, n_e^{(\ell)}). \quad (4.67)$$

The total number of integration variables of the wavefunction is  $n = n_{\ell} + n_s$ , where  $n_s$  is the number of vertices. Let us refer to the set of loop integration variables as  $\mathcal{L}$ , where  $n_{\ell} = |\mathcal{L}|$ . The Bunch-Davies wavefunction at 1-loop takes the form:

$$\tilde{\psi}_{\mathcal{G}} = \int_{X_v}^{+\infty} \prod_{v \in \mathcal{V}} [dx_v \lambda_k \cdot (x_v - X_v)^{\gamma_k-1}] \int_{\Gamma} \left[ \prod_{j \in \mathcal{L}} dy_j \right] \mu_{\ell}(y_j) \psi_{\mathcal{G}}(x_v, y_j). \quad (4.68)$$

Here,  $\mu_{\ell}(y_j) \equiv \mu_{\ell}(y_1, \dots, y_{n_{\ell}})$  and  $\psi_{\mathcal{G}}(x_v, y_j) \equiv \psi_{\mathcal{G}}(x_1, \dots, x_{n_s}; y_1, \dots, y_{n_{\ell}})$ .

The physical poles of the wavefunction  $\tilde{\psi}_{\mathcal{G}}$  are the same as in the tree-level case and are given by the poles of the universal integrand. Provided that there are no branch points in the measure  $\mu_{\ell}$ , we can apply the same computation as in the tree-level case.

### 4.4.1 Wavefunction integral basis

In analogy with the tree-level case, we exploit the 1-1 correspondence between singularities of the wavefunction and subgraphs to construct the integral basis. Each term of the integral basis corresponds to a set of subgraphs.

For a given process, consider all the compatible sets of  $d$  subgraphs where  $d \in [1, n]$  and  $n = n_s + n_\ell$ . We refer to this set as  $\mathfrak{G}^d$  and its elements are  $\mathfrak{g}_i^d$ . The compatibility rules for subgraphs are derived in [9]. Let us define a term of the basis associated to the set of subgraphs  $\mathfrak{g}_i^d$ :

$$I_{\mathfrak{g}_i^d} = \int_{X_v}^{+\infty} \prod_{v \in \mathcal{V}} [dx_v \lambda_k \cdot (x_v - X_v)^{\gamma_k - 1}] \int_{\Gamma} \left[ \prod_{j \in \mathcal{L}} dy_j \right] \mu_\ell(y_j) \prod_{j=1}^d \frac{1}{E_j}, \quad (4.69)$$

where  $E_j$  are the energies of the  $d$  subgraphs contained in  $\mathfrak{g}_i^d$ .

We can expand the wavefunction as a linear combination of this basis up to a rational function  $R$ :

$$\begin{aligned} \tilde{\psi}_{\mathcal{G}} &= \sum_{d=1}^n \sum_{i=1}^{|\mathfrak{G}^d|} C_{\mathfrak{g}_i^d} I_{\mathfrak{g}_i^d} + R \\ &= \sum_{i=1}^{|\mathfrak{G}^1|} C_{\mathfrak{g}_i^1} I_{\mathfrak{g}_i^1} + \cdots + \sum_{k=1}^{|\mathfrak{G}^n|} C_{\mathfrak{g}_k^n} I_{\mathfrak{g}_k^n} + R. \end{aligned} \quad (4.70)$$

where, in the first line, the first summation runs over the  $d$ -gon basis terms, where  $d \in [1, n]$ , and the second summation runs over every compatible set of  $d$  subgraphs  $\mathfrak{g}_i^d$  belonging to  $\mathfrak{G}^d$ .

#### 4.4.2 Computation of the coefficients at 1-loop

The wavefunction and its integral representation are equal up to a rational function:

$$\int_{X_v}^{+\infty} \prod_{v \in \mathcal{V}} [dx_v \lambda_k \cdot (x_v - X_v)^{\gamma_k - 1}] \int_{\Gamma} \left[ \prod_{j \in \mathcal{L}} dy_j \right] \mu(y_j) \psi_{\mathcal{G}}(x_v, y_j) = \sum_{d=1}^n \sum_{i=1}^{|\mathfrak{G}^d|} C_{\mathfrak{g}_i^d} I_{\mathfrak{g}_i^d} + R. \quad (4.71)$$

Since we are going to compute residues on the whole integrand, it is convenient to write the measure more compactly:

$$\mu(x_v, y_j) = \prod_{v \in \mathcal{V}} [\lambda_k \cdot (x_v - X_v)^{\gamma_k - 1}] \cdot \mu_\ell(y_j), \quad (4.72)$$

where  $\mu_\ell(y_j) \equiv \mu_\ell(y_1, \dots, y_{n_\ell})$ .

Let us describe the algorithm for computing the coefficients. As in the tree-level case, we start by matching the discontinuities of highest codimension and then we consider the discontinuities of lower codimension, until we get to the lowest codimension, which is 1.

- (Codimension  $n$ ) We start by computing the coefficients  $C_{\mathfrak{g}_i^n}$  such that  $\mathfrak{g}_i^n \in \mathfrak{G}^n$ . For each  $\mathfrak{g}_i^n \in \mathfrak{G}^n$ , we compute the corresponding set of residues, enforcing energy conservation, on the integrands of both sides of (4.71). Since we compute  $n$  residues, the wavefunction and the integral basis, which are defined by integration over  $n$  variables, are completely localized. On the l.h.s. we obtain a factorized wavefunction and on the r.h.s. we are left with only one basis term. We obtain immediately the expression of the coefficient  $C_{\mathfrak{g}_i^n}$ :

$$C_{\mathfrak{g}_i^n} = \text{Res}_{\mathfrak{g}_i^n} \psi_{\mathcal{G}} \quad (4.73)$$

where  $\text{Res}_{\mathfrak{g}_i^n}$  means taking  $n$  residues for the energies of the subgraphs belonging to  $\mathfrak{g}_i^n$  going to zero. The order of the residues matters, since two incompatible residues taken sequentially lead to a null amplitude. After calculating all the coefficients  $C_{\mathfrak{g}_i^n}$ , we proceed to compute the coefficients  $C_{\mathfrak{g}_i^{n-1}}$  associated to integral terms of dimension  $d = n - 1$ .

It is important to emphasize that the coefficients, associated with integral terms having the highest number of poles, are fully determined by flat-space amplitudes and do not depend on the cosmology or the loop measure.

- (Codimension  $d < n$ ) We now compute the coefficients  $C_{\mathfrak{g}_i^d}$  such that  $\mathfrak{g}_i^d \in \mathfrak{G}^d$ , by matching the discontinuities of codimension  $d$ . For each set of subgraphs  $\mathfrak{g}_i^d$  belonging to  $\mathfrak{G}^d$ , we compute the corresponding set of residues on the integrands of both sides of (4.71). The wavefunction contains  $n - d$  integration variables left. On the l.h.s. we obtain a factorized wavefunction into flat-space amplitudes and simpler subgraphs wavefunctions. On the r.h.s., we have contributions from basis terms of dimensions  $n, n - 1, \dots, d + 1$ , and one term of dimension  $d$ :

$$\begin{aligned} & \int_{X_v}^{+\infty} \prod_{v \in \mathcal{V}'} [dx_v] \int_{\Gamma} \left[ \prod_{j \in \mathcal{L}'} dy_j \right] \mu'(x_v, y_j) \psi_{\mathfrak{g}_i^d}(x_v, y_e) \\ &= \sum_k C_{\mathfrak{g}_i^d \cup \mathfrak{g}_k^{n-d}} \int_{X_v}^{+\infty} \prod_{v \in \mathcal{V}'} [dx_v] \int_{\Gamma} \left[ \prod_{j \in \mathcal{L}'} dy_j \right] \mu'(x_v, y_j) \prod_{g_j \in \mathfrak{g}_k^{n-d}} \frac{1}{E_j} \\ &+ \sum_k C_{\mathfrak{g}_i^d \cup \mathfrak{g}_k^{n-d-1}} \int_{X_v}^{+\infty} \prod_{v \in \mathcal{V}'} [dx_v] \int_{\Gamma} \left[ \prod_{j \in \mathcal{L}'} dy_j \right] \mu'(x_v, y_j) \prod_{g_j \in \mathfrak{g}_k^{n-d-1}} \frac{1}{E_j} \\ &+ \dots \\ &+ \sum_k C_{\mathfrak{g}_i^d \cup \mathfrak{g}_k^1} \int_{X_v}^{+\infty} \prod_{v \in \mathcal{V}'} [dx_v] \int_{\Gamma} \left[ \prod_{j \in \mathcal{L}'} dy_j \right] \mu'(x_v, y_j) \frac{1}{E_k} \end{aligned}$$

$$+ C_{\mathfrak{g}_i^d} \int_{X_v}^{+\infty} \prod_{v \in \mathcal{V}'} [dx_v] \int_{\Gamma} \left[ \prod_{j \in \mathcal{L}'} dy_j \right] \mu'(x_v, y_j) \quad (4.74)$$

where the measure is evaluated at

$$\mu'(x_v, y_j) = \prod_{v \in \mathcal{V}} [\lambda_k \cdot (x_v - X_v)^{\gamma_k - 1}] \cdot \mu_\ell(y_j) \Big|_{\mathfrak{g}_i^d} \quad (4.75)$$

and

$$\psi_{\mathfrak{g}_i^d} = \text{Res}_{\mathfrak{g}_i^d} \psi_{\mathcal{G}}(x_v, y_e). \quad (4.76)$$

The first sum runs through all the sets  $\mathfrak{g}_k^{n-d}$  such that  $\mathfrak{g}_i^d \cup \mathfrak{g}_k^{n-d}$  is a compatible set of subgraphs, i.e.  $\mathfrak{g}_i^d \cup \mathfrak{g}_k^{n-d} \in \mathfrak{G}^n$ . The second sum runs through all the sets  $\mathfrak{g}_k^{n-d-1}$  such that  $\mathfrak{g}_i^d \cup \mathfrak{g}_k^{n-d-1} \in \mathfrak{G}^{n-1}$ . The same applies to the other sums. Each energy  $E_j$  represents the energy of the subgraph  $g_j$ . The product of the inverse of the energies  $E_j$  corresponds to the remaining poles of the basis terms.

By taking  $d$  residues, we are left with  $n - d$  integration variables. While there is some arbitrariness in choosing which integration variables to integrate out, the total number of integration variables remaining is  $n - d = |\mathcal{V}'| + |\mathcal{L}'|$ . It is crucial to emphasize that we must integrate out the same variables on both the left-hand side and right-hand side of (4.71).

We now have to isolate the contributions to the coefficient  $C_{\mathfrak{g}_i^d}$ . We expand the integrands on both sides of (4.21) using the relation (A.4), where the energy variables  $x_v$  have been shifted by  $x_v \rightarrow x_v + \alpha_v z$ . By matching the singularities, we obtain that the contributions to the coefficient  $C_{\mathfrak{g}_i^d}$  come from the zeroth terms of the Laurent series for  $z \rightarrow \infty$ :

$$\begin{aligned} & \int_{X_v}^{+\infty} \prod_{v \in \mathcal{V}'} [dx_v] \int_{\Gamma} \left[ \prod_{j \in \mathcal{L}'} dy_j \right] \mathcal{L}_{z \rightarrow \infty}^{(0)} \left\{ \mu'(x_v, y_j) \psi_{\mathfrak{g}_i^d}(x_v, y_e) \right\} \\ &= \sum_k C_{\mathfrak{g}_i^d \cup \mathfrak{g}_k^{n-d}} \int_{X_v}^{+\infty} \prod_{v \in \mathcal{V}'} [dx_v] \int_{\Gamma} \left[ \prod_{j \in \mathcal{L}'} dy_j \right] \mathcal{L}_{z \rightarrow \infty}^{(0)} \left\{ \mu'(x_v, y_j) \prod_{g_j \in \mathfrak{g}_k^{n-d}} \frac{1}{E_j} \right\} \\ &+ \sum_k C_{\mathfrak{g}_i^d \cup \mathfrak{g}_k^{n-d-1}} \int_{X_v}^{+\infty} \prod_{v \in \mathcal{V}'} [dx_v] \int_{\Gamma} \left[ \prod_{j \in \mathcal{L}'} dy_j \right] \mathcal{L}_{z \rightarrow \infty}^{(0)} \left\{ \mu'(x_v, y_j) \prod_{g_j \in \mathfrak{g}_k^{n-d-1}} \frac{1}{E_j} \right\} \\ &+ \dots \\ &+ \sum_k C_{\mathfrak{g}_i^d \cup \mathfrak{g}_k^1} \int_{X_v}^{+\infty} \prod_{v \in \mathcal{V}'} [dx_v] \int_{\Gamma} \left[ \prod_{j \in \mathcal{L}'} dy_j \right] \mathcal{L}_{z \rightarrow \infty}^{(0)} \left\{ \mu'(x_v, y_j) \frac{1}{E_k} \right\} \end{aligned}$$

$$+ C_{\mathfrak{g}_i^d} \int_{X_v}^{+\infty} \prod_{v \in \mathcal{V}'} [dx_v] \int_{\Gamma} \left[ \prod_{j \in \mathcal{L}'} dy_j \right] \mathcal{L}_{z \rightarrow \infty}^{(0)} \left\{ \mu'(x_v, y_j) \right\} \quad (4.77)$$

We have computed all the coefficients of the previous iterations, thus by inverting the above equation we obtain an expression for  $C_{\mathfrak{g}_i^d}$ .

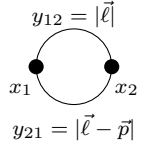
After computing all the coefficients  $C_{\mathfrak{g}_i^d}$  for every  $\mathfrak{g}_i^d \in \mathfrak{G}^d$ , we proceed to compute the coefficients associated with integral terms having a lower number of poles.

An important remark is in order. In the previous step of the algorithm we have shown that the coefficients associated with integral terms having the highest number of poles are fully determined by flat-space amplitudes and do not depend on the cosmology or the loop measure. The coefficients associated with integral terms having a lower number of poles, depend on the cosmology, which is encoded in the integral measure, and on the loop measure.

## 4.5 1-Loop example

We present one example for the integral reduction of a 1-loop wavefunction. We consider a bubble graph in flat-space cosmology.

**Bubble graph** The bubble graph is given by the following reduced Feynman diagram



$$\quad (4.78)$$

and its Bunch-Davies wavefunction is

$$\tilde{\psi}_{\mathcal{G}}(x_1, x_2) = \int d^D \vec{\ell} \psi_{\mathcal{G}}(x_1, x_2, y_{12} = |\vec{\ell}|, y_{21} = |\vec{\ell} - \vec{p}|), \quad (4.79)$$

where  $\vec{p}$  is the external momentum,  $\vec{\ell}$  is the free loop momentum,  $D$  is the dimension of spatial momentum. In a flat-space cosmology, the external energies  $x_1$  and  $x_2$  are fixed.

In the case of the bubble graph,  $n_e^{(\ell)} = 2$ . Therefore, for  $D \geq 2$ , the number of integration variables is  $n_{\ell} = 2$ , namely  $y_{12}$  and  $y_{21}$ , while for  $D = 1$ , there is only one integration variable,  $y_{12}$ .

For  $D \geq 2$ , the wavefunction of the bubble graph, in terms of integration in the internal energies, is given by:

$$\tilde{\psi}_{\mathcal{G}}(x_1, x_2) = \int_{\Gamma} dy_{12} dy_{21} \mu_{\ell}(y_{12}, y_{21}) \psi_{\mathcal{G}}(x_1, x_2, y_{12}, y_{21}), \quad (4.80)$$

where the integral measure  $\mu_\ell(y_{12}, y_{21})$  and integral domain  $\Gamma$  are derived in [24]. For  $D = 1$ ,

$$\tilde{\psi}_{\mathcal{G}}(x_1, x_2) = \int_{\Gamma} dy_{12} \mu_\ell(y_{12}) \psi_{\mathcal{G}}(x_1, x_2, y_{12}). \quad (4.81)$$

In this case, the one-dimensional momentum  $\ell$  is a scalar so  $y_{12} = \ell$  and  $y_{21} = \ell - p = y_{12} - p$ .

It is convenient to define  $\bar{\psi}_{\mathcal{G}}$  as the integrand of the bubble graph wavefunction (4.80), including the measure:

$$\bar{\psi}_{\mathcal{G}} = \mu_\ell(y_{12}, y_{21}) \psi_{\mathcal{G}}(x_1, x_2, y_{12}, y_{21}). \quad (4.82)$$

Let us now construct the basis considering all the compatible sets of subgraphs with cardinality  $d \in [1, n_\ell]$ . For  $D = 1$ ,  $n_\ell$  is equal to 1 and the basis has only 1-gon terms. The integral basis is given by:

$$\begin{aligned} \tilde{\psi}_{\mathcal{G}} &= C_{g(1)} \int_{\Gamma} dy_{12} \mu_\ell(y_{12}) \frac{1}{(x_1 + y_{21} + y_{12})} \\ &+ C_{g(2)} \int_{\Gamma} dy_{12} \mu_\ell(y_{12}) \frac{1}{(x_2 + y_{21} + y_{12})} \\ &+ C_{g(1,2)} \int_{\Gamma} dy_{12} \mu_\ell(y_{12}) \frac{1}{(x_1 + x_2 + 2y_{21})} \\ &+ C_{g(2,1)} \int_{\Gamma} dy_{12} \mu_\ell(y_{12}) \frac{1}{(x_1 + x_2 + 2y_{12})} \end{aligned} \quad (4.83)$$

where  $y_{21} = y_{12} - p$ .

For  $D \geq 2$ ,  $n_\ell$  is equal to 2 and the basis has 1-gon and 2-gon terms. The integral basis has 9 terms and it is given by:

$$\begin{aligned} \tilde{\psi}_{\mathcal{G}} &= C_{g(1)g(1,2)} \int_{\Gamma} dy_{12} dy_{21} \mu_\ell(y_{12}, y_{21}) \frac{1}{(x_1 + x_2 + 2y_{21})(x_1 + y_{21} + y_{12})} \\ &+ C_{g(2)g(1,2)} \int_{\Gamma} dy_{12} dy_{21} \mu_\ell(y_{12}, y_{21}) \frac{1}{(x_1 + x_2 + 2y_{21})(x_2 + y_{21} + y_{12})} \\ &+ C_{g(1)g(2,1)} \int_{\Gamma} dy_{12} dy_{21} \mu_\ell(y_{12}, y_{21}) \frac{1}{(x_1 + x_2 + 2y_{12})(x_1 + y_{21} + y_{12})} \\ &+ C_{g(2)g(2,1)} \int_{\Gamma} dy_{12} dy_{21} \mu_\ell(y_{12}, y_{21}) \frac{1}{(x_1 + x_2 + 2y_{12})(x_2 + y_{21} + y_{12})} \\ &+ C_{g(1)g(2)} \int_{\Gamma} dy_{12} dy_{21} \mu_\ell(y_{12}, y_{21}) \frac{1}{(x_1 + y_{21} + y_{12})(x_2 + y_{21} + y_{12})} \\ &+ C_{g(1)} \int_{\Gamma} dy_{12} dy_{21} \mu_\ell(y_{12}, y_{21}) \frac{1}{(x_1 + y_{21} + y_{12})} \end{aligned}$$

$$\begin{aligned}
& + C_{g(2)} \int_{\Gamma} dy_{12} dy_{21} \mu_{\ell}(y_{12}, y_{21}) \frac{1}{(x_2 + y_{21} + y_{12})} \\
& + C_{g(1,2)} \int_{\Gamma} dy_{12} dy_{21} \mu_{\ell}(y_{12}, y_{21}) \frac{1}{(x_1 + x_2 + 2y_{21})} \\
& + C_{g(2,1)} \int_{\Gamma} dy_{12} dy_{21} \mu_{\ell}(y_{12}, y_{21}) \frac{1}{(x_1 + x_2 + 2y_{12})}. \tag{4.84}
\end{aligned}$$

We represent the basis expansion graphically as:

$$\begin{aligned}
& \begin{array}{c} y_{12} \\ \square \quad \square \\ \text{---} \text{---} \text{---} \\ x_1 \quad x_2 \\ \text{---} \text{---} \text{---} \\ y_{21} \end{array} = C_{g(1)g(1,2)} \begin{array}{c} \text{---} \text{---} \text{---} \\ \bullet \quad \bullet \\ \text{---} \text{---} \text{---} \end{array} + C_{g(2)g(1,2)} \begin{array}{c} \text{---} \text{---} \text{---} \\ \bullet \quad \bullet \\ \text{---} \text{---} \text{---} \end{array} + C_{g(1)g(2,1)} \begin{array}{c} \text{---} \text{---} \text{---} \\ \bullet \quad \bullet \\ \text{---} \text{---} \text{---} \end{array} \\
& + C_{g(2)g(2,1)} \begin{array}{c} \text{---} \text{---} \text{---} \\ \bullet \quad \bullet \\ \text{---} \text{---} \text{---} \end{array} + C_{g(1)g(2)} \begin{array}{c} \text{---} \text{---} \text{---} \\ \bullet \quad \bullet \\ \text{---} \text{---} \text{---} \end{array} + C_{g(1)} \begin{array}{c} \text{---} \text{---} \text{---} \\ \bullet \quad \bullet \\ \text{---} \text{---} \text{---} \end{array} \\
& + C_{g(2)} \begin{array}{c} \text{---} \text{---} \text{---} \\ \bullet \quad \bullet \\ \text{---} \text{---} \text{---} \end{array} + C_{g(1,2)} \begin{array}{c} \text{---} \text{---} \text{---} \\ \bullet \quad \bullet \\ \text{---} \text{---} \text{---} \end{array} + C_{g(2,1)} \begin{array}{c} \text{---} \text{---} \text{---} \\ \bullet \quad \bullet \\ \text{---} \text{---} \text{---} \end{array} \tag{4.85}
\end{aligned}$$

In this example, we consider a theory with an action that does not contain couplings with time derivatives. In this case, we can use the recursive relation (3.61) to split the universal integrand into two 2-vertex graphs:

$$(x_1 + x_2) \begin{array}{c} y_{12} \\ \bullet \quad \bullet \\ \text{---} \text{---} \text{---} \\ x_1 \quad x_2 \\ \text{---} \text{---} \text{---} \\ y_{21} \end{array} = \begin{array}{c} y_{12} \\ \bullet \quad \bullet \\ \text{---} \text{---} \text{---} \\ x_1 + y_{21} \quad x_2 + y_{21} \\ \text{---} \text{---} \text{---} \\ y_{21} \end{array} + \begin{array}{c} x_1 + y_{12} \quad x_2 + y_{12} \\ \bullet \quad \bullet \\ \text{---} \text{---} \text{---} \\ y_{21} \end{array} \tag{4.86}$$

Let us consider the case  $D \geq 2$  and apply the algorithm. We compute one coefficient for each singularity codimension.

- (Codimension  $d = 2$ ) The coefficients of the basis terms containing two poles are computed by taking two residues and, thus, localizing completely the integrals of the wavefunction and the basis. For instance, let us compute the coefficient  $C_{g(1)g(1,2)}$ . We compute the two residues on the wavefunction integrand (4.82) and obtain:

$$\text{Res}_{g(1)g(1,2)} \bar{\psi}_{\mathcal{G}} = \mu(y_{12}, y_{21}) \Big|_{g(1)g(1,2)} \frac{\mathcal{A}_1(x_1 + y_{21} + y_{12}) \cdot \mathcal{A}_2(x_2 + y_{21} - y_{12})}{2y_{12}(x_1 + x_2)}, \tag{4.87}$$



The contributing terms of the integral basis are given by:

$$\begin{aligned}
\tilde{\psi}_{g(1)} &= C_{g(1)g(1,2)} \int_{\Gamma}' dy_{21} \mu'(y_{21}) \frac{1}{(x_1 + x_2 + 2y_{21})} \\
&+ C_{g(1)g(2,1)} \int_{\Gamma}' dy_{21} \mu'(y_{21}) \frac{1}{(-x_1 + x_2 - 2y_{21})} \\
&+ C_{g(1)g(2)} \int_{\Gamma}' dy_{21} \mu'(y_{21}) \frac{1}{(x_2 - x_1)} \\
&+ C_{g(1)} \int_{\Gamma}' dy_{21} \mu'(y_{21}). \tag{4.94}
\end{aligned}$$

We represent the above equation graphically as:

$$\begin{aligned}
&= C_{g(1)g(1,2)} \text{ (diagram)} + C_{g(1)g(2,1)} \text{ (diagram)} \\
&+ C_{g(1)g(2)} \text{ (diagram)} + C_{g(1)} \text{ (diagram)} \tag{4.95}
\end{aligned}$$

We match the codimension-1 discontinuities given by (4.92) and (4.94):

$$\begin{aligned}
\int_{\Gamma'} dy_{21} \mu'(y_{21}) \psi_{g(1)}(y_{21}) &= C_{g(1)g(1,2)} \int_{\Gamma'} dy_{21} \mu'(y_{21}) \frac{1}{(x_1 + x_2 + 2y_{21})} \\
&+ C_{g(1)g(2,1)} \int_{\Gamma'} dy_{21} \mu'(y_{21}) \frac{1}{(-x_1 + x_2 - 2y_{21})} \\
&+ C_{g(1)g(2)} \int_{\Gamma'} dy_{21} \mu'(y_{21}) \frac{1}{(x_2 - x_1)} \\
&+ C_{g(1)} \int_{\Gamma'} dy_{21} \mu'(y_{21}). \tag{4.96}
\end{aligned}$$

We expand the integrands of both sides of the above equation using relation (A.4), where  $y_{21}$  is shifted to  $y_{21} \rightarrow y_{21} + z$ . The coefficient  $C_{g(1)}$  is obtained by selecting the zeroth order terms of the Laurent series for  $z \rightarrow \infty$ :

$$\begin{aligned}
&\int_{\Gamma'} dy_{21} \mathcal{L}_{z \rightarrow \infty}^0 \left\{ \mu'(y_{21}) \psi_{g(1)}(y_{21}) \right\} \\
&= C_{g(1)g(1,2)} \int_{\Gamma'} dy_{21} \mathcal{L}_{z \rightarrow \infty}^0 \left\{ \mu'(y_{21}) \frac{1}{(x_1 + x_2 + 2y_{21})} \right\}
\end{aligned}$$

$$\begin{aligned}
& + C_{g(1)g(2,1)} \int_{\Gamma'} dy_{21} \mathcal{L}_{z \rightarrow \infty}^0 \left\{ \mu'(y_{21}) \frac{1}{(-x_1 + x_2 - 2y_{21})} \right\} \\
& + C_{g(1)g(2)} \int_{\Gamma'} dy_{21} \mathcal{L}_{z \rightarrow \infty}^0 \left\{ \mu'(y_{21}) \frac{1}{(x_2 - x_1)} \right\} \\
& + C_{g(1)} \int_{\Gamma'} dy_{21} \mathcal{L}_{z \rightarrow \infty}^0 \left\{ \mu'(y_{21}) \right\}
\end{aligned} \tag{4.97}$$

where  $\psi_{g(1)}(y_{21})$  is given by (4.92). Inverting the above equation we find an expression for  $C_{g(1)}$  in terms of flat-space amplitudes and simpler wavefunctions.

# Chapter 5

## Conclusion

In this thesis, we have addressed the challenge of developing a systematic technique to compute inflationary correlations. To achieve this goal, a promising approach is represented by the wavefunction of the universe, whose squared modulus provides the probability distribution to compute inflationary correlations.

The inflationary correlations are the field correlations at the end of inflation and determine the initial conditions for the universe's evolution. A central challenge in cosmology is to extract fundamental physics from these correlations, shedding light on the physics of inflation and improving our understanding of physics at very high energies. Indeed, inflation serves as a 'cosmological' particle accelerator, allowing us to probe physics at energy levels beyond what terrestrial experiments can achieve.

The advantage of considering the wavefunction of the universe is that, for conformally coupled scalars in FRW cosmology, it can be cast into a relatively simple form. In fact, in this context, the information on the cosmology can be extracted from the wavefunction of the universe by integrating a rational function, the universal integrand, on the space external energies with an appropriate measure, depending on the cosmology.

We have begun this work by reviewing the flat-space scattering amplitudes, focusing on their analytic properties, and integral reduction techniques for flat-space 1-loop amplitudes. Such analytic properties can be exploited to compute 1-loop amplitudes using integral reduction. Specifically, the amplitude is expanded in a basis of integrals that capture its singularity structure. The coefficients are determined by matching the discontinuities of the amplitude and those of the basis, and they are fixed by tree-level amplitudes.

We have drawn inspiration from the integral reduction in flat-space to perform the integral reduction of the Bunch-Davies wavefunction, in the context of a toy model of conformally-coupled scalars in FRW spacetime. In order to do so, we have reviewed the progress that has been done towards understanding the singularity structure of the Bunch-Davies wavefunction for a single Feynman graph, with particular focus on the factorization conditions near singularities.

Then, we developed an algorithm to perform the integral reduction for the Bunch-Davies wavefunction of a single Feynman graph at tree-level and we extended the treatment to the 1-loop case. We defined a basis of integrals reflecting the singularity structure of the wavefunction. Then, by matching the discontinuities of the wavefunction and the basis, we determined the coefficients in terms of flat-space amplitudes and simpler wavefunctions, given by the factorization conditions.

In the algorithm for computing the coefficients, we start by matching the discontinuities of highest codimension and then proceed considering the discontinuities of lower codimension. The coefficients associated to basis terms with the highest number of poles are fully fixed by flat-space amplitudes. The coefficients associated to basis terms with a lower number of poles are determined by the residues at infinity in the energy variables of the integrands of the factorized wavefunction and the contributing basis terms. The presence of these residues at infinity is contingent upon the measure of the integral. In the tree-level case, the measure is solely dependent on the cosmology. In fact, for a flat-space cosmology, the residues at infinity vanish. In the loop case, there is an additional measure stemming from the loop integration. In this case, contributions from residues at infinity result from both the loop measure and the measure encoding the information on the cosmology. In fact, there can be contributions from residues at infinity even when considering a flat-space cosmology.

This computational technique possesses two crucial strengths. First, it is a general method that works for any topology of Feynman graph at tree-level and 1-loop. Second, it is a systematic way to perform the computation of the Bunch-Davies wavefunction, therefore it can, in principle, be implemented in software.

In conclusion, in this work, we introduced a systematic computational technique for calculating the Bunch-Davies wavefunction for a single Feynman graph at tree-level and 1-loop. Such wavefunction provides the probability distribution for computing inflationary correlations. A deeper understanding of such correlations is crucial, as it would shed more light on the physics of inflation and on physics at very high energy.

**Future directions** In this thesis, the integral reduction was performed using a basis of integrals. The issue of computing and regularizing such basis terms was not addressed. This is the most crucial aspect of future work to make this integral reduction practical. Other areas of focus for future work involve addressing the weaknesses of this approach. First, a crucial aspect of our computation relies on employing Cauchy's theorem to perform partial fractions on the wavefunction's and integral basis integrands. This implies that the integral measure must not contain branch points. This limitation restricts the cosmologies that we can consider in our toy model. Second, the integral basis is defined up to a rational function, denoted as  $R$ . It is not possible to determine  $R$  by exploiting the discontinuities of the wavefunction, since it does not have branch cuts.

# Appendix A

## Cauchy theorem and partial fractions

The Cauchy theorem states the following.

Suppose  $f(z)$  is a meromorphic function inside a simply connected region, and  $C$  is a positively oriented simple closed curve within that region. If  $f(z)$  has isolated singularities inside  $C$  at points  $z_1, z_2, \dots, z_n$ , then the integral of  $f(z)$  along  $C$  is given by

$$\oint_C f(z) dz = 2\pi i \sum_{k=1}^n \text{Res}(f, z_k), \quad (\text{A.1})$$

where  $\text{Res}(f, z_k)$  denotes the residue of  $f(z)$  at the isolated singularity  $z_k$ .

Let us now trace the curve  $C$  in the opposite direction, and suppose that  $f(z)$  is meromorphic in the entire complex plane, we get:

$$\oint_C f(z) dz = -2\pi i \sum_{j=n+1}^m \text{Res}(f, z_j), \quad (\text{A.2})$$

where the points  $z_{n+1}, \dots, z_m$  are the isolated singularities of  $f(z)$  in the region outside of the curve  $C$ .

Therefore, a direct consequence of the Cauchy theorem is that the sum of the residues over the entire complex plane of a meromorphic function  $f(z)$  is zero. The same is true for the function  $\frac{f(z)}{z}$ , where we have inserted a simple pole at  $z = 0$ :

$$\begin{aligned} 0 &= \sum_k \text{Res} \left( \frac{f(z)}{z}, z_k \right) \\ &= \text{Res} \left( \frac{f(z)}{z}, 0 \right) + \sum_{k, k \neq 0} \text{Res} \left( \frac{f(z)}{z}, z_k \right) + \text{Res} \left( \frac{f(z)}{z}, z \rightarrow \infty \right) \end{aligned}$$

$$= f(0) + \sum_{k, k \neq 0} \text{Res} \left( \frac{f(z)}{z}, z_k \right) - \mathcal{L}_{z \rightarrow \infty}^{(0)} f(z) \quad (\text{A.3})$$

where  $z = z_k$  are the locations of the poles.

Let us consider a function  $g(x)$ , we want to expand it in partial fractions. Let us define the function  $f(z) = g(x+z)$ , by shifting  $x \rightarrow x+z$ , where  $z \in \mathbf{C}$ .

Notice that  $f(0)$  is the pole at  $z = 0$  of  $\frac{f(z)}{z}$  and it is also our original function  $f(0) = g(x)$ . Thus, we have found a way to express  $g(x)$ :

$$g(x) = - \sum_{k, k \neq 0} \text{Res} \left( \frac{f(z)}{z}, z_k \right) + \mathcal{L}_{z \rightarrow \infty}^{(0)} f(z). \quad (\text{A.4})$$

Let us generalize this result to  $n$  variables. Consider the function  $g(x_1, \dots, x_n)$ , we define the function  $f(z)$  by shifting all the variables as:  $x_i \rightarrow x_i + \alpha_i z$ , where  $\alpha_i$  is a real non-null constant and  $z \in \mathbf{C}$ . The constants  $\alpha_i$  need to be set appropriately such that we do not miss any pole. For instance, consider a 2-variable function  $g(x, y) = N(x, y)/(x-y)$ . This function has a pole in  $x = y$ . If we shift the variables  $x, y \rightarrow (x+z), (y+z)$  and consider  $f(z) = N(x+z, y+z)/(x-y)$ . The  $z$  shifts in the denominator cancel off and we miss the pole. This is why, in general, we need appropriate  $\alpha_i$  constants. After the computation of all the residues we can set the constants  $\alpha_i$  to one.

The Cauchy theorem applies as before, since  $f(z)$  is a one dimensional complex function. The formula (A.4) is still valid.

Let us consider an example:

$$\begin{aligned} g(x) &= \frac{x^2 + y^2 + 1}{(x+1)(y+2)(x+4)} \\ f(z) &= \frac{(x + \alpha_x z)^2 + (y + \alpha_y z)^2 + 1}{(x + \alpha_x z + 1)(y + \alpha_y z + 2)(x + \alpha_x z + 4)} \end{aligned} \quad (\text{A.5})$$

$$\begin{aligned} g(x) &= - \text{Res}_{z=(-1-x)/\alpha_x} \frac{f(z)}{z} - \text{Res}_{z=(-4-x)/\alpha_x} \frac{f(z)}{z} - \text{Res}_{z=(-2-y)/\alpha_y} \frac{f(z)}{z} + \mathcal{L}_{z \rightarrow \infty}^{(0)} f(z) \\ &= - \frac{-x^2 + 2xy - 8x - y^2 + 8y + 47}{3(x+4)(x-y+2)} - \frac{x^2 - 2xy + 2x + y^2 - 2y + 1}{3(x+1)(x-y-1)} - \\ &\quad - \frac{-x^3 + 3x^2y + 6x^2 - 3xy^2 - 12xy - 12x + y^3 + 6y^2 + 12y + 3}{(y+2)(-x+y-2)(-x+y+1)} + 1, \end{aligned} \quad (\text{A.6})$$

where in the last line we have set  $\alpha_x = \alpha_y = 1$ , which is allowed after having computed the residues. Notice that the contribution without poles is given by the zeroth term of the Laurent series,

$$\mathcal{L}_{z \rightarrow \infty}^{(0)} f(z) = 1. \quad (\text{A.7})$$

# Bibliography

- [1] Adam G. Riess, Lucas M. Macri, Samantha L. Hoffmann, Dan Scolnic, Stefano Casertano, Alexei V. Filippenko, Brad E. Tucker, Mark J. Reid, David O. Jones, Jeffrey M. Silverman, Ryan Chornock, Peter Challis, Wenlong Yuan, Peter J. Brown, and Ryan J. Foley. A 2.4 *The Astrophysical Journal*, 826(1):56, July 2016.
- [2] A. A. Penzias and R. W. Wilson. A Measurement of Excess Antenna Temperature at 4080 Mc/s. , 142:419–421, July 1965.
- [3] D. J. Fixsen, E. S. Cheng, J. M. Gales, J. C. Mather, R. A. Shafer, and E. L. Wright. The cosmic microwave background spectrum from the fullcobefiras data set. *The Astrophysical Journal*, 473(2):576–587, December 1996.
- [4] Raul Jimenez. The age of the universe, 1997.
- [5] Daniel Baumann. *Cosmology*. Cambridge University Press, 7 2022.
- [6] David Tong. Lectures on cosmology.
- [7] Alan H. Guth. The Inflationary Universe: A Possible Solution to the Horizon and Flatness Problems. *Phys. Rev. D*, 23:347–356, 1981.
- [8] de Bernardis et al. A flat universe from high-resolution maps of the cosmic microwave background radiation. *Nature*, 404(6781):955–959, April 2000.
- [9] Paolo Benincasa. Amplitudes meet cosmology: A (scalar) primer. *International Journal of Modern Physics A*, 37(26), September 2022.
- [10] Nima Arkani-Hamed, Paolo Benincasa, and Alexander Postnikov. Cosmological polytopes and the wavefunction of the universe, 2017.
- [11] Paolo Benincasa. Cosmological polytopes and the wavefuncton of the universe for light states, 2019.
- [12] Nima Arkani-Hamed, Freddy Cachazo, and Jared Kaplan. What is the simplest quantum field theory? *Journal of High Energy Physics*, 2010(9), sep 2010.

- [13] Michael E. Peskin and Daniel V. Schroeder. *An Introduction to quantum field theory*. Addison-Wesley, Reading, USA, 1995.
- [14] Steven Weinberg. *The quantum theory of fields*, volume 1. Cambridge university press, 1995.
- [15] Matthew D. Schwartz. *Quantum Field Theory and the Standard Model*. Cambridge University Press, 3 2014.
- [16] Paolo Benincasa. New structures in scattering amplitudes: A review. *International Journal of Modern Physics A*, 29(05):1430005, feb 2014.
- [17] Simon Badger, Johannes Henn, Jan Plefka, and Simone Zoia. Scattering amplitudes in quantum field theory, 2023.
- [18] G. Passarino and M. J. G. Veltman. One Loop Corrections for  $e^+ e^-$  Annihilation Into  $\mu^+ \mu^-$  in the Weinberg Model. *Nucl. Phys. B*, 160:151–207, 1979.
- [19] R. E. Cutkosky. Singularities and Discontinuities of Feynman Amplitudes. *Journal of Mathematical Physics*, 1(5):429–433, 09 1960.
- [20] Aaron Hillman and Enrico Pajer. A differential representation of cosmological wavefunctions. *Journal of High Energy Physics*, 2022(4), April 2022.
- [21] Robert M. Wald. *General Relativity*. Chicago Univ. Pr., Chicago, USA, 1984.
- [22] Robert M. Wald. *Quantum Field Theory in Curved Space-Time and Black Hole Thermodynamics*. Chicago Lectures in Physics. University of Chicago Press, Chicago, IL, 1995.
- [23] Daniel Green and Rafael A. Porto. Signals of a quantum universe. *Physical Review Letters*, 124(25), June 2020.
- [24] Paolo Benincasa and Francisco Vazão. The Asymptotic Structure of Cosmological Integrals. 2 2024.